

EPA-600/4-77-020
March 1977

AIR QUALITY DATA FOR THE NORTHEAST OXIDANT TRANSPORT STUDY, 1975

Final Data Report

by

G.W. Siple, C.K. Fitzsimmons, J.J. van Ee, and K.F. Zeller
Monitoring Operations Division
Environmental Monitoring and Support Laboratory
Las Vegas, Nevada 89114

U.S. ENVIRONMENTAL PROTECTION AGENCY
OFFICE OF RESEARCH AND DEVELOPMENT
ENVIRONMENTAL MONITORING AND SUPPORT LABORATORY
LAS VEGAS, NEVADA 89114

RESEARCH REPORTING SERIES

Research reports of the Office of Research and Development, U.S. Environmental Protection Agency, have been grouped into nine series. These nine broad categories were established to facilitate further development and application of environmental technology. Elimination of traditional grouping was consciously planned to foster technology transfer and a maximum interface in related fields. The nine series are:

1. Environmental Health Effects Research
2. Environmental Protection Technology
3. Ecological Research
4. Environmental Monitoring
5. Socioeconomic Environmental Studies
6. Scientific and Technical Assessment Reports (STAR)
7. Interagency Energy-Environment Research and Development
8. "Special" Reports
9. Miscellaneous Reports

This report has been assigned to the ENVIRONMENTAL MONITORING series. This series describes research conducted to develop new or improved methods and instrumentation for the identification and quantification of environmental pollutants at the lowest conceivably significant concentrations. It also includes studies to determine the ambient concentrations of pollutants in the environment and/or the variance of pollutants as a function of time or meteorological factors.

This document is available to the public through the National Technical Information Service, Springfield, Virginia 22161.

DISCLAIMER

This report has been reviewed by the Environmental Monitoring and Support Laboratory-Las Vegas, U. S. Environmental Protection Agency, and approved for publication. Mention of trade names or commercial products does not constitute endorsement or recommendation for use.

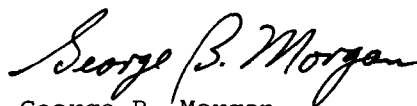
FOREWORD

Protection of the environment requires effective regulatory actions which are based on sound technical and scientific information. This information must include the quantitative description and linking of pollutant sources, transport mechanisms, interactions, and resulting effects on man and his environment. Because of the complexities involved, assessment of specific pollutants in the environment requires a total systems approach which transcends the media of air, water, and land. The Environmental Monitoring and Support Laboratory-Las Vegas contributes to the formation and enhancement of a sound integrated monitoring data base through multidisciplinary, multimedia programs designed to:

develop and optimize systems and strategies for monitoring pollutants and their impact on the environment

demonstrate new monitoring systems and technologies by applying them to fulfill special monitoring needs of the Agency's operating programs

This report presents the results of a study directed at determining the extent of pollutant transport, specifically oxidant, into and through the EPA Region I area. The results of this study could provide a basis for modifying the transportation control plans for the Boston metropolitan area particularly since they demonstrate that the origin of the photochemical pollution resides in areas upwind of that city. As this study demonstrates the phenomenon of oxidant transport, that mechanism should be considered by policymakers and investigators in other geographical areas. Further details concerning this subject can be obtained by contacting the Air Quality Branch, Monitoring Operations Division, Environmental Monitoring & Support Laboratory-Las Vegas.



George B. Morgan

Acting Director

Environmental Monitoring and Support Laboratory
Las Vegas

CONTENTS

	<u>Page</u>
List of Figures	v
List of Tables	viii
List of Abbreviations and Symbols	ix
Introduction	1
Summary of EPA-LV Involvement	1
Monitoring System Description	2
Instrument Layout	2
System Design Rationale	4
Temperature and Pressure Sensitivity of Instruments	5
Data Handling	6
Quality Control	9
Quality Assurance Program	9
Data Anomalies/Aberrations	14
Air Quality Data	16
References	90

LIST OF FIGURES

<u>Number</u>		<u>Page</u>
1	On-site data treatment	8
2	Off-site data treatment	8
3	EMSL-LV field calibration scheme for ozone measurement	10
4	Northeast Oxidant Transport Study ozone measurement intercomparison	13
5	Flight #1 (August 9, 1975): Flight pattern and ozone distribution map	18
6	Flight #2 (August 10, 1975): Flight pattern	19
7	Flight #2: Vertical profiles of parameters for Spiral #1	20
8	Flight #2: Vertical profiles of parameters for Spiral #2	21
9	Flight #2: Vertical profiles of parameters for Spiral #3	22
10	Flight #2: Vertical profiles of parameters for Spiral #4	23
11	Flight #2: Vertical profiles of parameters for Spiral #5	24
12	Flight #2: Vertical profiles of parameters for Spiral #6	25
13	Flight #2: Vertical profiles of parameters for Spiral #7	26
14	Flight #2: Vertical profiles of parameters for Spiral #8	27
15	Flight #2: Vertical profiles of parameters for Spiral #9	28
16	Flight #3 (August 11, 1975): Flight pattern and ozone distribution map	29
17	Flight #3: Vertical profiles of parameters for Spiral #1	30
18	Flight #3: Vertical profiles of parameters for Spiral #2	31
19	Flight #3: Vertical profiles of parameters for Spiral #3	32
20	Flight #3: Vertical profiles of parameters for Spiral #4	33
21	Flight #3: Vertical profiles of parameters for Spiral #5	34
22	Flight #3: Vertical profiles of parameters for Spiral #6	35
23	Flight #4 (August 12, 1975): Flight pattern and ozone distribution map	36
24	Flight #5 (August 12, 1975): Flight pattern and ozone distribution map	37
25	Flight #5: Vertical profiles of parameters for Spiral #1	38
26	Flight #5: Vertical profiles of parameters for Spiral #2	39
27	Flight #5: Vertical profiles of parameters for Spiral #3	40
28	Flight #5: Vertical profiles of parameters for Spiral #4	41
29	Flight #6 (August 13, 1975): Flight pattern and ozone distribution map	42
30	Flight #6: Vertical profiles of parameters for Spiral #1	43
31	Flight #6: Vertical profiles of parameters for Spiral #2	44
32	Flight #6: Vertical profiles of parameters for Spiral #3	45
33	Flight #6: Vertical profiles of parameters for Spiral #4	46
34	Flight #7 (August 13, 1975): Flight pattern and ozone distribution map	47

LIST OF FIGURES (Continued)

<u>Number</u>		<u>Page</u>
35	Flight #7: Vertical profiles of parameters for Spiral #1	48
36	Flight #7: Vertical profiles of parameters for Spiral #2	49
37	Flight #7: Vertical profiles of parameters for Spiral #3	50
38	Flight #7: Vertical profiles of parameters for Spiral #4	51
39	Flight #8 (August 14, 1975): Flight pattern and ozone distribution map	52
40	Flight #8: Vertical profiles of parameters for Spiral #1	53
41	Flight #8: Vertical profiles of parameters for Spiral #2	54
42	Flight #9 (August 14, 1975): Flight pattern and ozone distribution map	55
43	Flight #9: Vertical profiles of parameters for Spiral #1	56
44	Flight #10 (August 15, 1975): Flight pattern and ozone distribution map	57
45	Flight #10: Vertical profiles of parameters for Spiral #1	58
46	Flight #10: Vertical profiles of parameters for Spiral #2	59
47	Flight #10: Vertical profiles of parameters for Spiral #3	60
48	Flight #10: Vertical profiles of parameters for Spiral #4	61
49	Flight #11 (August 17, 1975): Flight pattern and ozone distribution map	62
50	Flight #11: Vertical profiles of parameters for Spiral #1	63
51	Flight #11: Vertical profiles of parameters for Spiral #2	64
52	Flight #11: Vertical profiles of parameters for Spiral #3	65
53	Flight #11: Vertical profiles of parameters for Spiral #4	66
54	Flight #11: Vertical profiles of parameters for Spiral #5	67
55	Flight #12 (August 19, 1975): Flight pattern and ozone distribution map	68
56	Flight #12: Vertical profiles of parameters for Spiral #1	69
57	Flight #12: Vertical profiles of parameters for Spiral #2	70
58	Flight #12: Vertical profiles of parameters for Spiral #3	71
59	Flight #13 (August 19, 1975): Flight pattern and ozone distribution map	72
60	Flight #13: Vertical profiles of parameters for Spiral #1	73
61	Flight #14 (August 20, 1975): Flight pattern and ozone distribution map	74
62	Flight #14: Vertical profiles of parameters for Spiral #1	75
63	Flight #14: Vertical profiles of parameters for Spiral #2	76
64	Flight #14: Vertical profiles of parameters for Spiral #3	77
65	Flight #15 (August 20, 1975): Flight pattern and ozone distribution map	78
66	Flight #16 (August 24, 1975): Flight pattern and ozone distribution map	79

LIST OF FIGURES (Continued)

<u>Number</u>		<u>Page</u>
67	Flight #16: Vertical profiles of parameters for Spiral #1	80
68	Flight #16: Vertical profiles of parameters for Spiral #2	81
69	Flight #16: Vertical profiles of parameters for Spiral #3	82
70	Flight #17 (August 26, 1975): Flight pattern and ozone distribution map	83
71	Flight #18 (August 27, 1975): Flight pattern and ozone distribution map	84
72	Flight #18: Vertical profiles of parameters for Spiral #1	85
73	Flight #18: Vertical profiles of parameters for Spiral #2	86
74 a	Flight #19 (August 27, 1975): Flight pattern and ozone distribution map, northbound	87
74 b	Flight #19 (August 27, 1975): Flight pattern and ozone distribution map, southbound	88
75	Flight #20 (August 28, 1975): Flight pattern and ozone distribution map	89

LIST OF TABLES

<u>Number</u>		<u>Page</u>
I	Instrument Characteristics	3
II	Data Acquisition System	7
III	Traceability of EMSL-LV Ozone Calibration	11
IV	Summary of Data Presented	17

LIST OF ABBREVIATIONS AND SYMBOLS

ABBREVIATIONS

BEN	-- Bendix model 8002 ozone analyzer
BMI	-- Battelle Memorial Institute
cm	-- centimeter(s)
DAS B-26	-- Dasibi model 1003-AAS used in Boston
DAS-LV	-- Dasibi model 1003-AH used in Las Vegas
EDT	-- U.S. Eastern Daylight Time
EMSL-LV	-- Environmental Monitoring and Support Laboratory- Las Vegas
EPA	-- U.S. Environmental Protection Agency
GPT	-- gas-phase titration
IC	-- integrated circuit
KI	-- potassium iodide
km	-- kilometer(s)
LORAMA	-- Long Range Air Monitoring Aircraft
LV	-- Las Vegas
m	-- meter(s)
MOA	-- Air Quality Branch
mm Hg	-- millimeters mercury
MSL	-- mean sea level
NBKI	-- neutral buffered potassium iodide
NBS	-- National Bureau of Standards
NO	-- nitric oxide
NO ₂	-- nitrogen dioxide
NOTS	-- Northeast Oxidant Transport Study
NPR	-- Normalized Pressure Response
O ₃	-- ozone
PHOT	-- ultraviolet photometer in Las Vegas laboratory
ppb	-- parts per billion by volume
RTP	-- Research Triangle Park
SRM	-- Standard Reference Material
STP	-- Standard Temperature and Pressure
uv	-- ultra violet
v/v	-- volume of O ₃ per volume of air
WSU	-- Washington State University

LIST OF ABBREVIATIONS AND SYMBOLS (Continued)

SYMBOLS

$^{\circ}\text{C}$	-- degrees Celsius
$^{\circ}\text{K}$	-- degrees absolute (Kelvin)
K_a	-- photo dissociation constant for nitrogen dioxide
$K(\text{O}_3 + \text{NO})$	-- rate constant for the reaction between ozone and nitric oxide
μ_{BMI}	-- mean ozone concentration in Boston on August 12, 1975, as measured by BMI
μ_{EPA}	-- mean ozone concentration in Boston on August 12, 1975, as measured by EMSL-LV
μ_{WSU}	-- mean ozone concentration in Boston on August 12, 1975, as measured by WSU
Φ	-- quantum yield for photo dissociation of nitrogen dioxide

INTRODUCTION

The transport of oxidant and oxidant precursors over short and long-range distances has gained more attention as Air Quality Control Regions implement strategies to control photochemical pollution within their mandated areas. Policy makers have promoted studies which investigate the transport of oxidant and oxidant precursors in such areas as the Midwest (Johnston et al., 1974; Decker et al., 1975), South Coast Basin of California (Blumenthal et al., 1973), the Northeast (Cleveland et al., 1976), and the heavily industrialized areas of the East (Coffey and Stasiuk, 1975). The promulgation of a Transportation Control Plan for the Boston metropolitan area elicited an urgent need to investigate the possibility of oxidant and oxidant precursors transport from the metropolitan New York - New Jersey area into Southern New England. Subsequently, Region I of the U.S. Environmental Protection Agency (EPA) sought to conduct an extensive monitoring effort directed at determining the extent of pollutant transport into and through Region I. Emission reductions in the areas accountable for the origin of the photochemical pollution problem in Region I can have extensive economic implications.

The field project involved research teams from Washington State University (WSU), Battelle Memorial Institute (BMI), EPA-Research Triangle Park (RTP), EPA-Region I, and EPA-Las Vegas (LV). WSU conducted airborne monitoring of ozone primarily through eastern New York and western Connecticut, as well as operated ground stations monitoring ozone and ozone precursors. BMI had a similar approach, primarily in eastern Connecticut and in Massachusetts. EPA-RTP operated a hydrocarbon analytical lab for samples collected throughout the area during the study. EPA-Region I administered the overall project and provided cross-calibration audits of those groups involved, including the various State agencies. EPA-LV involvement is discussed below.

SUMMARY OF EPA-LV INVOLVEMENT

The participation of the Air Quality Branch (MOA) of the Monitoring Operations Division (MOD) of the Environmental Monitoring and Support Laboratory at Las Vegas, Nevada (EMSL-LV), was twofold. A staff meteorologist with MOA was responsible for the day-to-day coordination of the various airborne monitoring teams, including the EMSL-LV team. A report of meteorological data covering the period of the study was also compiled. In addition, the EMSL-LV field team gathered extensive air quality data utilizing the Long Range Air Monitoring Aircraft (LORAMA); these data are

reported here in final form. The purpose of this report is to document all phases of the EMSL-LV participation in the Northeast Oxidant Transport Study and to present all data collected by LORAMA during the NOTS. The data are presented graphically for ease in noting trends; no interpretation of the data is provided. Hydrocarbon samples were analyzed by EPA-RTP and results are not presented herein.

MONITORING SYSTEM DESCRIPTION

INSTRUMENT LAYOUT

Since the completion of participation in NOTS, a number of changes have been made on the LORAMA system. However, this section describes the system as it existed during the summer of 1975. Table I lists the instruments installed on board. Ambient air data were collected primarily for ozone (O_3) and nitric oxide (NO); no data were collected on nitrogen dioxide (NO_2).

An air-handling system was installed in the aircraft, a Monarch B-26, which operated as an air monitoring platform. A probe which admits ram air into an integrating nephelometer consisted of a cylindrical aluminum tube, 3.5 centimeters (cm) in diameter. This tube extends about 0.9 meter (m) in front of the nose of the aircraft and allows air to flow into the instrument, which was located in the nose of the ship. The air then flowed on through an exhaust manifold and exited at the rear of the aircraft.

The hygrometer, designed specifically for aircraft use, responds to air let in through a small probe extending through the skin of the aircraft on the underside of the nose.

The temperature probe consisted of an integrated circuit projecting from the underside of the nose of the aircraft forward about 0.3 m. The probe was encased in a small cylindrical tube with an opening at the forward end.

The pressure transducer was mounted freely hanging inside the nose of the aircraft. This transducer was not attached to a static line since the air in the nose of the aircraft remains static during flight.

The remaining equipment was mounted in standard racks in the cabin of the aircraft. An S-shaped cylindrical aluminum probe, 3.5 cm in diameter, and internally coated with Kynar (a relatively inert plastic compound), was mounted on the roof of the cabin extending about 45 cm into undisturbed ambient air. Sample air entered the probe due to ram pressure. This air flowed through a manifold system and exited through the exhaust manifold. Each of the air quality instruments in the cabin continuously drew sample air from the inlet manifold for analysis. Air for sample bags was also drawn from this manifold. The operation was conducted remotely from the rear of the cabin.

TABLE I. INSTRUMENT CHARACTERISTICS

<u>Substance</u>	<u>Method</u>	<u>Model</u>	<u>Range</u>
Ozone	Chemiluminescence	Bendix 8002	0 to 500 ppb
Nitric oxide	Chemiluminescence	Teco 14B (Modified)	0 to 50 ppb
Particulate light-scattering coefficient	Integrating Nephelometer	MRI 1550	$0-10 \times 10^{-4} \text{ m}^{-1}$
Temperature	IC Temperature Transducer	National Semiconductor LX 5700	-55° to +125° C
Dewpoint	Cooled mirror	EG&G 137-C3 Hygrometer	-50° to +50° C
Altitude	IC Pressure Transducer	National Semiconductor LX 3702A	$0-1.034 \times 10^5 \text{ N/m}^2$
Hydrocarbons	Grab bag samples (Tedlar)	Special design	---

SYSTEM DESIGN RATIONALE

There are a number of variables which affect the validity of data collected from airborne platforms. Among these are the reliability of instrument calibration, lag and response times of each instrument, statistical considerations of the size of the sample, chemical reactions of pollutants within the sampling system, and the response of each instrument to the stressful environment of an unpressurized aircraft (stresses such as vibration and temperature and pressure changes).

The quality of instrument calibration is limited by the accuracy of the calibration standard and the precision of the calibration procedure. The requisite details of the quality assurance program are discussed in a subsequent section of this report.

The lag time of an instrument is defined as the time interval between a step change in input concentration at the sampling system inlet to the first observable corresponding change in the instrument output. If the sampling system is defined as the aircraft-instrument combination, then the velocity of the aircraft will have some influence on what the system sees and when it responds. Since instantaneous data were recorded every 5 seconds, the average air speed of 320 kilometers (km) per hour, flown by the B-26 aircraft during NOTS, provided one data point approximately every 450 m. The effect of the response time, the time interval between initial response and some percentage of final response (e.g., 90 percent) after a step change in input concentration, is minimized when monitoring air of uniform composition, where strong pollution gradients do not exist. The data should be corrected when very rapid changes in input concentration occur, such as when source sampling. For the purpose of the regional ambient monitoring performed by our system, however, data have not been corrected for the effects of lag and response time.

Ambient air quality standards and modeling routines are generally based on data time-averaged over 1 hour or longer at a given location. Spatially static monitors can provide this type of information quite readily. Mobile monitors, such as airborne platforms, however, must provide averaged or spatially integrated data. It is apparent that a close examination of atmospheric variability is necessary before accepting the statistical validity of data taken from an airborne platform. The subject has been discussed in the literature (Mage, 1975) and the reader is referred to that article for a more in-depth discussion.

Air monitoring can be further complicated by the reactivity of species being measured. For example, a given compound can react on the walls of the system obviously biasing the sample. It is therefore necessary to take precautions to ensure that the portions of the system with which the compounds being measured come in contact are as chemically inert as possible. To this end, the internal surfaces of the air inlet probes are coated with Kynar, a relatively inert plastic compound.

Furthermore, reactive species can certainly react with one another; a good example is the reaction of NO with O₃. As long as these compounds exist at typical ambient concentrations, an equilibrium exists between them. Once they enter the confines of the monitoring system, the equilibrium is disturbed. For example, in a dark manifold, NO and O₃ will react according to their rapid dark-phase chemistry, biasing the measurement of both species. The error due to chemical interactions is strongly dependent on the residence time of sample air in the manifold system. This error can be estimated (Butcher and Ruff, 1971) by use of the appropriate rate constants. The residence time of this inlet manifold is calculated to be less than 1 second, while at typical ambient concentrations the reaction between NO and O₃ should take approximately 2 minutes to 99 percent completion; this obviates correction factors for this condition.

TEMPERATURE AND PRESSURE SENSITIVITY OF INSTRUMENTS

Since the B-26 aircraft is not pressurized, all equipment on board is subject to changes in ambient temperature and pressure. To isolate the sensitivity of each instrument to these factors, tests were conducted in an environmental chamber in Las Vegas before the beginning of the oxidant study. The following text will discuss only the Bendix ozone instrument and the TECO oxides of nitrogen instrument, since neither temperature nor pressure is expected to significantly affect the other instruments.

The Bendix ozone instrument showed an almost negligible effect from changing temperature in these tests. The zero level was unaffected throughout the range of 5° to 40° Celsius (C). The span varied up to 5 percent of full scale throughout this range, however, in the range of measurement covered by this report, approximately 15° to 30° C, it was practically unchanged.

The Bendix ozone instrument demonstrated an effect from changing altitude (pressure) in these tests. There was no demonstrable effect on the zero level. However, the span decreased with increasing altitude. Using the data obtained from these tests, a regression line was formulated ($r^2 = 0.94$) to relate instrument response to altitude; a correction factor is determined in terms of a Normalized Pressure Response (NPR).

$$\text{NPR}(\text{O}_3) = (-1.037 \times 10^{-4}) \times (\text{altitude in meters}) + (0.9968)$$

Ozone concentration is corrected for pressure sensitivity by dividing the Bendix output value by NPR(O₃). It should be noted that the change in signal was very similar to the expected theoretical output due to changing air density.

The TECO instrument, which was tested only for response to NO, showed some effect due to changing temperature in these tests. In the range 5° to 40° C, the zero level was noted to decrease for colder temperatures and increase for warmer temperature, relative to room temperature. The span was unaffected by changing temperature.

The TECO instrument, tested only for NO, also varied with changing altitude. The zero level was not affected by changing altitude, but the span decreased with increasing altitude. A regression analysis was also performed on this data ($r^2 = 0.92$).

$$\text{NPR (NO)} = (-4.315 \times 10^{-5}) \times (\text{altitude in meters}) + (0.9446)$$

NO concentration is corrected for pressure sensitivity by dividing the TECO output value by NPR(NO). NO₂ was not measured during the project. This variation of response with altitude is significantly different from the theoretical change in air density with altitude, presumably due to the low-pressure reaction chamber in the instrument. In applying these correction factors to the O₃ and NO data, it was assumed that the chamber test conditions closely simulated the range of aircraft operational conditions.

DATA HANDLING

The elements of the data acquisition system are listed in Table II. The signal voltages from each monitoring instrument were received, encoded (abbreviated ASCII), and stored on magnetic tape (7-track, 200 bits per inch, even parity) in 5-second increments, thus allowing ready accessibility for subsequent processing. The four-channel strip chart recorder provided a backup for the calculator-based storage and retrieval system. Figure 1 illustrates the availability of data during the study; the processing of the data followed the flow illustrated in Figure 2, after the field team returned to Las Vegas. The EMSL-LV field team now has the system capabilities for data processing (Figure 2) within 24-hours of collection, i.e., while still in the field. This is a great advantage for quality control considerations and for rapid initiation of data interpretation. The capability that now exists for final processing of the data corrects for zero and gain shifts (as linear functions of time), and also relates the data to sea-level pressure (altitude). In preparation of this final report, an error in the preliminary processing of the data was uncovered. The response of the O₃ analyzer and the NO analyzer, due to pressure sensitivity, was normalized to Las Vegas altitude (610 m Mean Sea Level (MSL) or 705 millimeters mercury (mm Hg) reference pressure) instead of sea-level altitude. This is a systematic error in the previously reported data values, and the proper pressure correction (to sea-level altitude) results in an approximate 7 percent increase in the O₃ data and in the NO data; i.e., the O₃ and NO data accompanying the preliminary draft of this report were low by 7 percent. The final data, presented in this report, incorporate the corrections as discussed above.

TABLE II. DATA ACQUISITION SYSTEM

<u>Item</u>	<u>Model</u>
Programmable Calculator	HP 9830 A
Multimeter	HP 3490 A
Scanner	HP 3495 A
Digital Clock	HP 59309 A
Magnetic Tape Recorder	Cipher 70
Strip Chart Recorder	MFE 4M3CAHA Modified
Printer	HP 9866 A

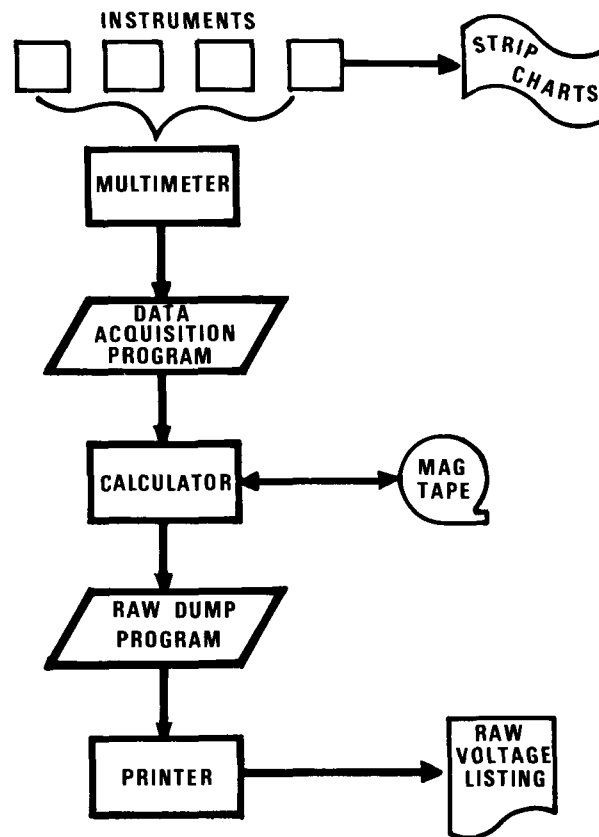


FIGURE 1. ON-SITE DATA TREATMENT.

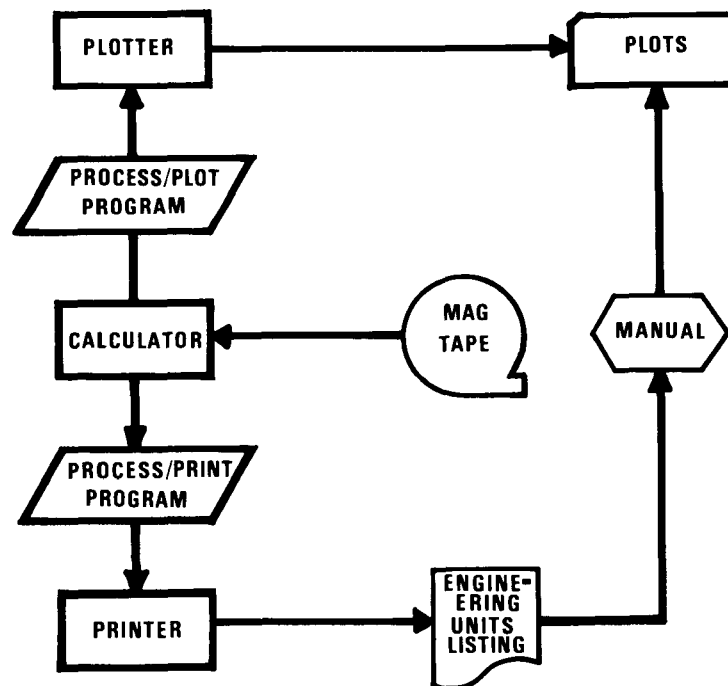


FIGURE 2. OFF-SITE DATA TREATMENT.

QUALITY CONTROL

QUALITY ASSURANCE PROGRAM

The validity of air quality data can be improved by the establishment of a well-documented and well-executed quality control program. Such a program must rely on accurate calibration standards and precise calibration techniques. Such a program was developed by the EMSL-LV field team for the successful participation of the LORAMA in the NOTS.

The accuracy of the ozone data was of primary importance. The literature was replete with difficulties with the Federal Register standard reference calibration method, Neutral Buffered Potassium Iodide (NBKI) (Behl, 1972; Boyd et al., 1970; Hodgeson et al., 1971; Kopczynski and Bufalini, 1971; Parry and Hern, 1973; Schmitz, 1973). Therefore, the quality control program chose the Dasibi 1003-AAS ozone monitor, based on the absorption of ultraviolet (uv) energy by ozone (an "absolute" measurement) to transfer the ozone standard from the laboratory to the Bendix 8002 ozone field analyzer. Previous experience with the Dasibi showed it to be stable and quite adequate for field work. Figure 3 shows the traceability of the ozone calibration from laboratory standards to the field instrument.

Under the supervision of J. Hodgeson, EMSL-LV, the uv-absorption method (Dasibi) was compared with the Federal Register NBKI method and with gas-phase titration (GPT) of ozone with a National Bureau of Standards (NBS) nitric oxide Standard Reference Material (SRM) which is maintained at Las Vegas. The results of these comparison studies are summarized in equations (1) and (2) in Table III (the numbers in parentheses in Figure 3 correspond to equations in Table III, and frequent references will be made to both Figure 3 and Table III in the following text). The Dasibi 1003-AAS was not calibrated directly against the laboratory-based uv photometer; instead, it was calibrated against a second, laboratory-based Dasibi (equation (4)), that is routinely calibrated against the uv photometer (equation (3)).

Some confusion arose in the field by calibrating the Dasibi under Las Vegas conditions without correcting to Standard Temperature and Pressure (STP) conditions. This situation was rectified after completion of the NOTS; equation (5) in Table III was used to correct the Dasibi readings made in the field to STP-based values. Furthermore, some doubt was generated during the study regarding the stability and accuracy of the Dasibi 1003-AAS. However, laboratory calibration of the instrument performed upon return to Las Vegas at the completion of the study indicated little variation from the laboratory calibration performed in Las Vegas prior to the study (compare equation (6) with equation (7)).

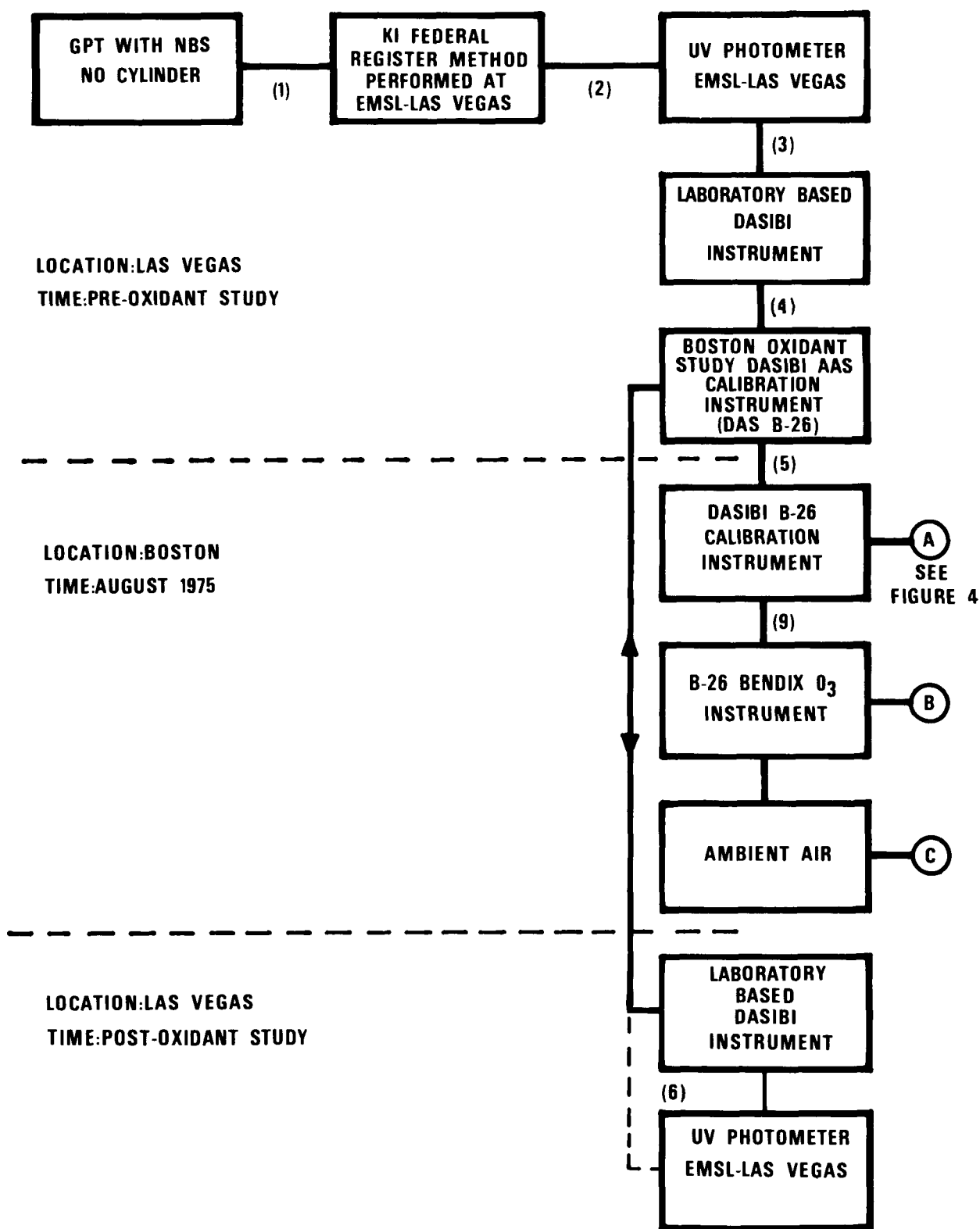


FIGURE 3. EMSL-LV FIELD CALIBRATION SCHEME FOR OZONE MEASUREMENT.

TABLE III. TRACEABILITY OF EMSL-LV OZONE CALIBRATION

Number	Equation	Date
(1)	$[O_3]^*_{NBKI} = 1.09 [O_3]^*_{GPT} - .034$	75
(2)	$[O_3]^*_{NBKI} + 1.11 [O_3]^*_{NBS-NO} - .035$	74-75
(3)	$[O_3]^*_{PHOT} + (1.060 \pm .011) [O_3]^*_{DAS-LV} + (.022 \pm .025)$	7/14/75
(4)	$[O_3]^*_{DAS-LV} + (1.017 \pm .001) [O_3]^*_{DAS B-26} + (.001 \pm .001)$	7/14/75
(5)	$[O_3]^*_{DAS B-26} = \frac{705}{P_{AMBIENT}} [O_3]^{**}_{DAS B-26}$	9/75
(6)	$[O_3]^*_{PHOT} + (1.105 \pm .002) [O_3]^*_{DAS B-26} + (.025 \pm .001)$	9/8/75
(3)+(4)→(7)	$[O_3]^*_{PHOT} + (1.078 \pm .012) [O_3]^*_{DAS B-26} + (.023 \pm .025)$	---
(2)+(7)→(8)	$[O_3]^*_{NBKI} + (1.197 \pm .012) [O_3]^*_{DAS B-26} - .010$	---
(9)	In Boston $[O_3]_{BEN} = [O_3]^{**}_{DAS B-26}$	8/75
(7)+(5)→(9)→(10)	$[O_3]^*_{PHOT} + (1.078 \pm .012) \frac{705}{P_{AMBIENT}} [O_3]^*_{BEN} + (.023 \pm .025)$	---
(8)+(5)→(9)→(11)	$[O_3]^*_{NBKI} + (1.197 \pm .012) \frac{705}{P_{AMBIENT}} [O_3]^*_{BEN} - .010$	---

*This value (v/v) is a concentration in parts per million corrected to STP conditions: $P_0 = 760$ mm Hg, $T_0 = 298^\circ K$.
 **This value is the panel meter reading of the Dasibi 1003-AAS (DAS B-26). In Las Vegas, prior to the study, the gain factor of this instrument was set to indicate ozone concentration corrected to STP conditions. When used at an ambient pressure other than that at Las Vegas ($P_{REFERENCE} = 705$ mm Hg) this gain factor must be adjusted as a function of the actual pressure change. For example, if the instrument is taken to a lower elevation, it displays concentration values which are high; these values must be corrected to STP conditions using Equation (5).

A Bendix 8851-X Dynamic Calibration System was utilized during the study to generate calibration atmospheres of ozone for the Bendix 8002 ozone analyzer. The Dasibi instrument was used to measure the concentration of the span gas and to check the quality of the zero air. The Bendix 8002 was calibrated before and after each day's flight, even though the stable performance of this instrument did not require such a frequent calibration schedule. Experience has shown it to be a good practice to calibrate frequently, especially when the instrument is subject to stressful aircraft environment, to minimize spurious data. Zero level checks were also made on the air quality instruments periodically during flight.

The ozone data reported for this study were scaled to an NBKI primary calibration standard, at STP, using equation (11) of Table III.

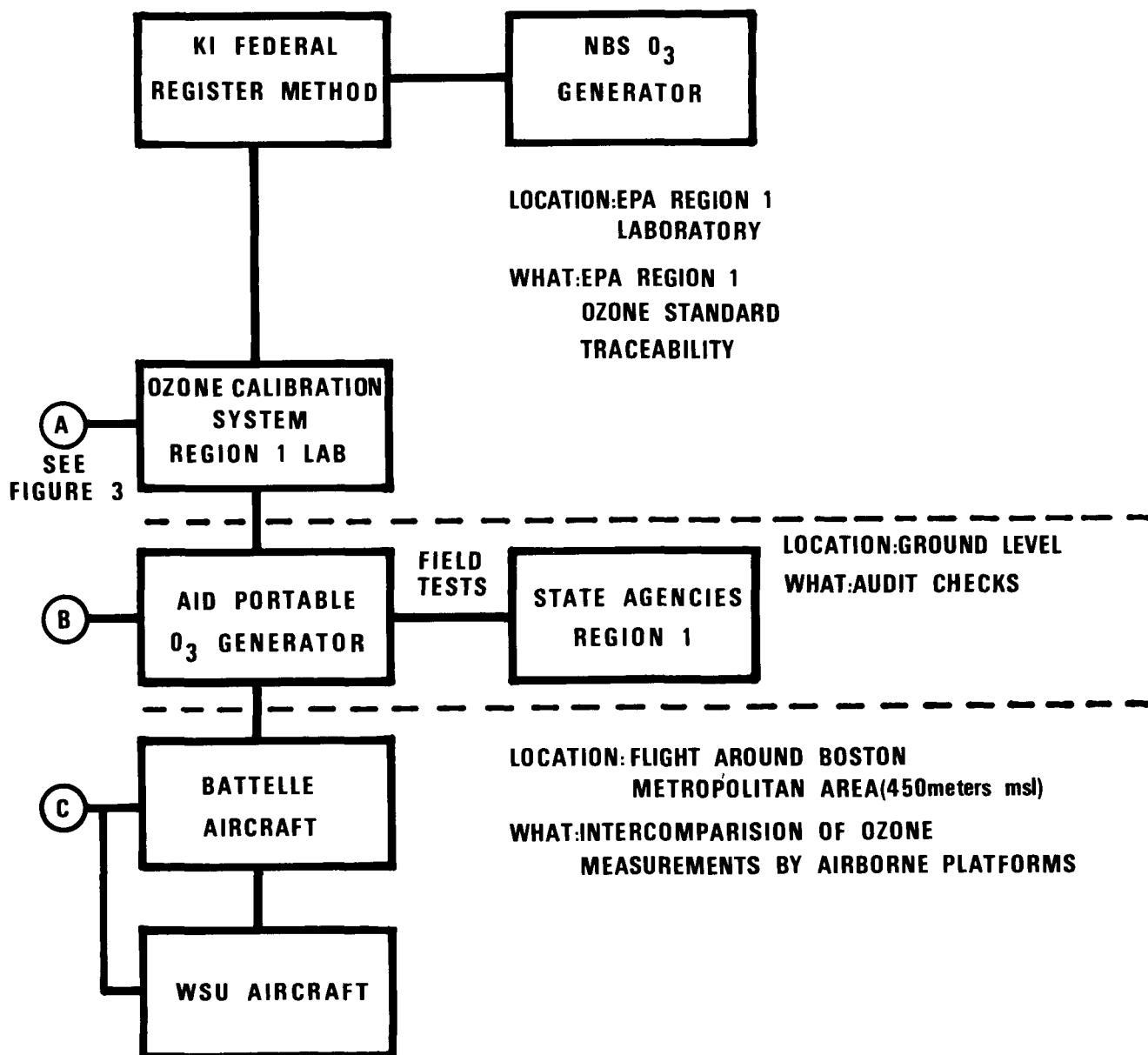
Figure 4 illustrates the various channels of intergroup ozone calibration carried out in Region I during the NOTS. Comparison data, in the form of ground-based audit checks, performed by the EPA-Region I laboratory are available from Region I. The three aircraft involved in the NOTS participated in a concomitant flight along a common path around the Boston metropolitan area on the morning of August 12, 1975. Analysis of variance of the ozone data populations sampled by WSU, BMI, and EMSL-LV infers that the hypothesis that all three population means are equivalent must be rejected. Further, this analysis indicates that at the 99 percent level of confidence, the difference between the WSU population mean (μ_{WSU}) is not significant, while the difference between the EMSL-LV population mean (μ_{EPA}) and both μ_{WSU} and μ_{BMI} is significant. At the 99 percent level of confidence,

$$\mu_{WSU} = \mu_{BMI} = (\mu_{EPA} + 6 \text{ ppb}).$$

The 6 ppb offset represents 8 percent of μ_{WSU} and appears to indicate a systematic bias in the EMSL-LV aircraft system since the other two sets of data are directly comparable. A linear regression analysis comparing all three sets of data yielded the following results:

$$\begin{aligned} \begin{bmatrix} O_3 \\ 3 \end{bmatrix}_{WSU} &= 0.934 \begin{bmatrix} O_3 \\ 3 \end{bmatrix}_{EPA} + 10.844; r^2 = 0.72 \\ \begin{bmatrix} O_3 \\ 3 \end{bmatrix}_{BMI} &= 0.988 \begin{bmatrix} O_3 \\ 3 \end{bmatrix}_{EPA} + 6.805; r^2 = 0.73 \\ \begin{bmatrix} O_3 \\ 3 \end{bmatrix}_{BMI} &= 0.956 \begin{bmatrix} O_3 \\ 3 \end{bmatrix}_{WSU} + 2.067; r^2 = 0.83 \end{aligned}$$

A modified TECO 14B gas-phase chemiluminescent instrument was used to measure NO only. No data were collected concerning NO₂. A cylinder of NO gas, bottled by Scott-Marrin, Inc., Riverside, California, was verified for concentration at the EMSL-LV lab by comparison to an NBS NO cylinder (SRM). The Scott-Marrin NO cylinder was taken into the field for calibration purposes. Gas from this cylinder was diluted with purified air in the Bendix Dynamic Calibration System, and zero level and one span level (approximately 40 percent of full scale) were checked before and after flight. Since none of the other instrumented aircraft measured NO regularly, no comparison data are included in this report.



Other instruments on board LORAMA, including the temperature sensor, dewpoint sensor, and nephelometer, were found to be extremely stable and calibration schedules were arranged accordingly.

DATA ANOMALIES/ABERRATIONS

Integrating Nephelometer

The integrating nephelometer is an instrument designed to indirectly measure the loading of solid particulate matter in the atmosphere. Particles in a given size range preferentially scatter visible light, altering the visibility through that column of light. However, the instrument cannot discriminate between various particle sizes or even particle composition. Liquid aerosols in the form of moisture droplets, therefore, act as a positive interference to determining pollutant-related particle loading. The instrument design calls for decreasing the relative humidity of the sample air in order to correct for the interference of water droplets. The residence time in the inlet line with the designed optimum flow rate of 10 cubic feet per minute (cfm) allows the installed heating element to accomplish this purpose.

In actual application, the sample flow rate provided by ram air is more than ten times faster than the optimum design, greatly reducing the residence time in the instrument and the effectiveness of the heater. For this reason, the scattering coefficient data reported are uncorrected for interference due to moisture droplets.

Ozone and Relative Humidity

As a general trend, the aircraft data showed an association between relative humidity and the indicated O₃ concentrations. Two possible reasons for this relationship are: (1) the moisture content of a parcel of air may play a role in the chemistry of smog-forming reactions; or (2) this moisture content may act as an interferent to the measurement method. (Naturally, these factors are not necessarily mutually exclusive.)

The role of humidity in the complex sequence of photochemical smog formation is, at best, confusing the contradictory. The literature offers no definitive statements when taken as a whole (Altshuller and Bufalini, 1971; Demerjian et al., 1974; Jeffries et al., 1975).

The possibility that moisture in the air interferes with the measurement technique may be attributed to the particular method (device) being used, or perhaps to the manner in which it is being used. The literature suggests that an interference effect does exist (Higuchi et al., 1976). During the study, an experiment was conducted to isolate the moisture effect relative to the instrumental method. Two instruments, based on different techniques (gas-phase chemiluminescence and uv absorption), were installed in the aircraft system and flown through areas of varying relative humidity. The chemiluminescent instrument had a positive correlation with the uv absorption instrument and with relative humidity, based on qualitative observations; i.e., both instruments indicated increased O₃ concentration in ambient air

of increased relative humidity. Laboratory-based experiments are planned to further test these instruments for the effects of relative humidity at various dewpoints.

Nitric Oxide Data

Significant challenges have arisen regarding the quantitative and qualitative validity of the NO data collected by the LORAMA system during the NOTS. The concentration levels of NO reported are relatively high, and one might expect to see lower levels, e.g., below 10 parts per billion (ppb) for the most part. In addition, considering the reactivity dynamics of the constituents of photochemical smog, one anticipates an inverse qualitative relationship between NO and O₃; however, a majority of the observations recorded in the LORAMA missions confound this expectation.

An easy solution to this dilemma is unduly complicated due to the dearth of NO₂ data. The fact is that NO concentrations up to 40 ppb (the highest recorded by LORAMA) are not unknown in the lower troposphere (Tebbens, 1968; Air Quality Criteria for Nitrogen Oxides, 1970), although data reported recently of NO aloft indicates concentrations near the limit of analytical techniques (Breeding et al., 1976). It is well-known that the equilibrium between NO, NO₂, and O₃ may exist at any level of concentration and the following equality exists:

$$\frac{[O_3] [NO]}{[NO_2]} = \frac{\phi K_a}{K_{(O_3 + NO)}}$$

This equality is constant under equilibrium conditions of constant temperature and irradiation, but outdoor conditions are seldom, if ever, constant. For example, if the O₃ concentration increases, the NO concentration can increase as long as the NO₂ concentration increases sufficiently to maintain the equilibrium. This argument, of course, says nothing about non-equilibrium conditions. (See Calvert (1976) for further discussion of the dynamic atmospheric relationship between NO, NO₂, and O₃.)

The lack of NO₂ data renders the above argument academic for the purposes of this report and necessarily constrains the possible approaches to validating the NO data. It could, of course, be said that in light of the foregoing arguments, the NO data are plausible. In support of this proposition, NO data were collected during three flights when the concentrations were, for the most part, below 10 ppb. Since calibration methods were not altered during the study, nor was the design of the air-handling system changed, all data might then represent a cross section of real values. On the other hand, the preponderance of the data appears to belie this argument; the NO data show little diurnal concentration variation. Several alternative explanations present themselves:

(1) It is possible the instrument was actually monitoring NO₂ plus NO. A suggestion has been proffered which implied that the residence time in the air-handling system might be sufficient for dissociation of NO₂ in the air and that the NO thus produced biased the measurements of "real" NO. Upon

further consideration, this argument is specious. For one thing, the dissociation of NO_2 is driven by light; since the manifold system is dark, the equilibrium for the reaction would lie on the side on NO_2 . Furthermore, if the residence time were relatively long, the subsequent reactions between NO and O_3 and NO_2 and O_3 would have the overall effect of reducing the NO values.

(2) It is possible that although the calibration procedure was rigorously followed, a systematic error was present. It has been suggested that the zero air generator may not have cleaned the incoming air of NO as thoroughly as expected. The result of such a situation would be a negative offset. If such an error existed, it would be necessary to increase the data by some amount to correct for this situation.

(3) It is possible there is a humidity interference in the measurement. Qualitative examination of the data shows an apparent association between dewpoint and NO , so that water vapor may be a positive interferent. This possibility needs to be followed up by laboratory investigation. Higuchi et al. (1976) found humidity to be negatively correlated with NO measured or a similar instrument under controlled conditions.

AIR QUALITY DATA

In general, there were four types of flight patterns performed by the LORAMA during the NOTS. These were: (1) broad area coverage; (2) long range eastern seaboard; (3) urban plume characterization; and (4) circumcity. The aircraft performed spiral descents at strategic points in all types of patterns to determine the vertical profiles of all parameters. Non-spiral flight consisted of horizontal flight along a predetermined path. The altitude of O_3 maximum as determined from the most recent vertical profile most often served to dictate the altitude of horizontal flight. Most of the flight hours were logged below 610 M MSL.

The final processed digital data have been reduced into analog (graphical) representations, which are presented here in two forms. Each flight is represented by a horizontal O_3 distribution map. These maps illustrate the flight pattern plus pertinent data: time during flight (Eastern Daylight Time (EDT)), flight level in meters MSL, instantaneous O_3 concentration in ppb (volume of O_3 per volume of air (v/v)) every two minutes (approximately every 11 km), and location of spiral descents. In addition, vertical profiles of all parameters for all spiral descents are presented. All data are arranged by flight, beginning with flight #1 on August 9 and going through flight #20 of August 28, 1975. Table IV summarizes the data to follow.

TABLE IV. SUMMARY OF DATA PRESENTED

I. Horizontal O₃ Distribution Maps

- A. Times are EDT
- B. Altitudes are m above MSL
- C. Locations marked every two minutes by "+" are determined by Collins-40 Distance Measuring Equipment (DME) and are accurate to within 200 m
- D. Instantaneous O₃ concentrations in ppb, corrected for zero and span drift and corrected to 760 mm Hg pressure (no correction for temperature or lag or response time of the instrument)

II. Vertical Profiles of Parameters

- A. Parameters reported
 - 1. O₃ (ppb)
 - 2. NO (ppb)
 - 3. Outside ambient temperature (°C)
 - 4. Dewpoint temperature (°C)
 - 5. Relative humidity (percent)
 - 6. Particulate light scattering coefficient (10^{-4} m^{-1})
- B. Instantaneous O₃ and NO concentrations in ppb, corrected for zero and span drift and corrected to 760 mm Hg
- C. Temperatures are reported in °C with no corrections applied
- D. Relative humidity calculated from dewpoint and outside ambient temperatures, based on appropriate equations in the Smithsonian Meteorological Tables (1971)
- E. Scattering coefficient reported without correction for high relative humidity

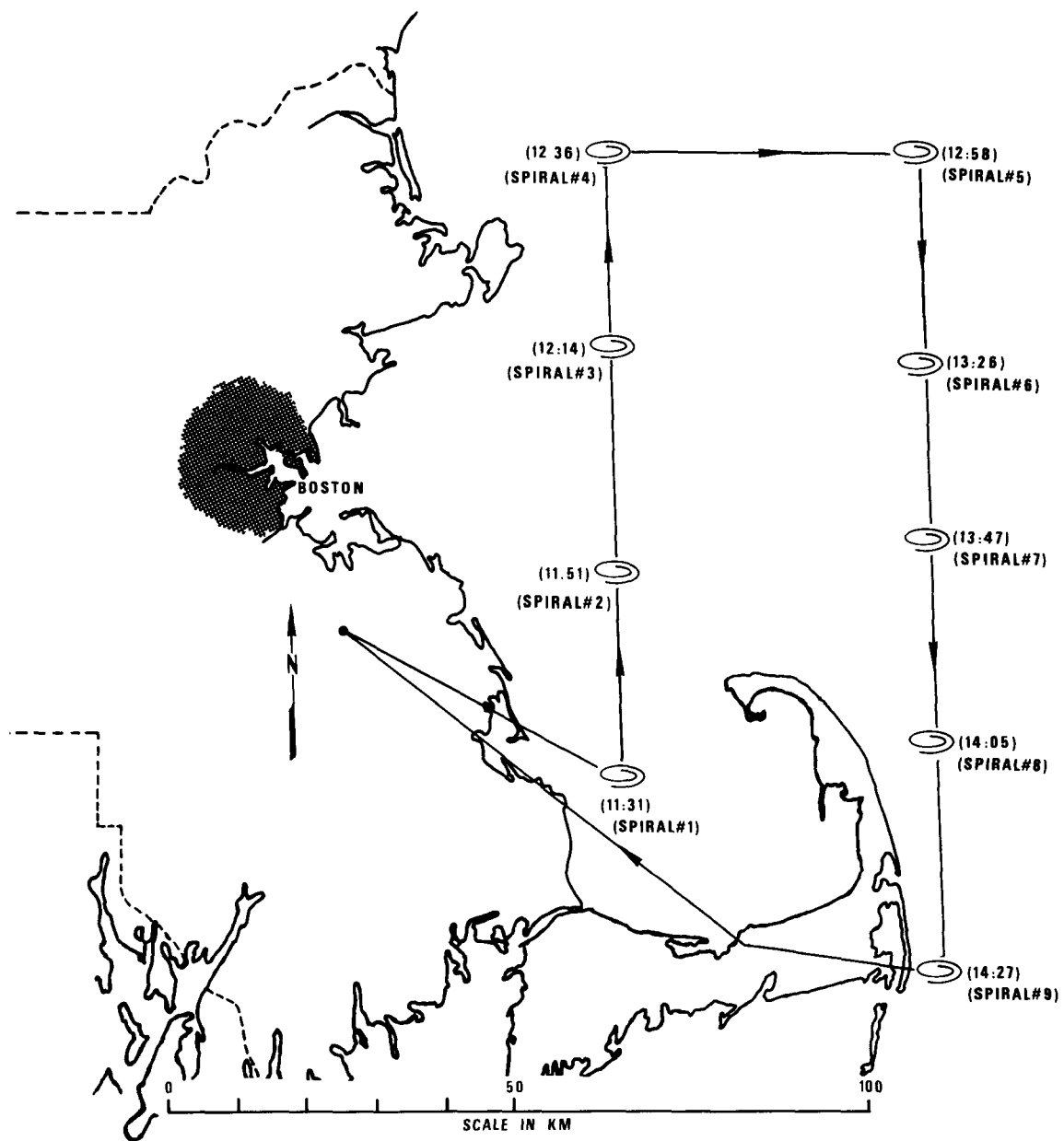
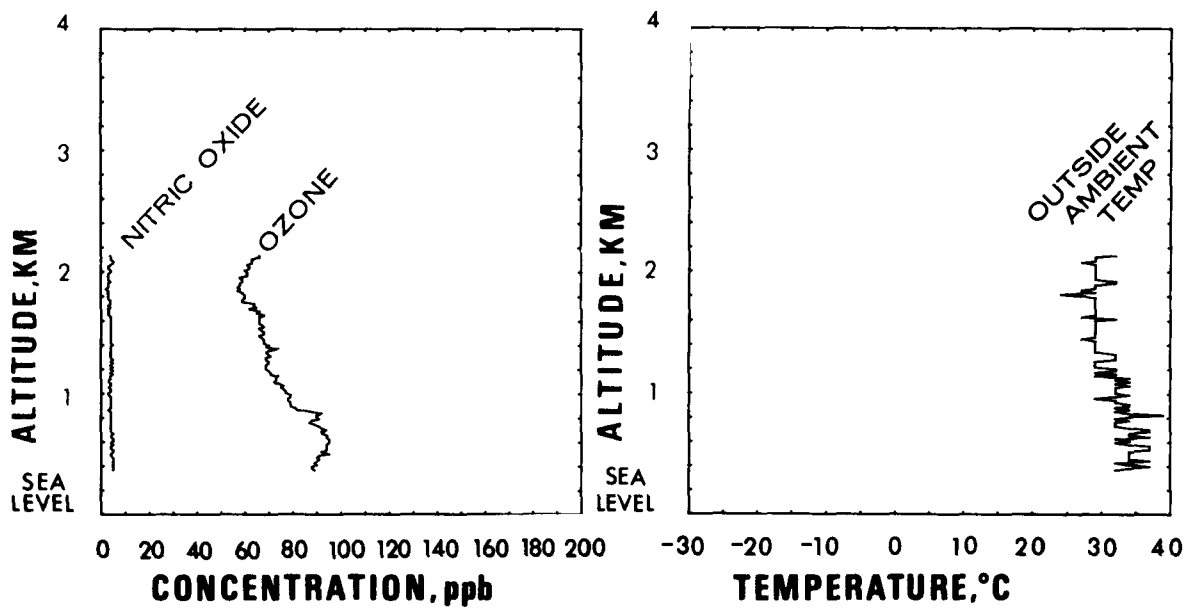


Figure 6. Flight #2 (August 10, 1975): Flight pattern



NO DATA

NO DATA

0 10 20 30 40 50 60 70 80 90 100
RELATIVE HUMIDITY, %

0 1 2 3 4 5 6 7 8 9 10
SCATTERING COEFFICIENT, 10^{-4} m^{-1}

Figure 7. Flight #2: Vertical profiles of parameters for Spiral #1

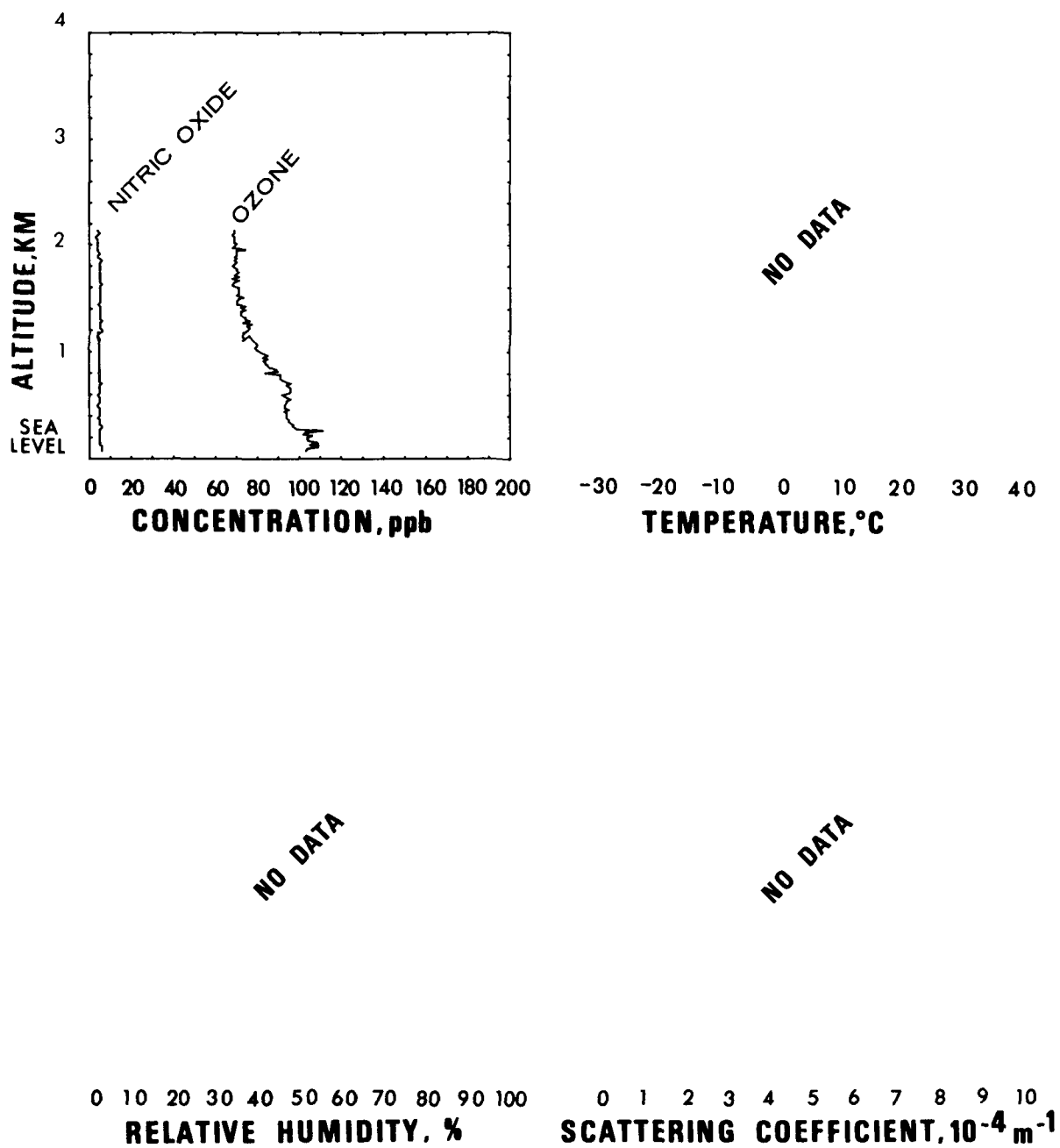


Figure 8. Flight #2: Vertical profiles of parameters for Spiral #2

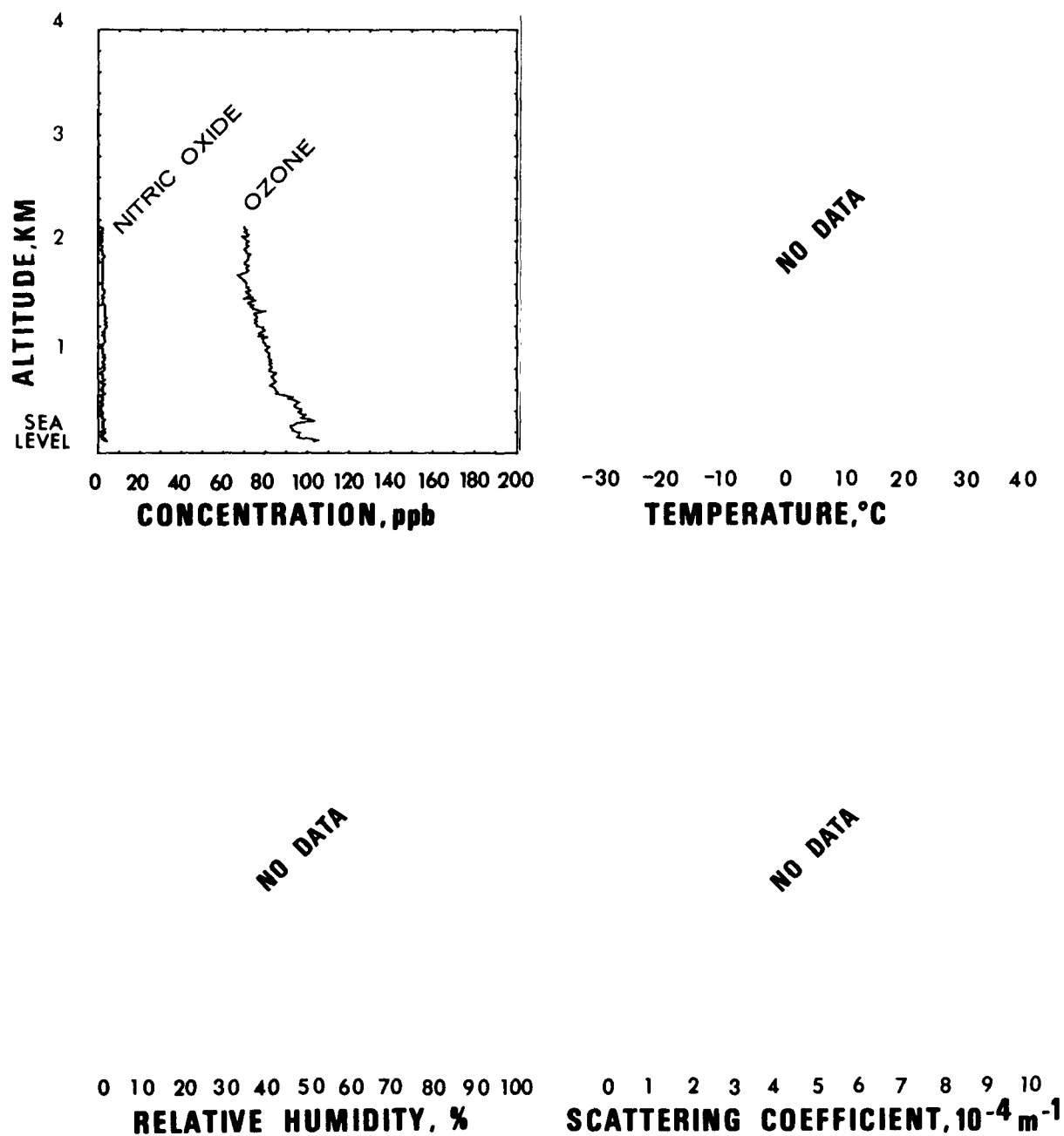
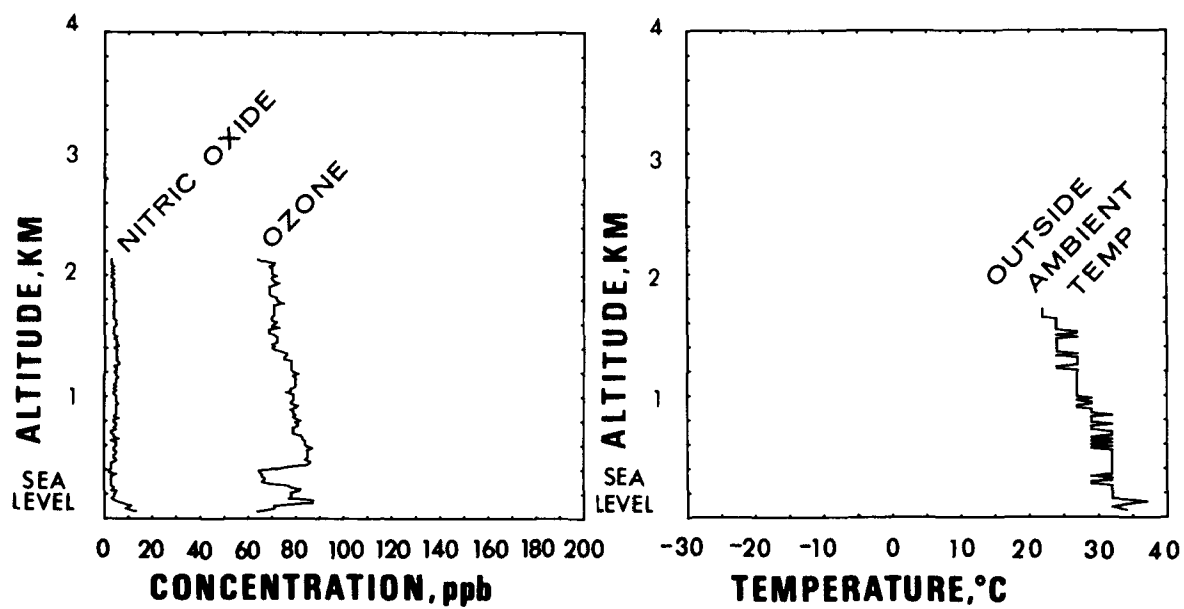


Figure 9. Flight #2: Vertical profiles of parameters for Spiral #3



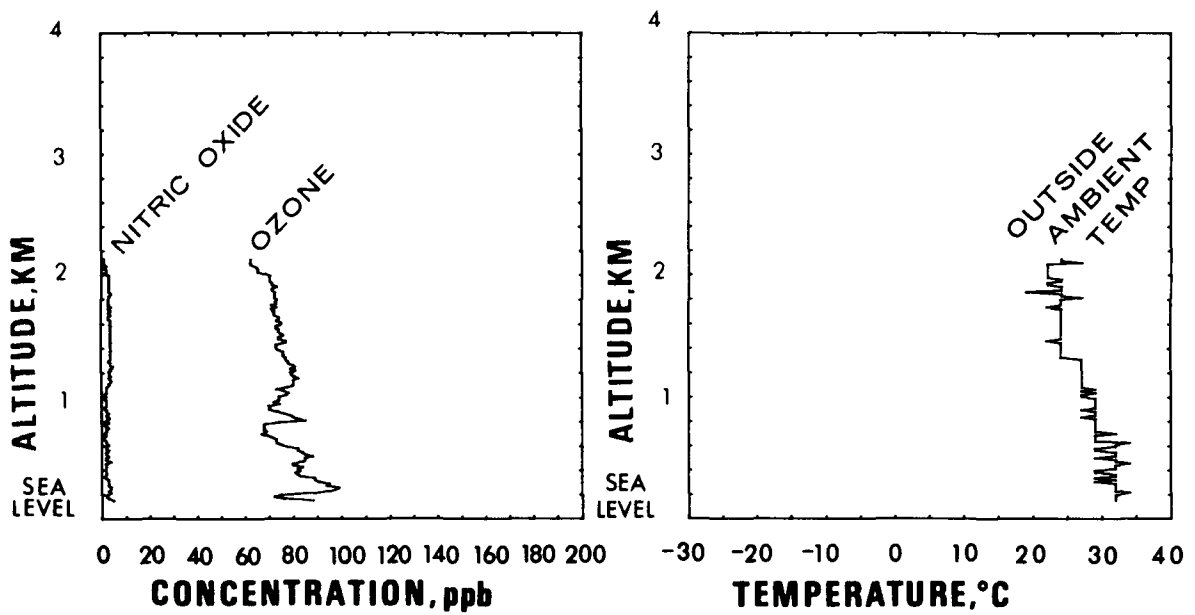
NO DATA

NO DATA

0 10 20 30 40 50 60 70 80 90 100
RELATIVE HUMIDITY, %

0 1 2 3 4 5 6 7 8 9 10
SCATTERING COEFFICIENT, $10^{-4} m^{-1}$

Figure 10. Flight #2: Vertical profiles of parameters for Spiral #4



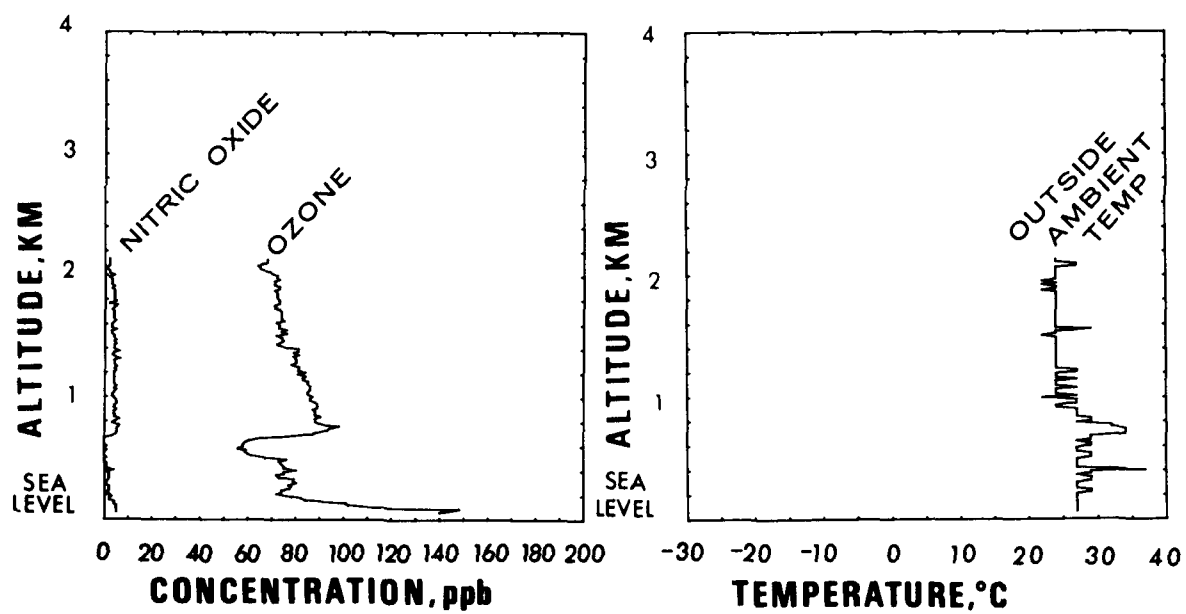
NO DATA

NO DATA

0 10 20 30 40 50 60 70 80 90 100
RELATIVE HUMIDITY, %

0 1 2 3 4 5 6 7 8 9 10
SCATTERING COEFFICIENT, 10^{-4} m^{-1}

Figure 11. Flight #2: Vertical profiles of parameters for Spiral #5



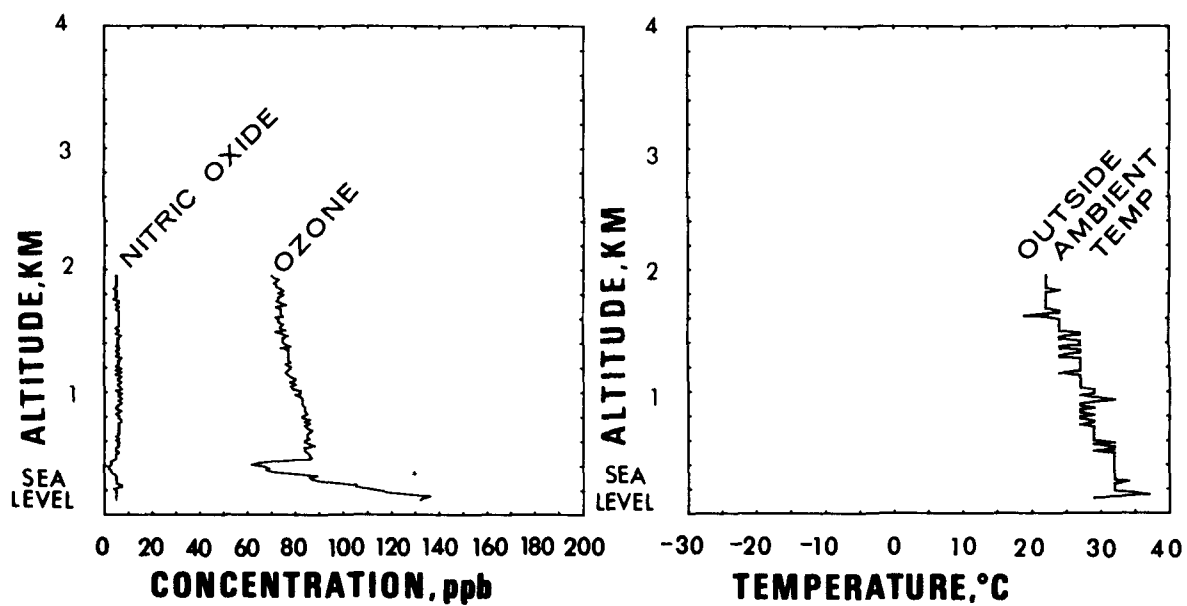
NO DATA

NO DATA

0 10 20 30 40 50 60 70 80 90 100
RELATIVE HUMIDITY, %

0 1 2 3 4 5 6 7 8 9 10
SCATTERING COEFFICIENT, $10^{-4} m^{-1}$

Figure 12. Flight #2: Vertical profiles of parameters for Spiral #6



NO DATA

NO DATA

0 10 20 30 40 50 60 70 80 90 100
RELATIVE HUMIDITY, %

0 1 2 3 4 5 6 7 8 9 10
SCATTERING COEFFICIENT, 10^{-4} m^{-1}

Figure 13. Flight #2: Vertical profiles of parameters for Spiral #7

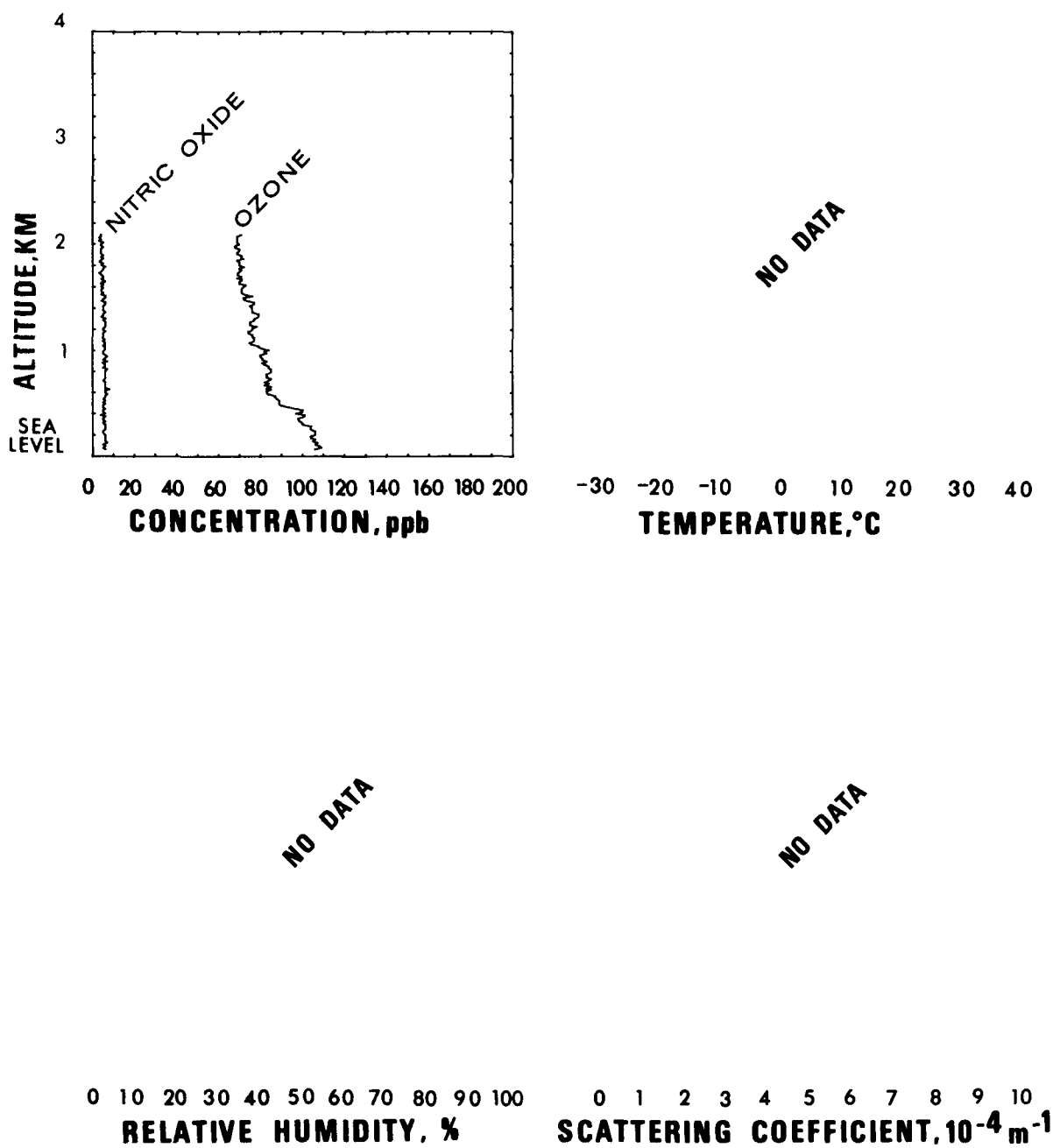


Figure 14. Flight #2: Vertical profiles of parameters for Spiral #8

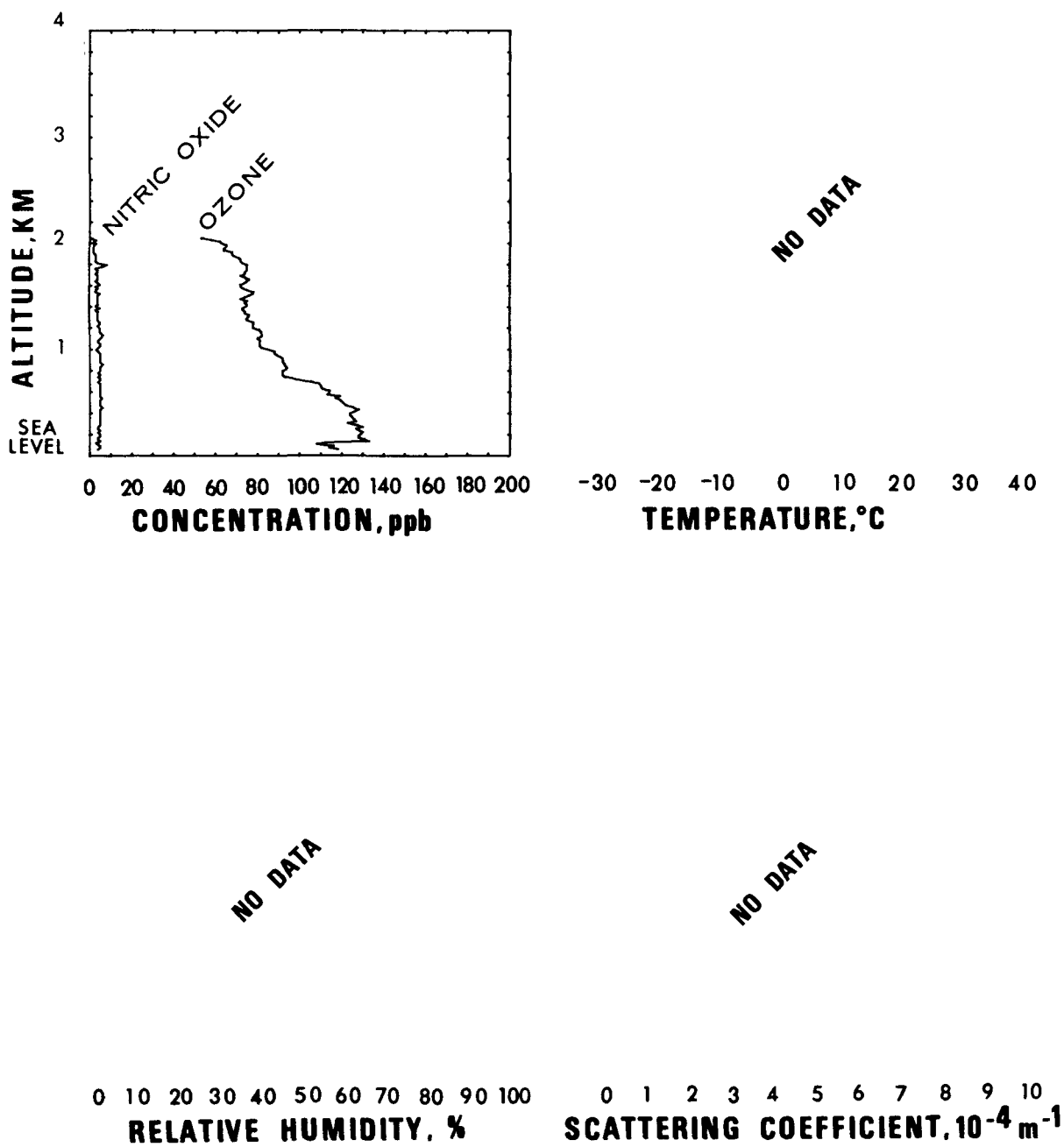


Figure 15. Flight #2: Vertical profiles of parameters for Spiral #9

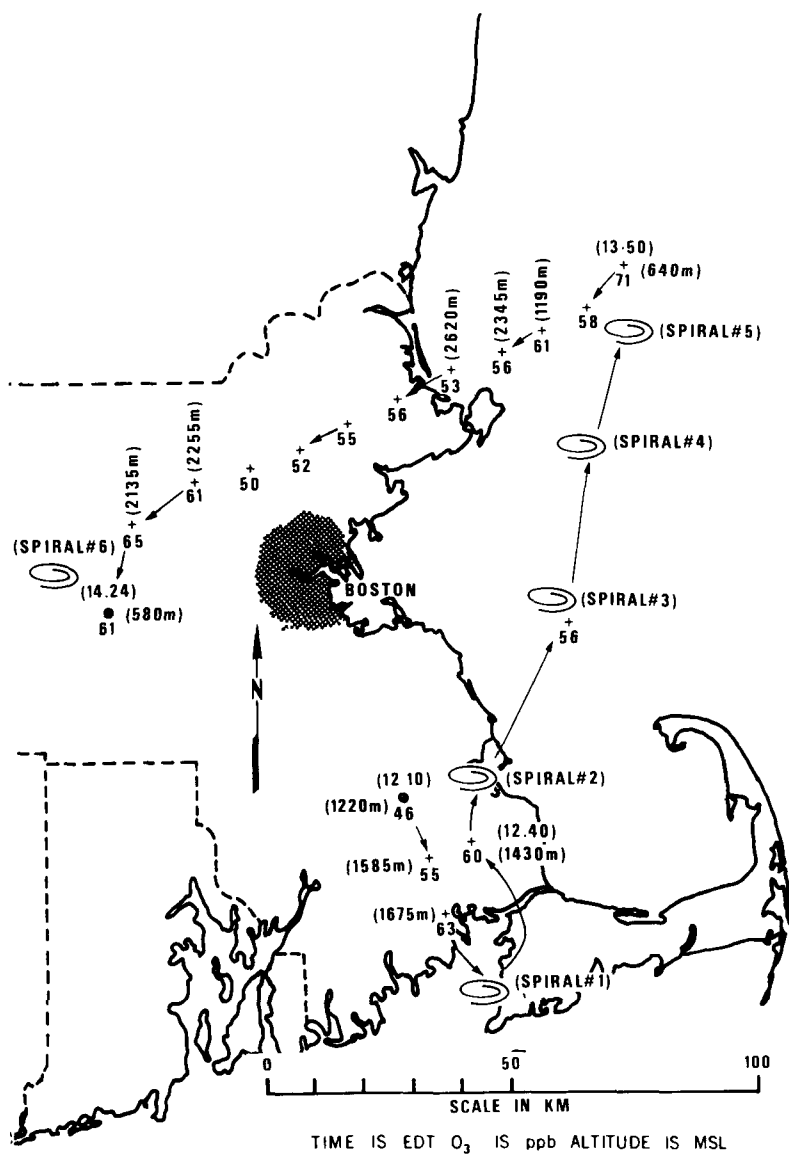


Figure 16. Flight #3 (August 11, 1975): Flight pattern and ozone distribution map

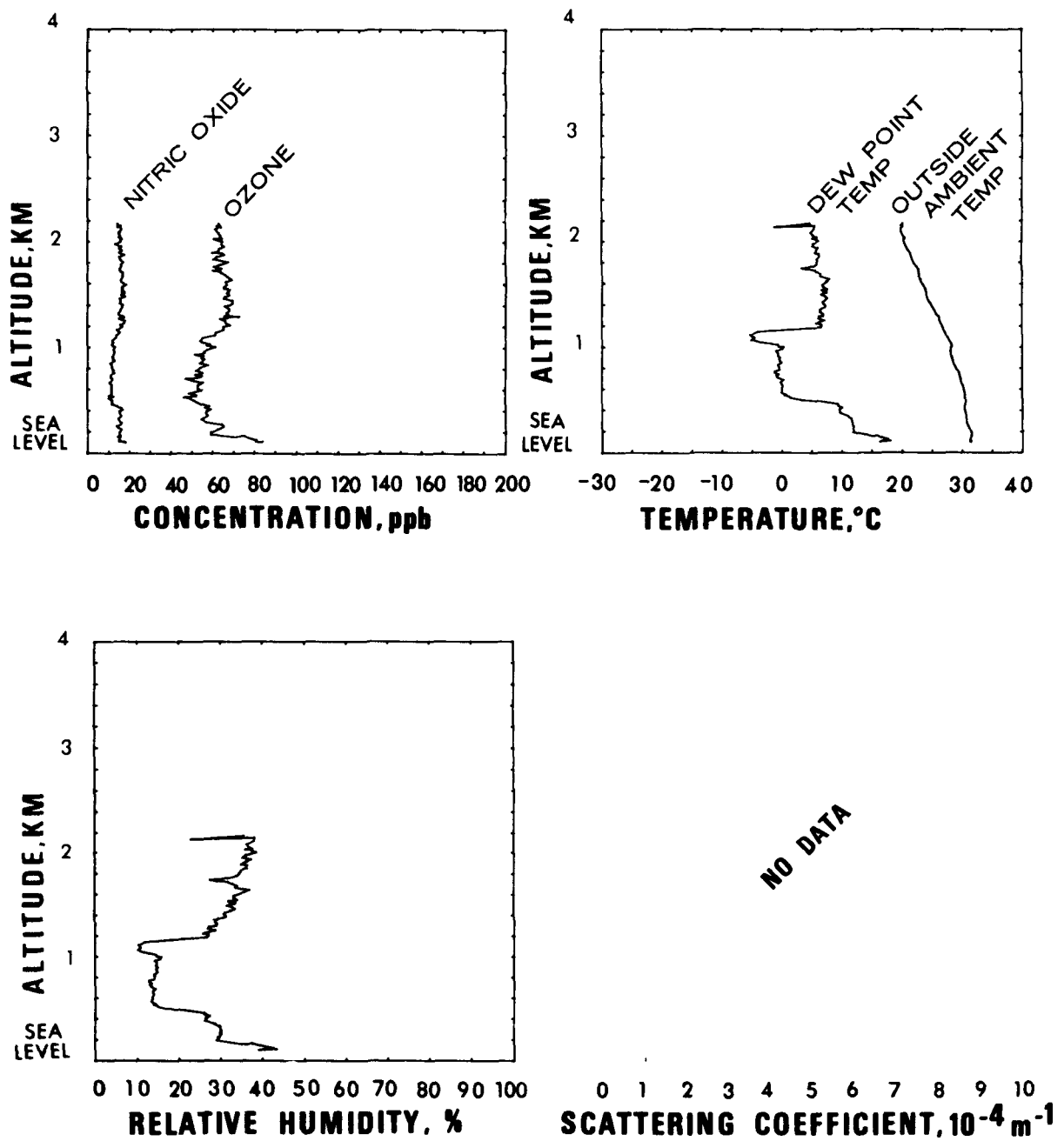


Figure 17. Flight #3: Vertical profiles of parameters for Spiral #1

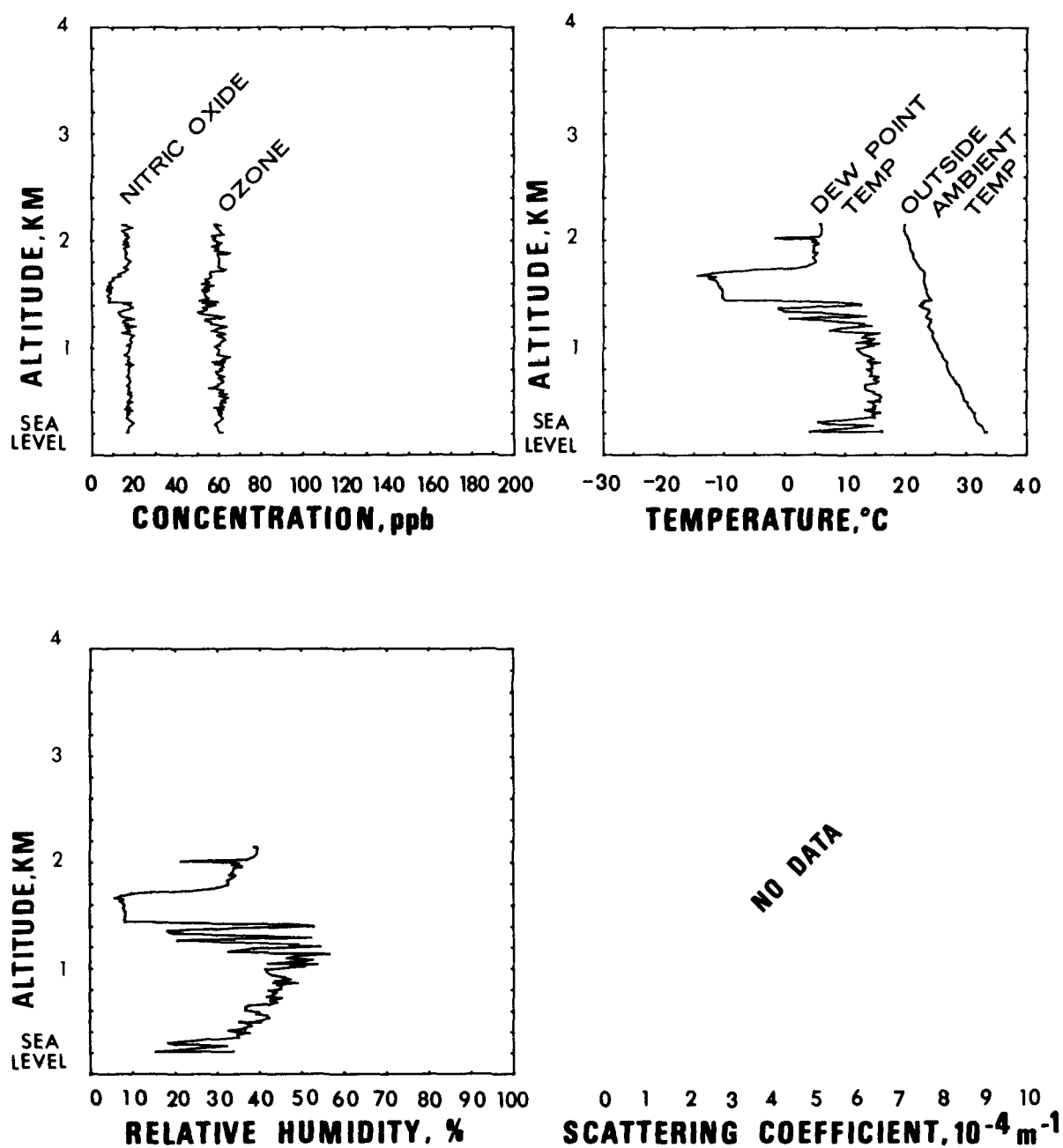


Figure 18. Flight #3: Vertical profiles of parameters for Spiral #2

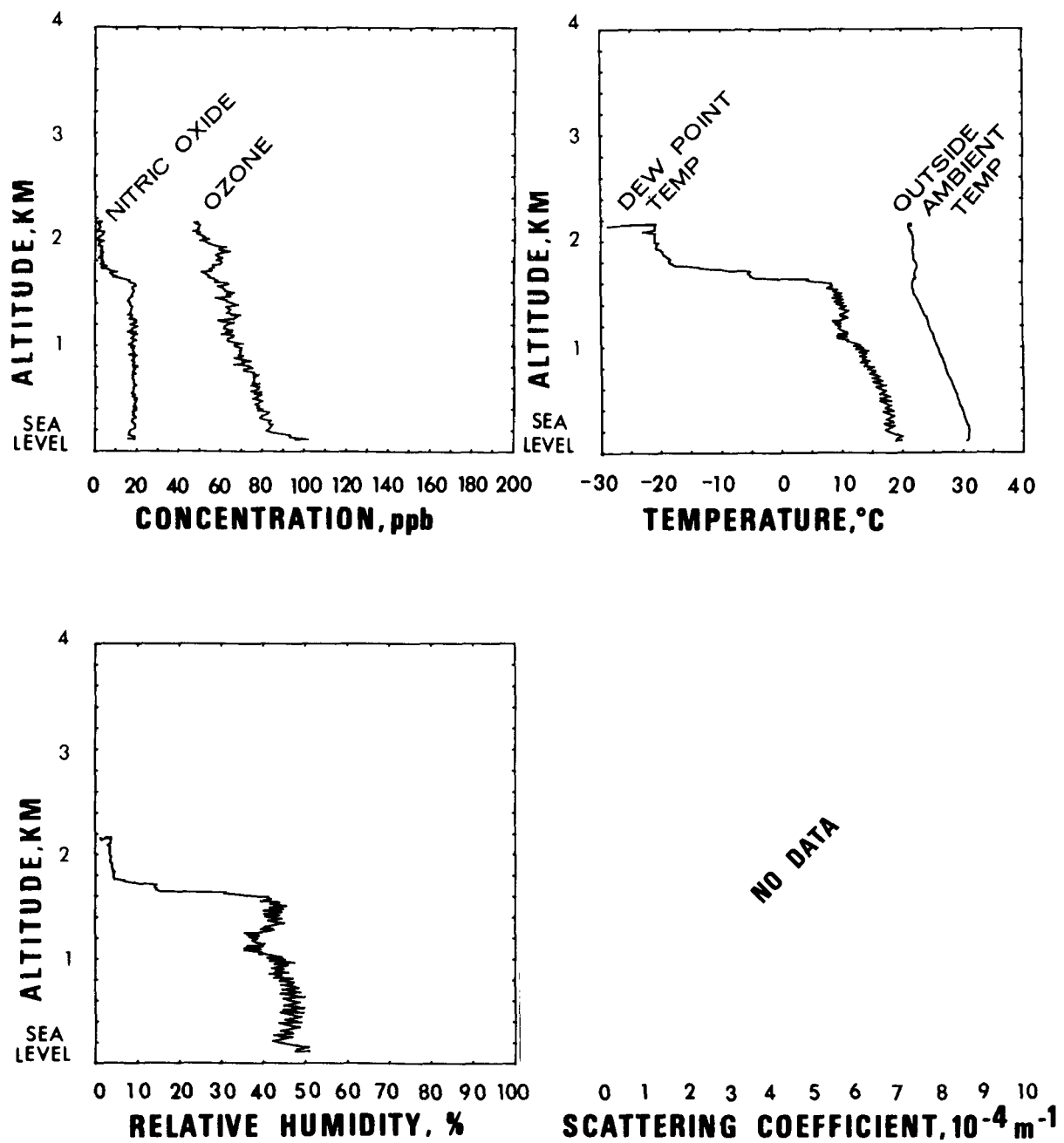


Figure 19. Flight #3: Vertical profiles of parameters for Spiral #3

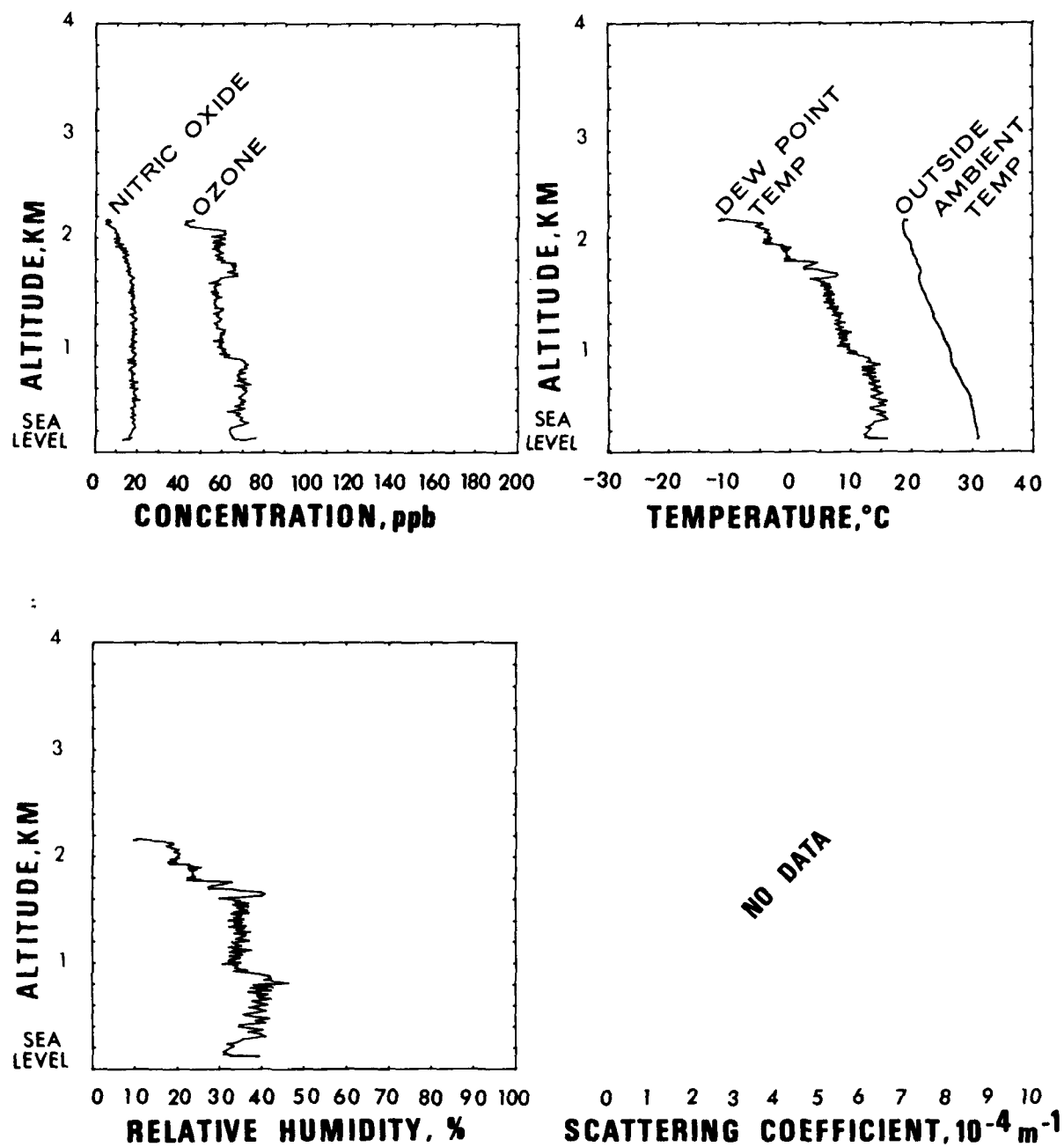


Figure 20. Flight #3: Vertical profiles of parameters for Spiral #4

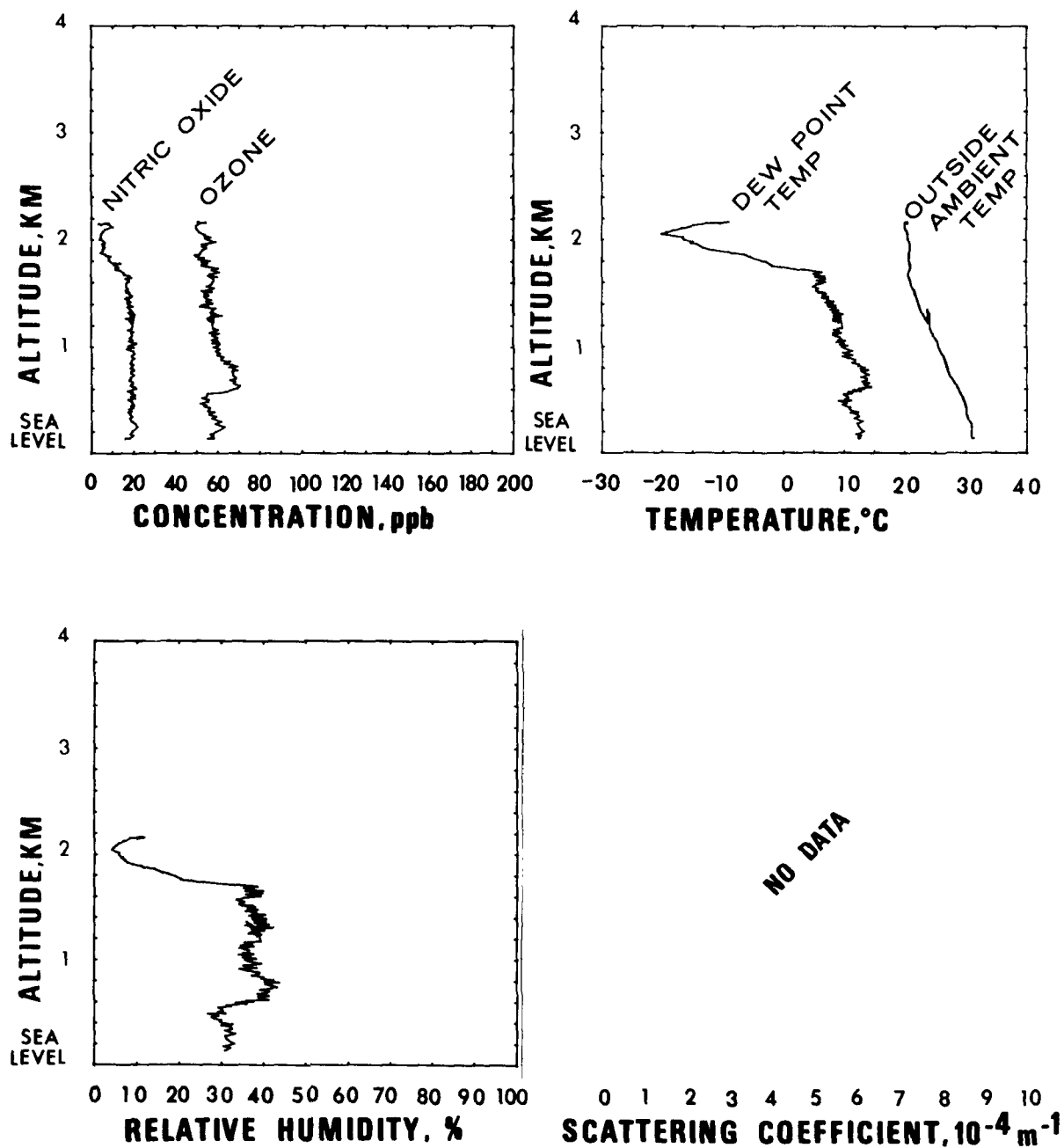


Figure 21. Flight #3: Vertical profiles of parameters for Spiral #5

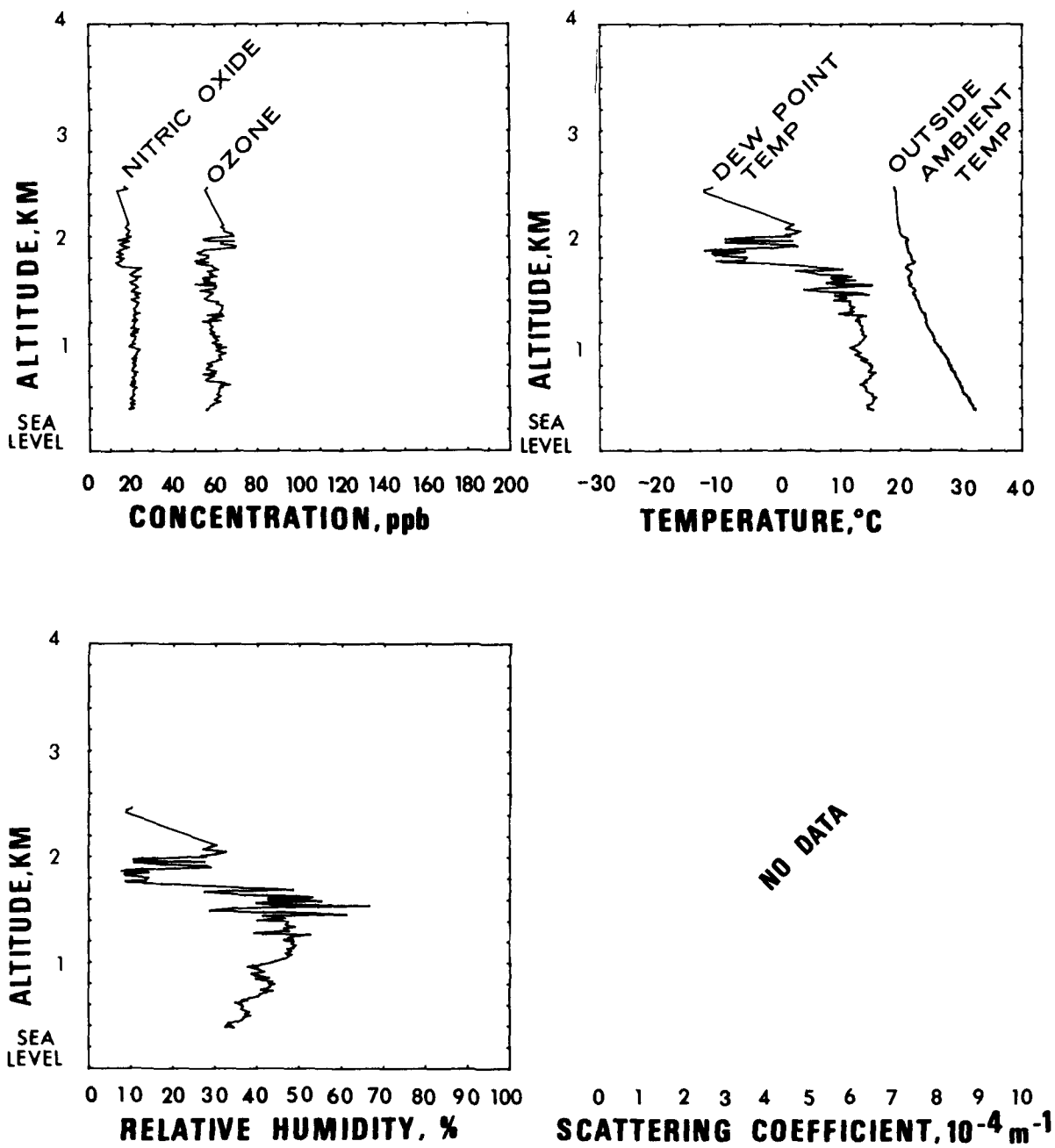


Figure 22. Flight #3: Vertical profiles of parameters for Spiral #6

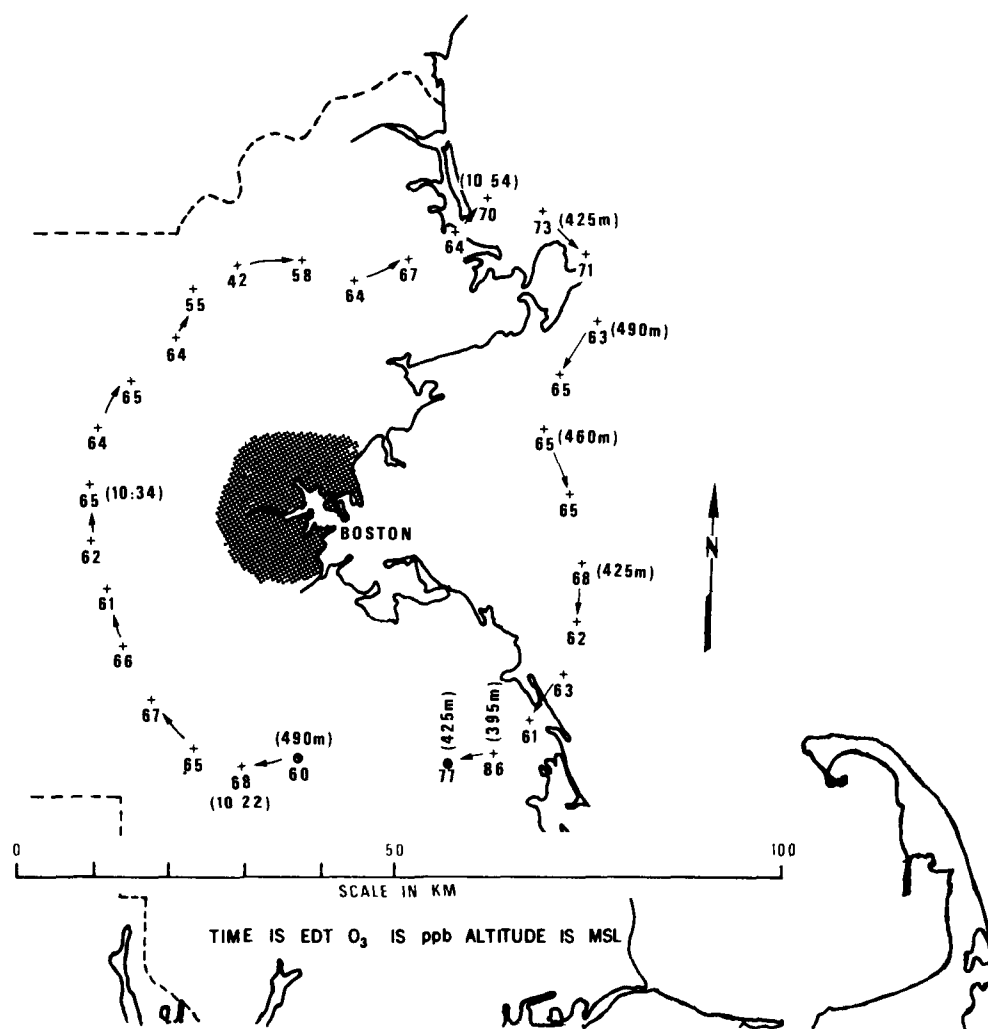


Figure 23. Flight #4 (August 12, 1975): Flight pattern and ozone distribution map

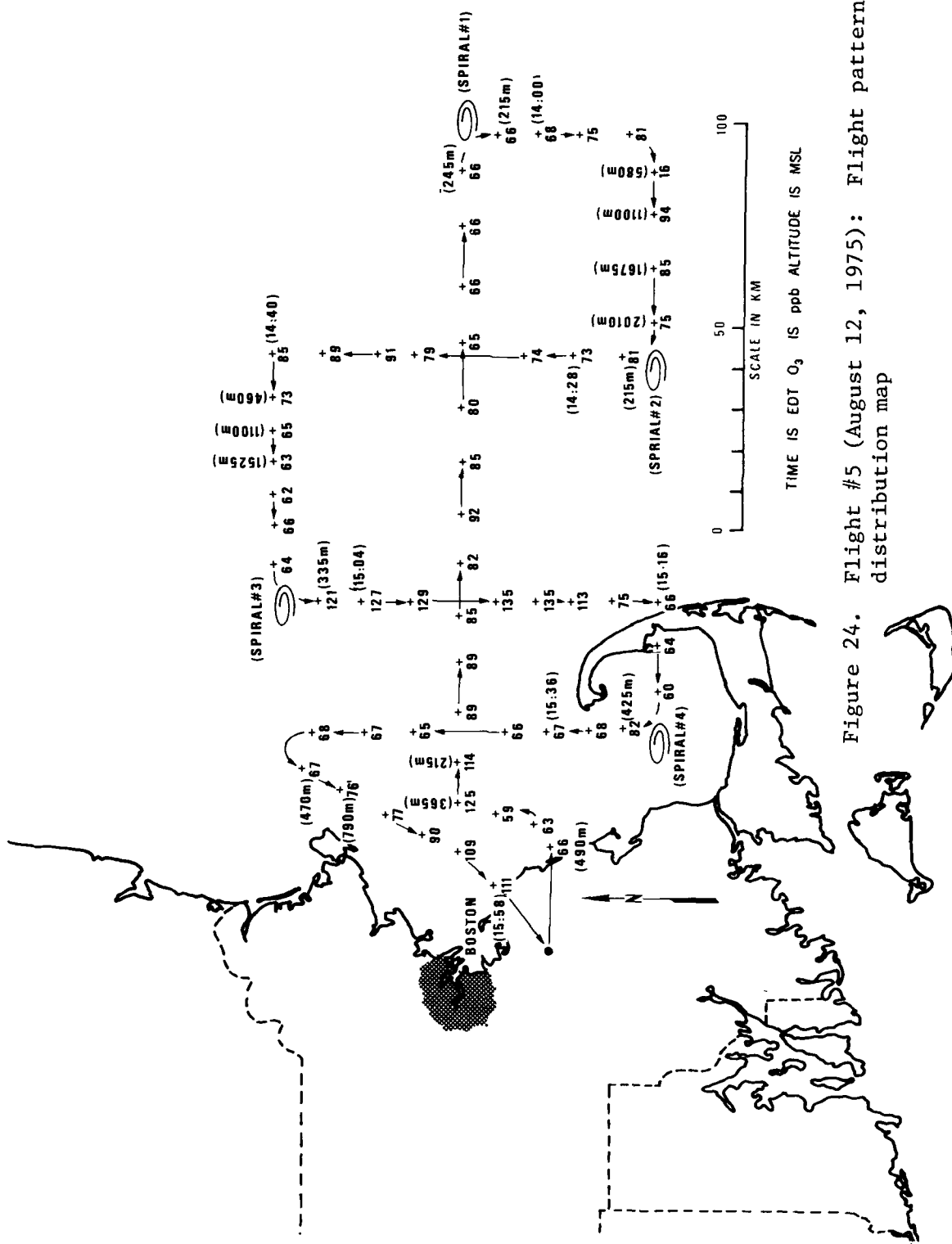


Figure 24. Flight #5 (August 12, 1975): Flight pattern and ozone distribution map

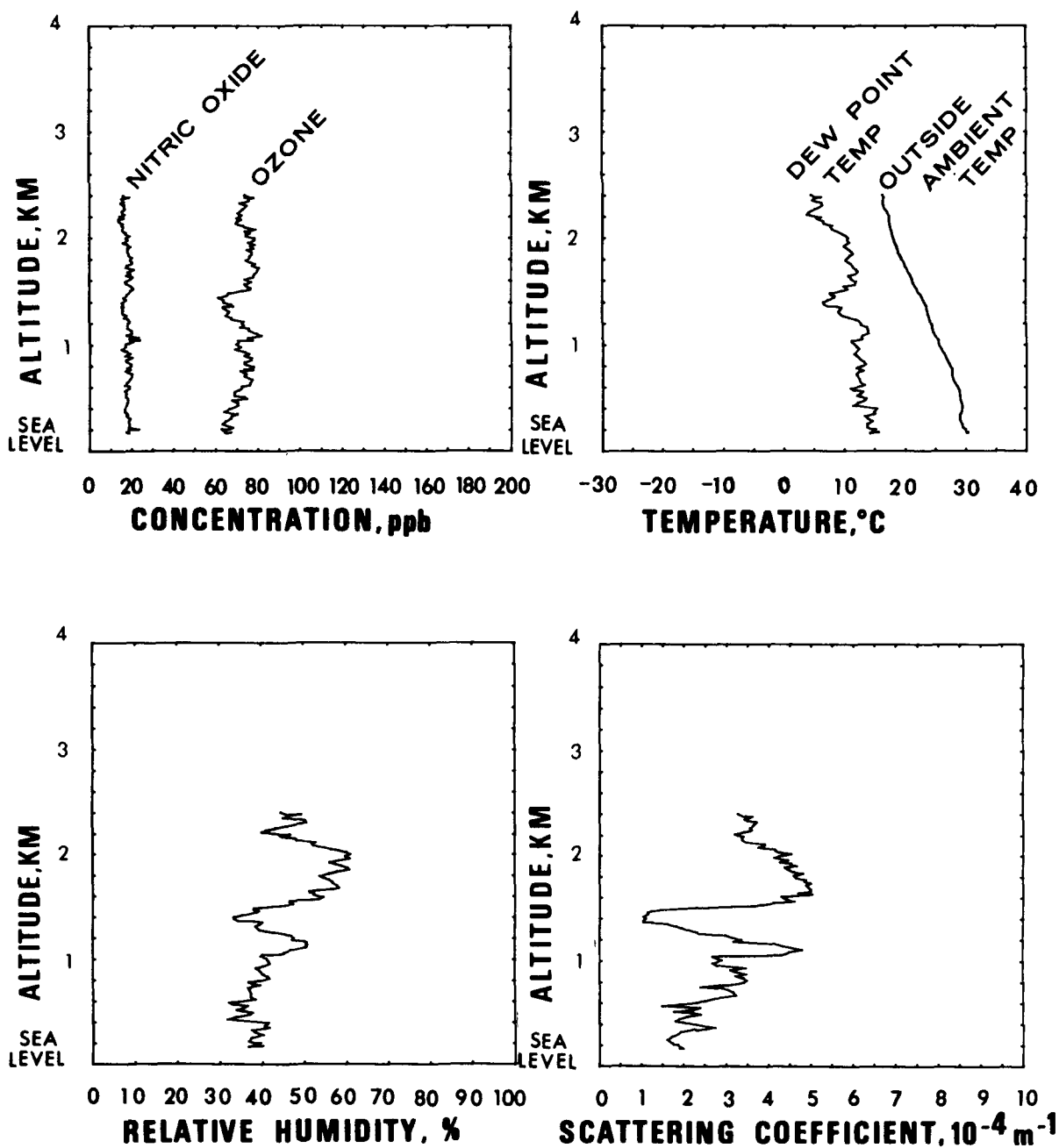


Figure 25. Flight #5: Vertical profiles of parameters for Spiral #1

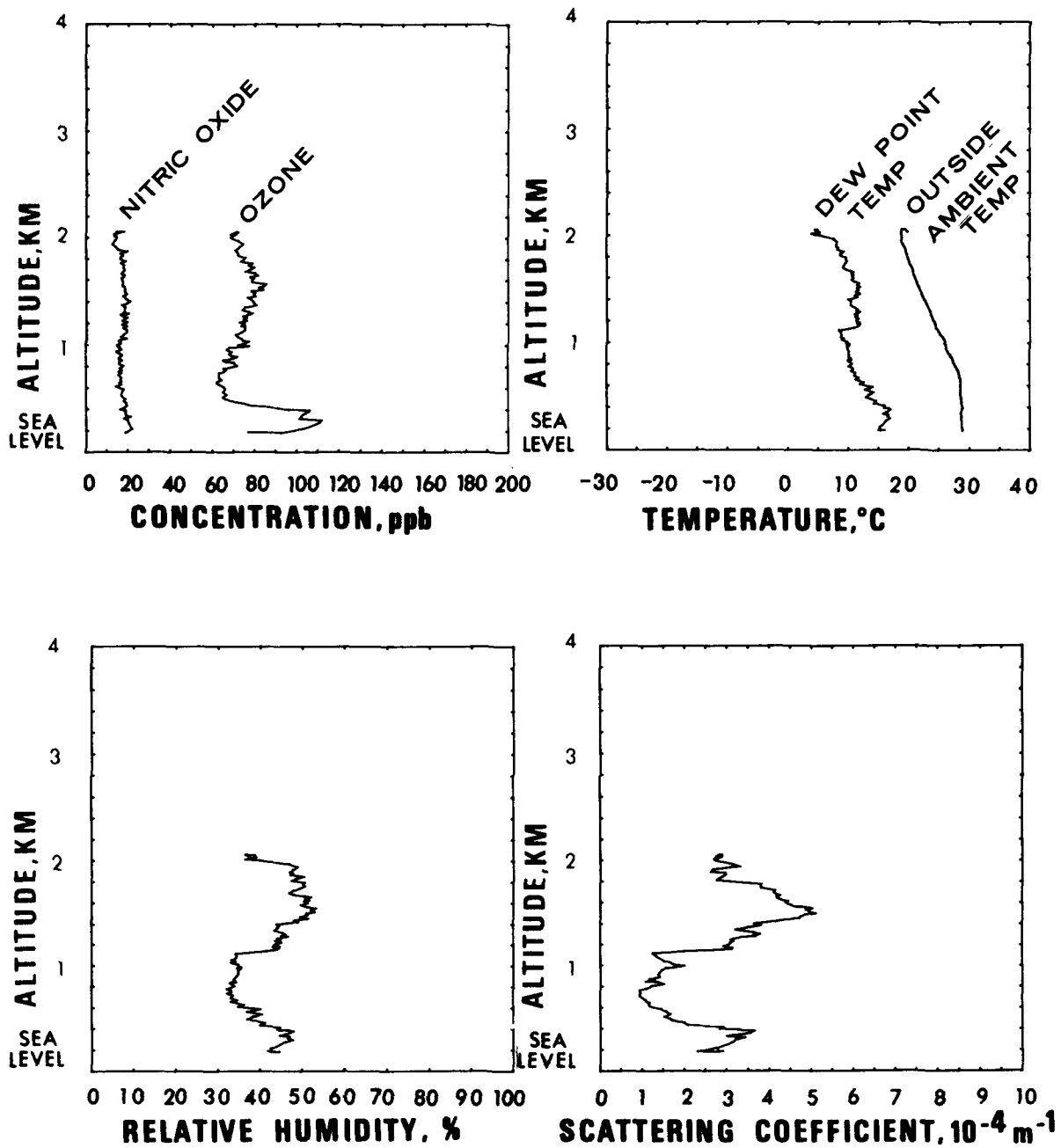


Figure 26. Flight #5: Vertical profiles of parameters for Spiral #2

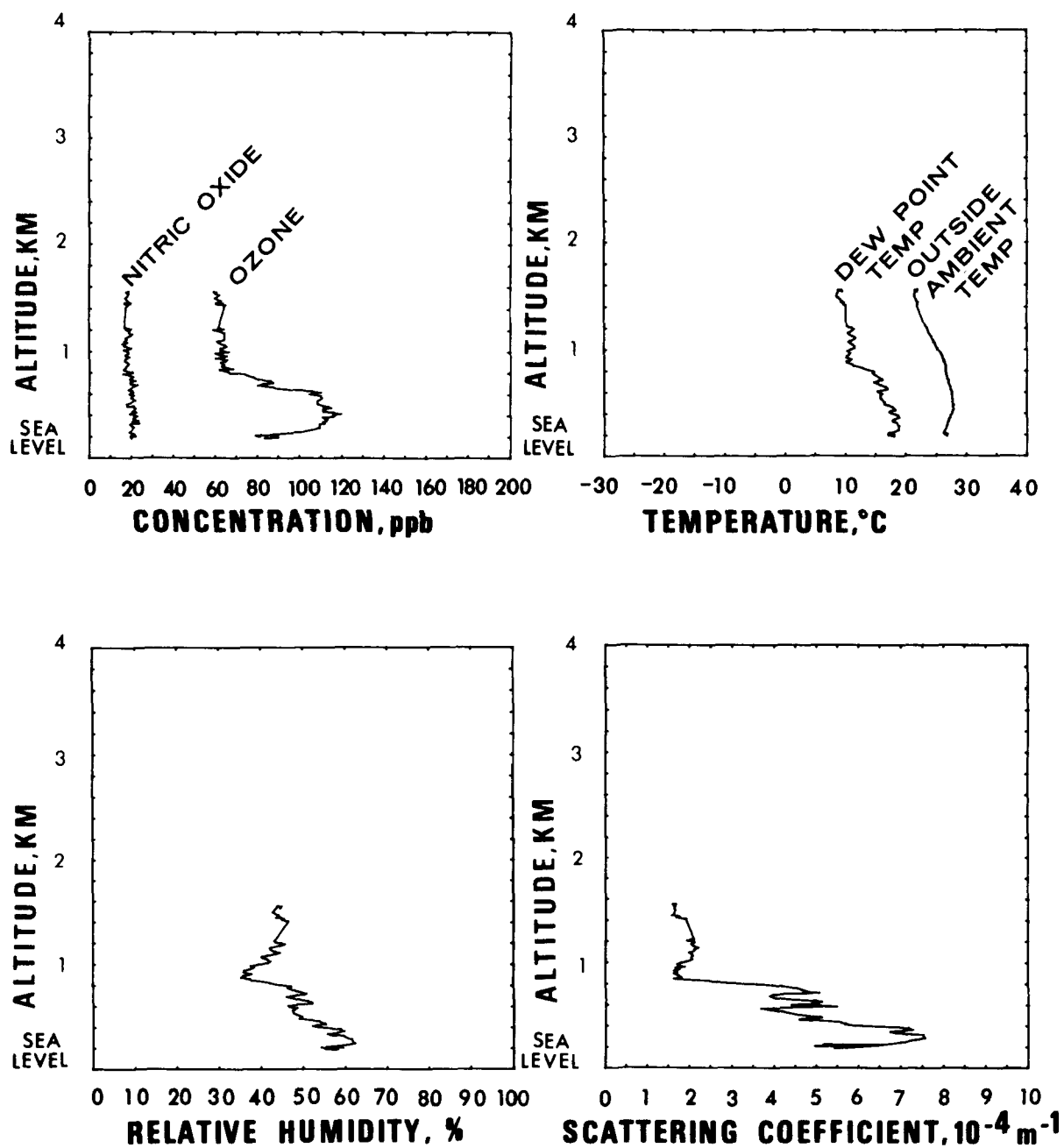


Figure 27. Flight #5: Vertical profiles of parameters for Spiral #3

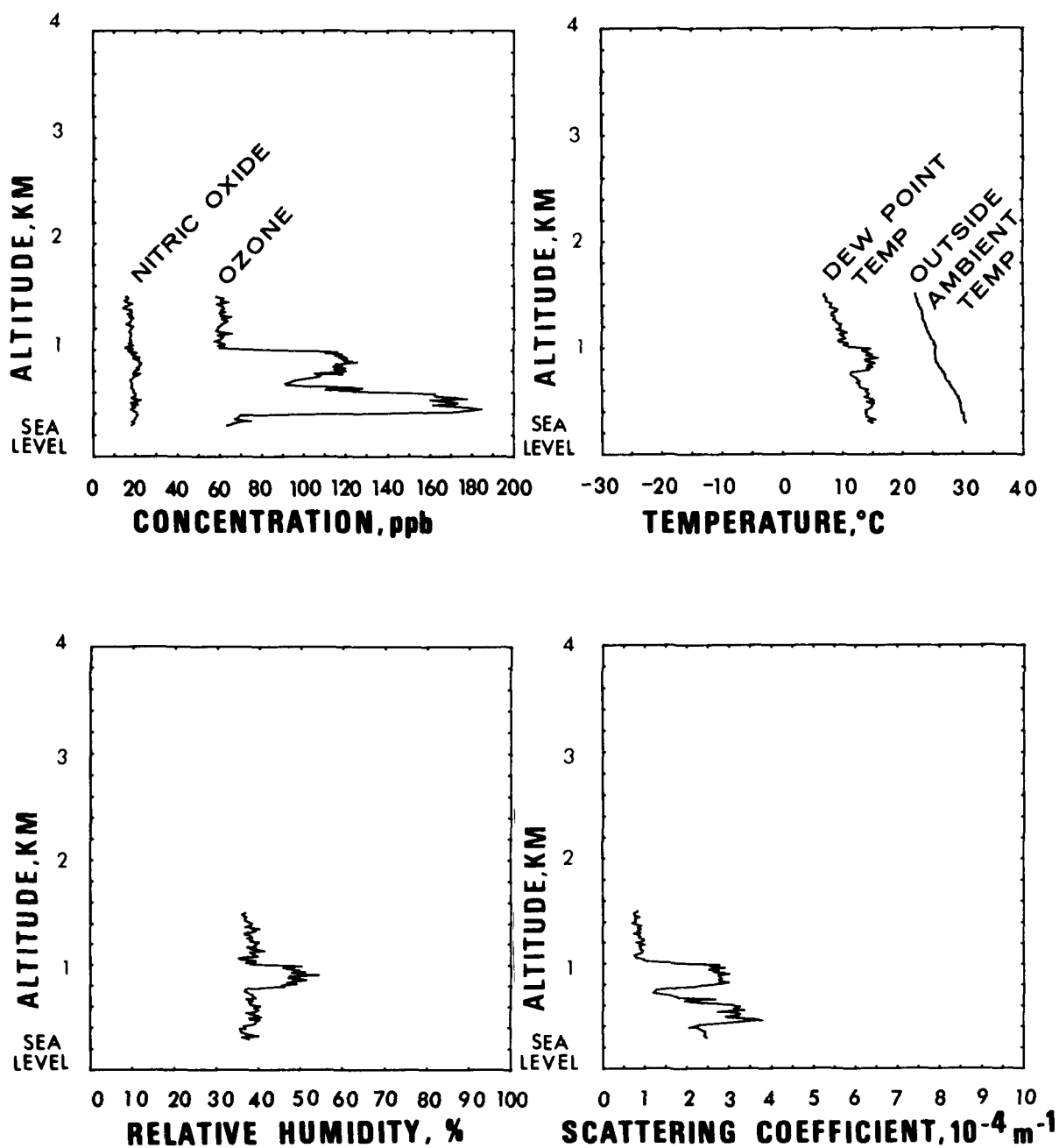
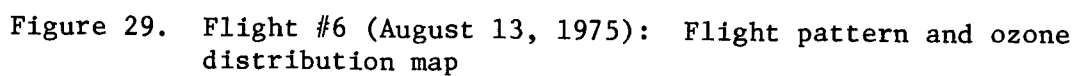


Figure 28. Flight #5: Vertical profiles of parameters for Spiral #4



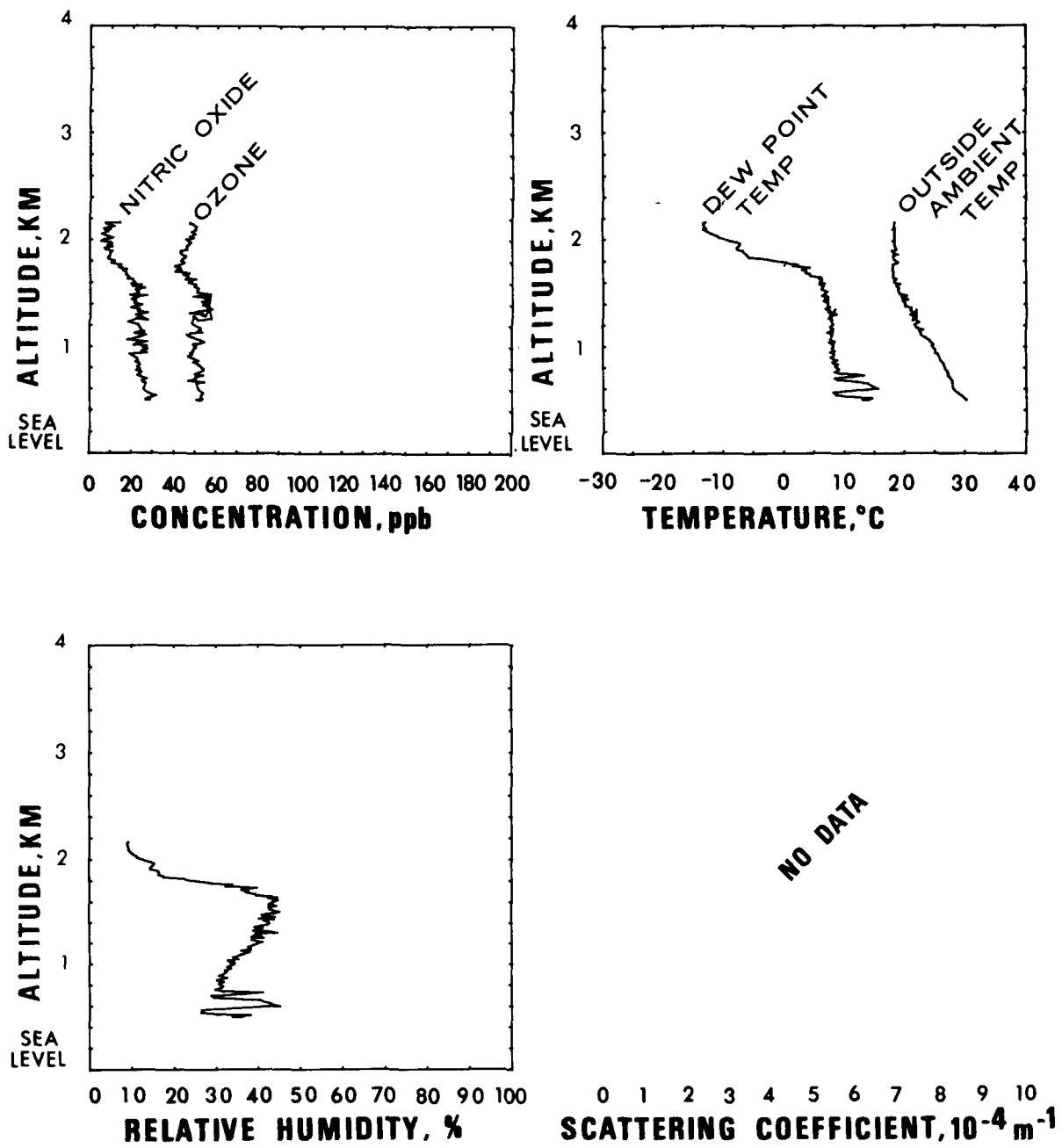


Figure 30. Flight #6: Vertical profiles of parameters for Spiral #1

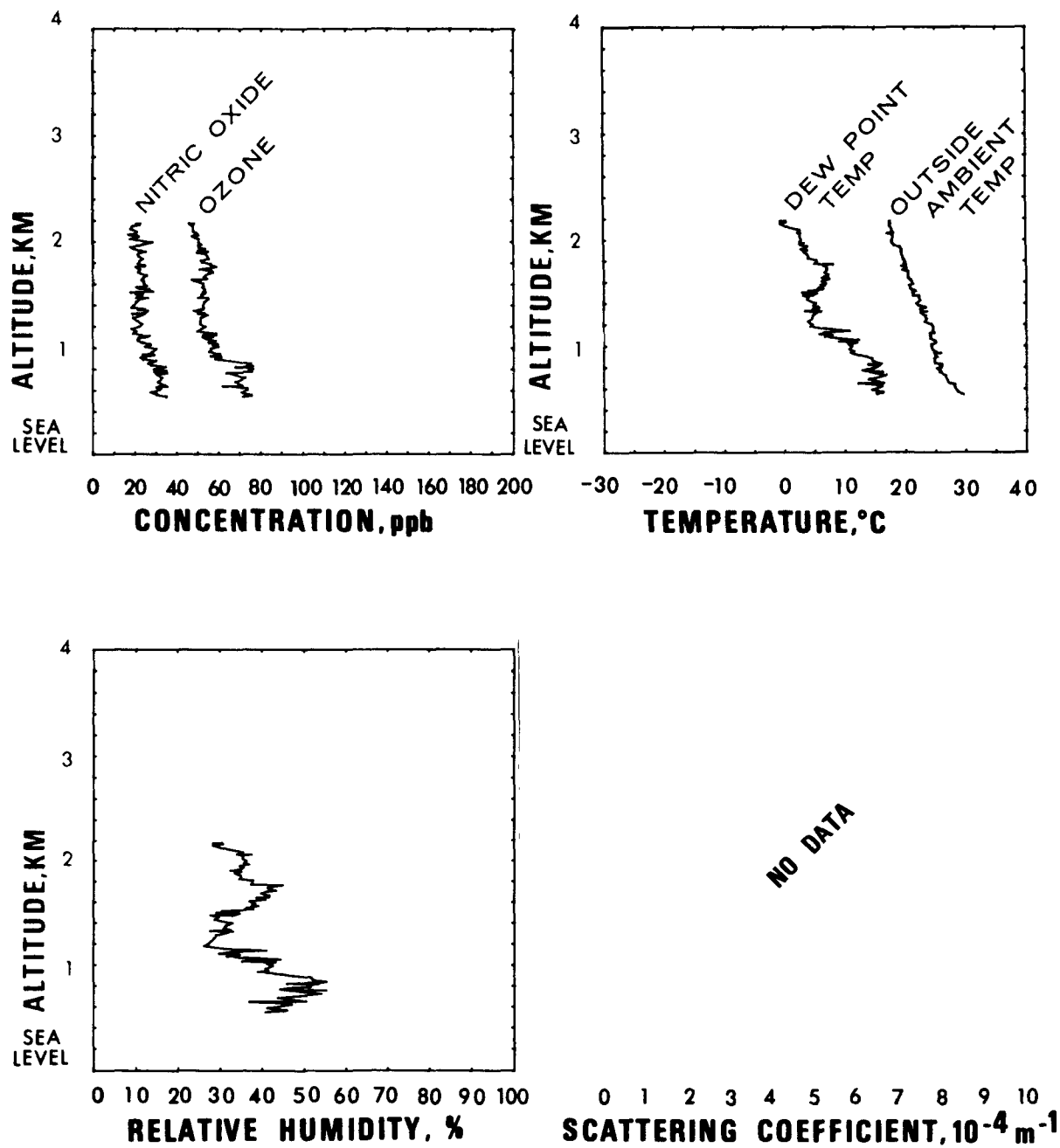


Figure 31. Flight #6: Vertical profiles of parameters for Spiral #2

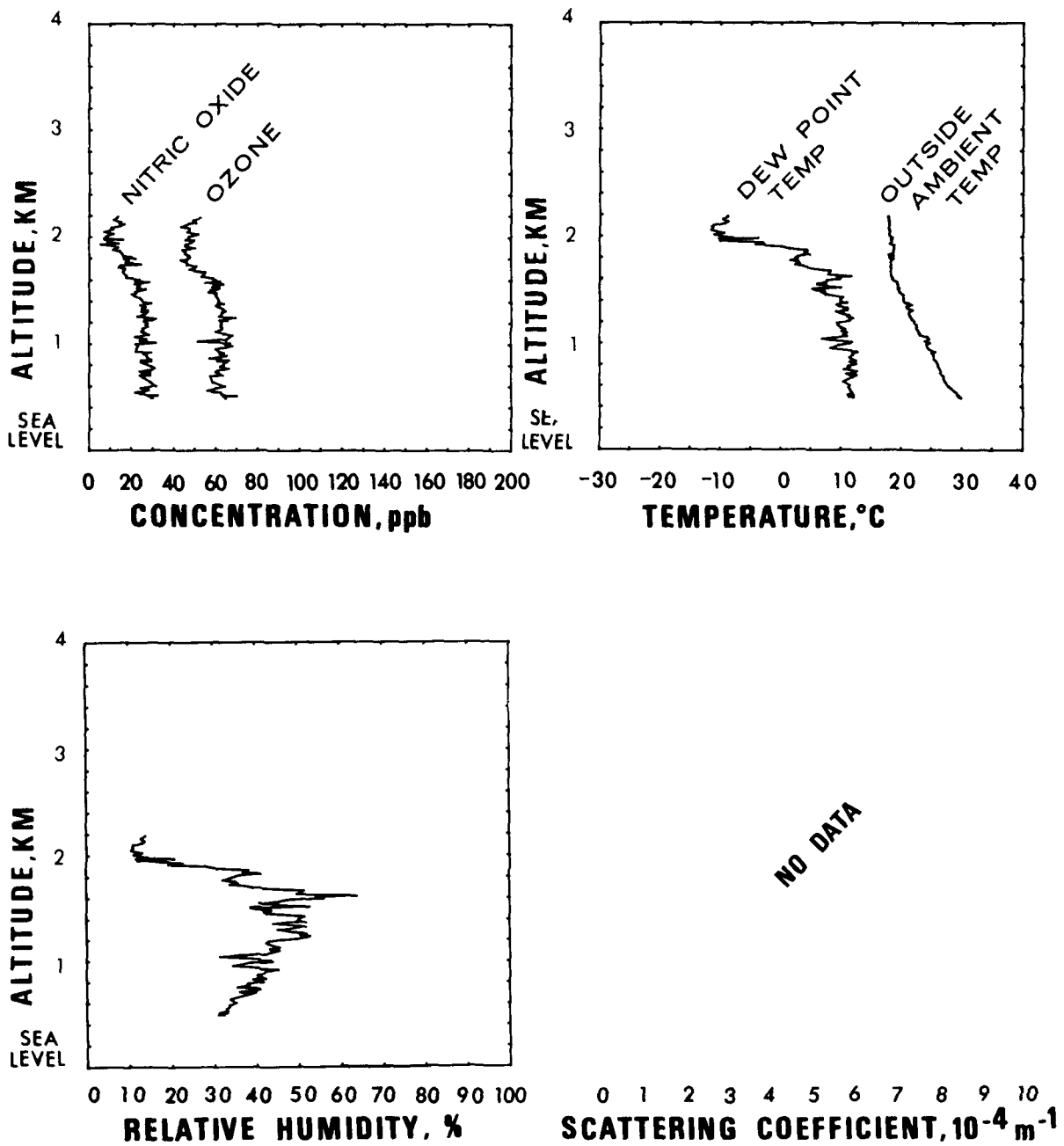


Figure 32. Flight #6: Vertical profiles of parameters for Spiral #3

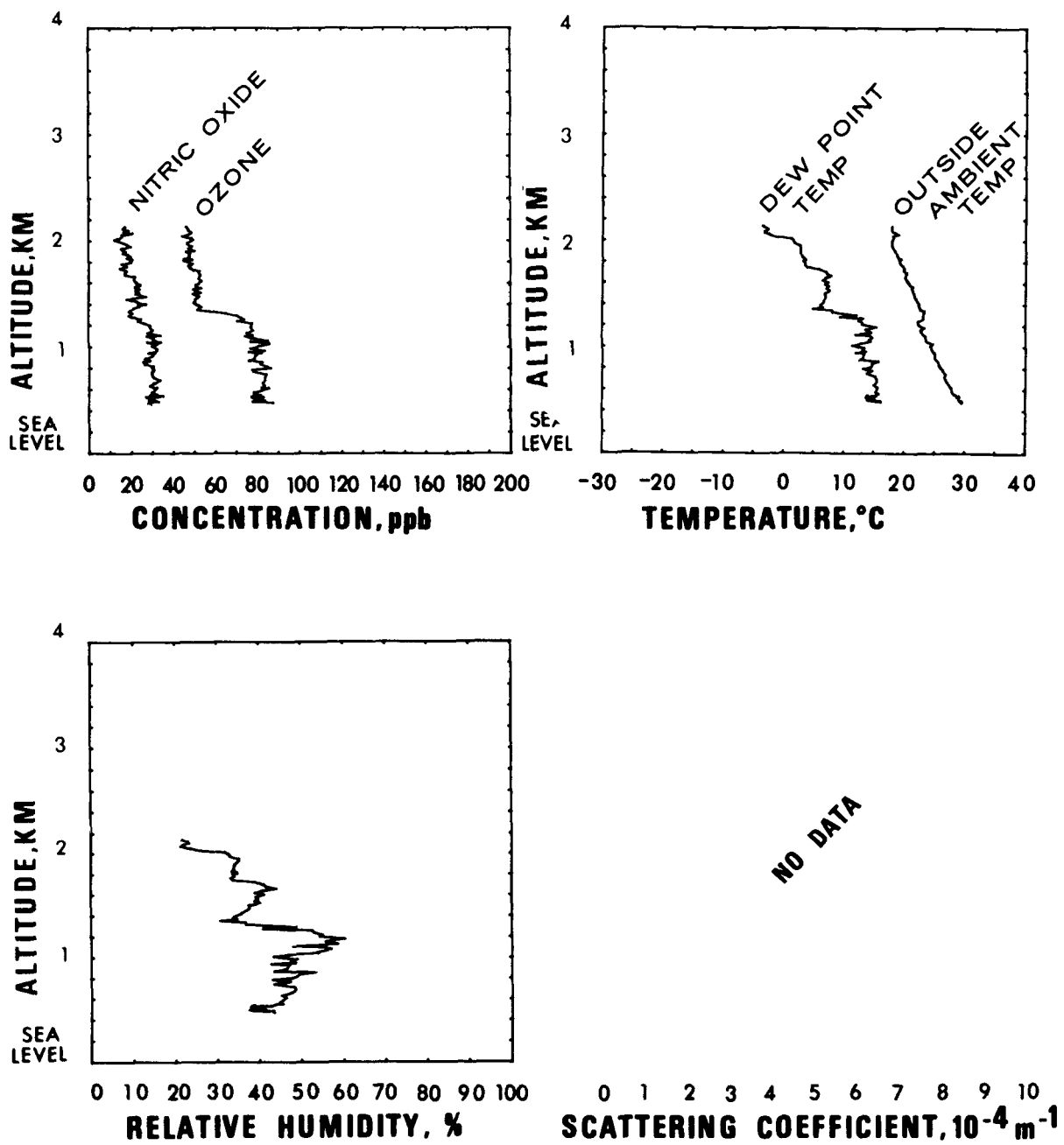


Figure 33. Flight #6: Vertical profiles of parameters for Spiral #4

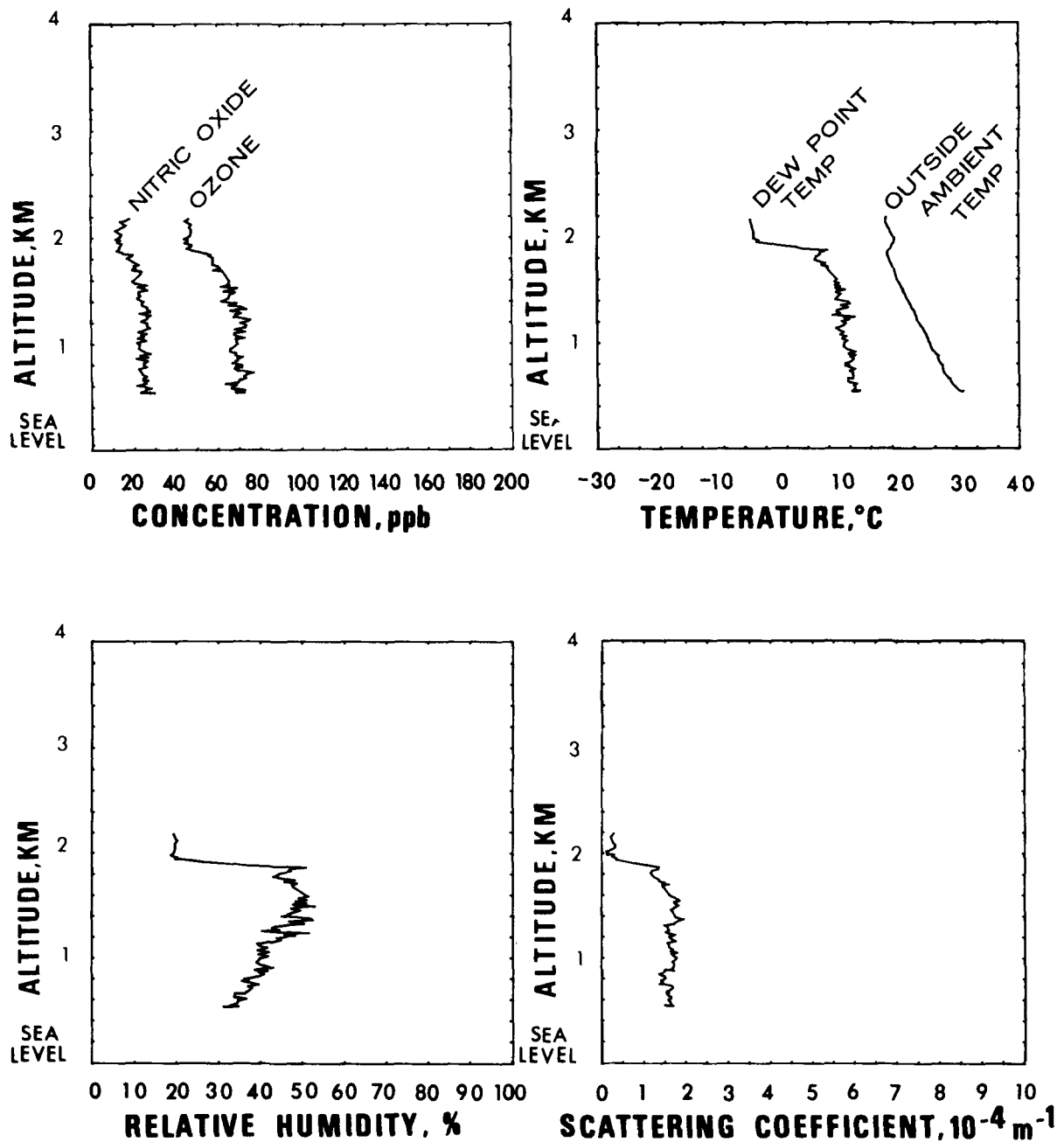


Figure 35. Flight #7: Vertical profiles of parameters for Spiral #1

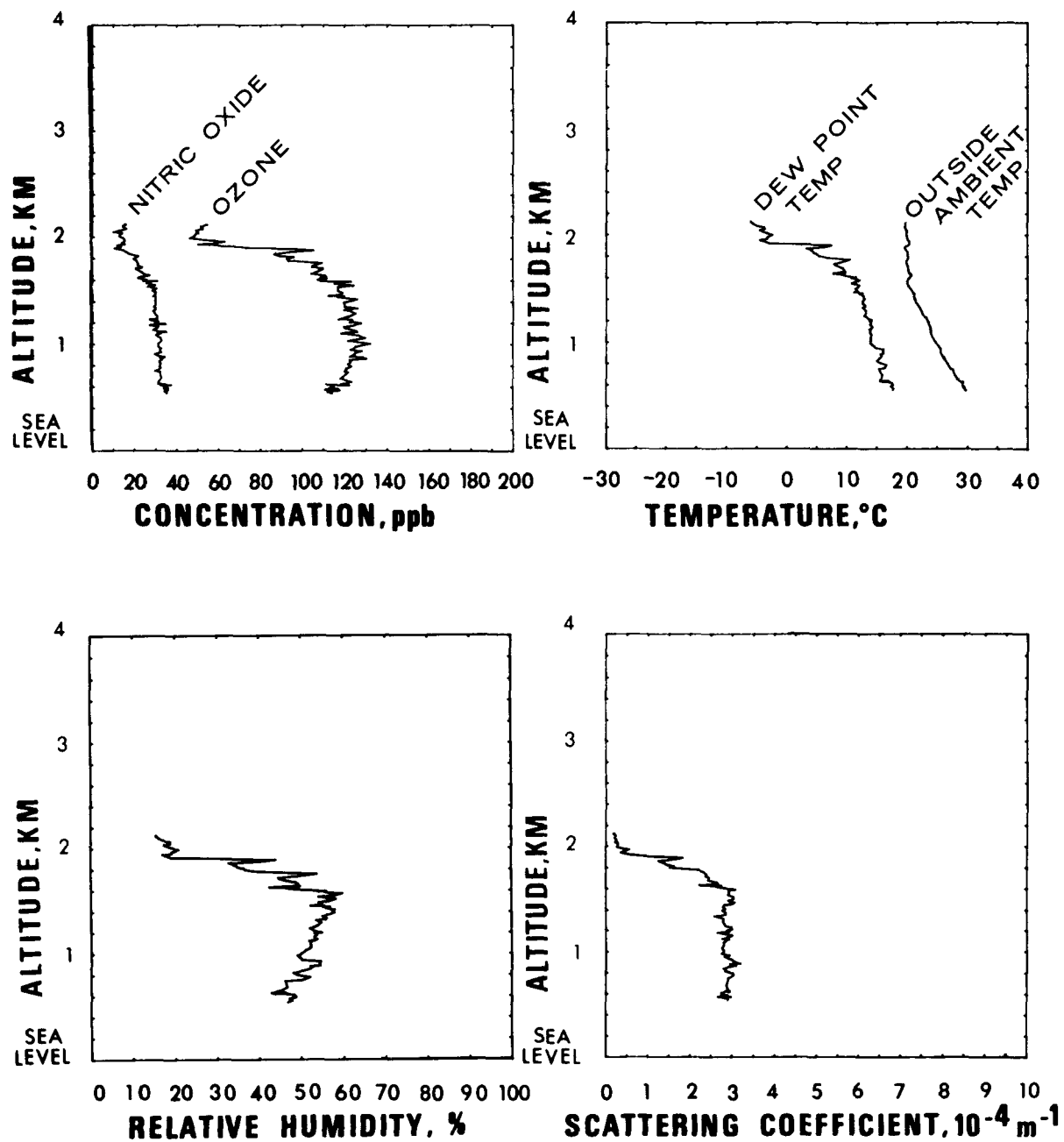


Figure 36. Flight #7: Vertical profiles of parameters for Spiral #2

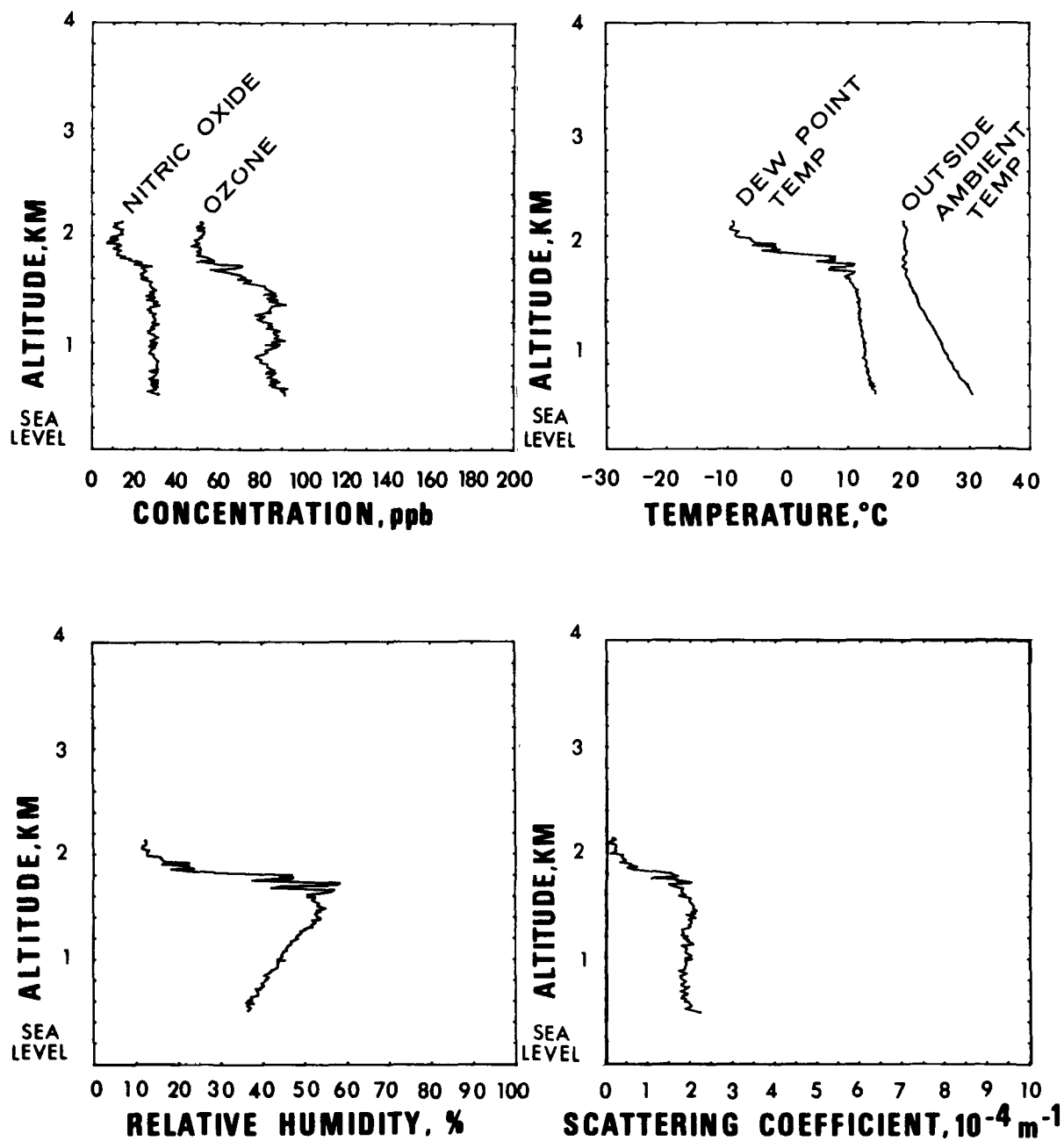


Figure 37. Flight #7: Vertical profiles of parameters for Spiral #3

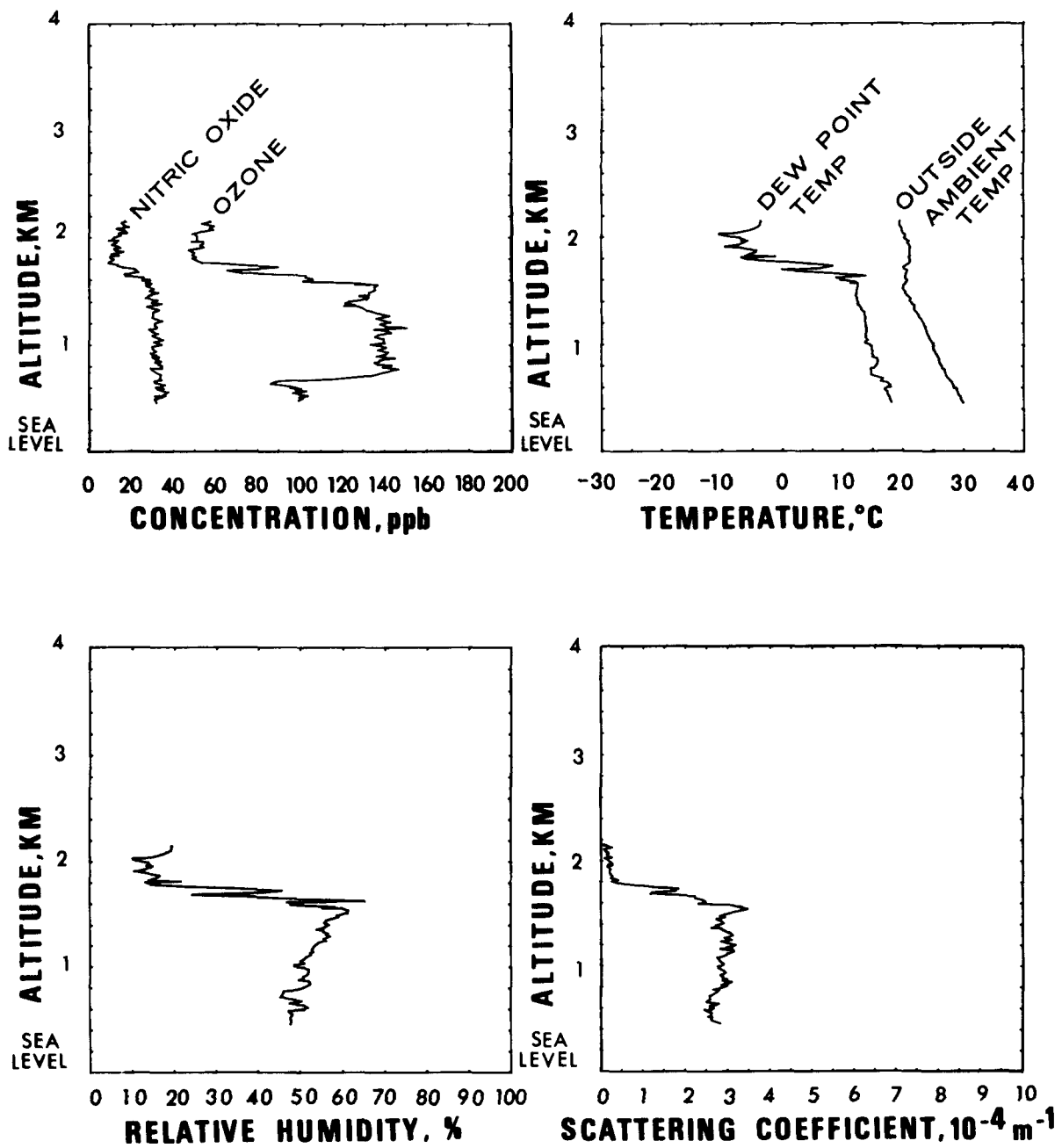


Figure 38. Flight #7: Vertical profiles of parameters for Spiral #4

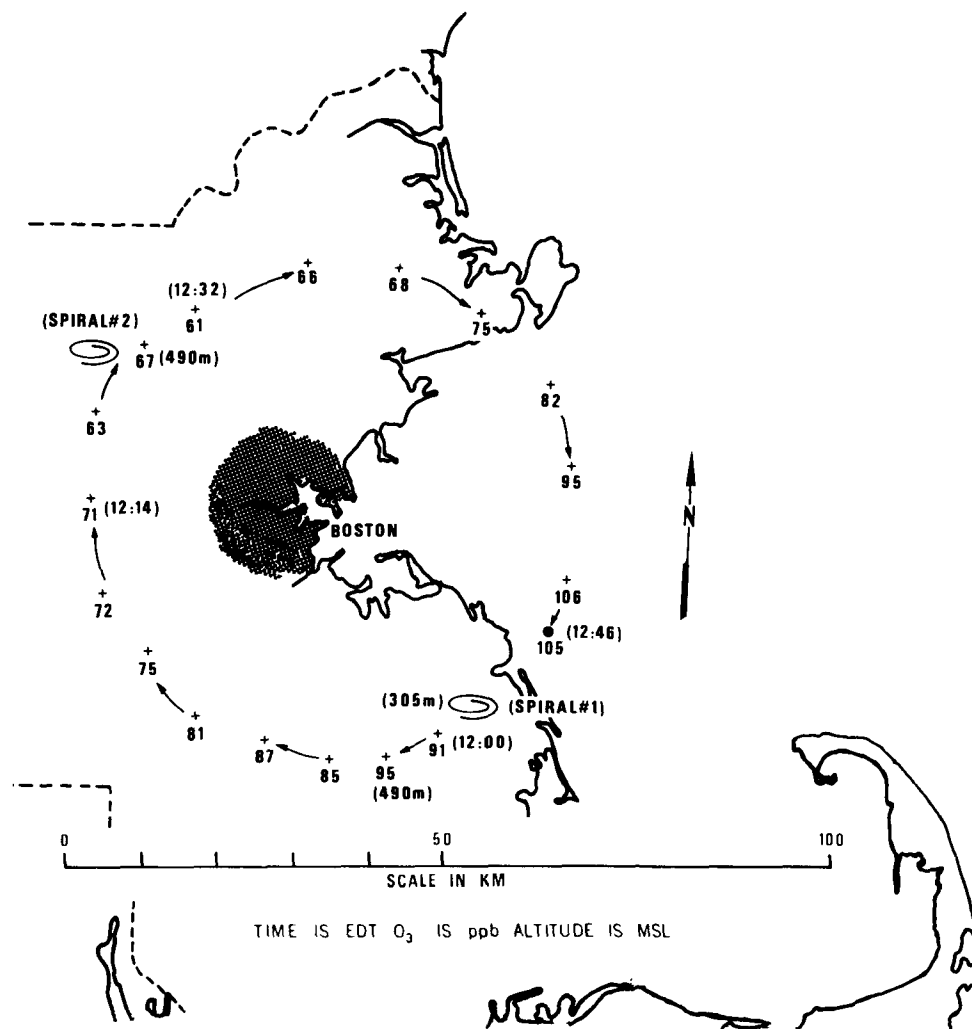


Figure 39. Flight #8 (August 14, 1975): Flight pattern and ozone distribution map

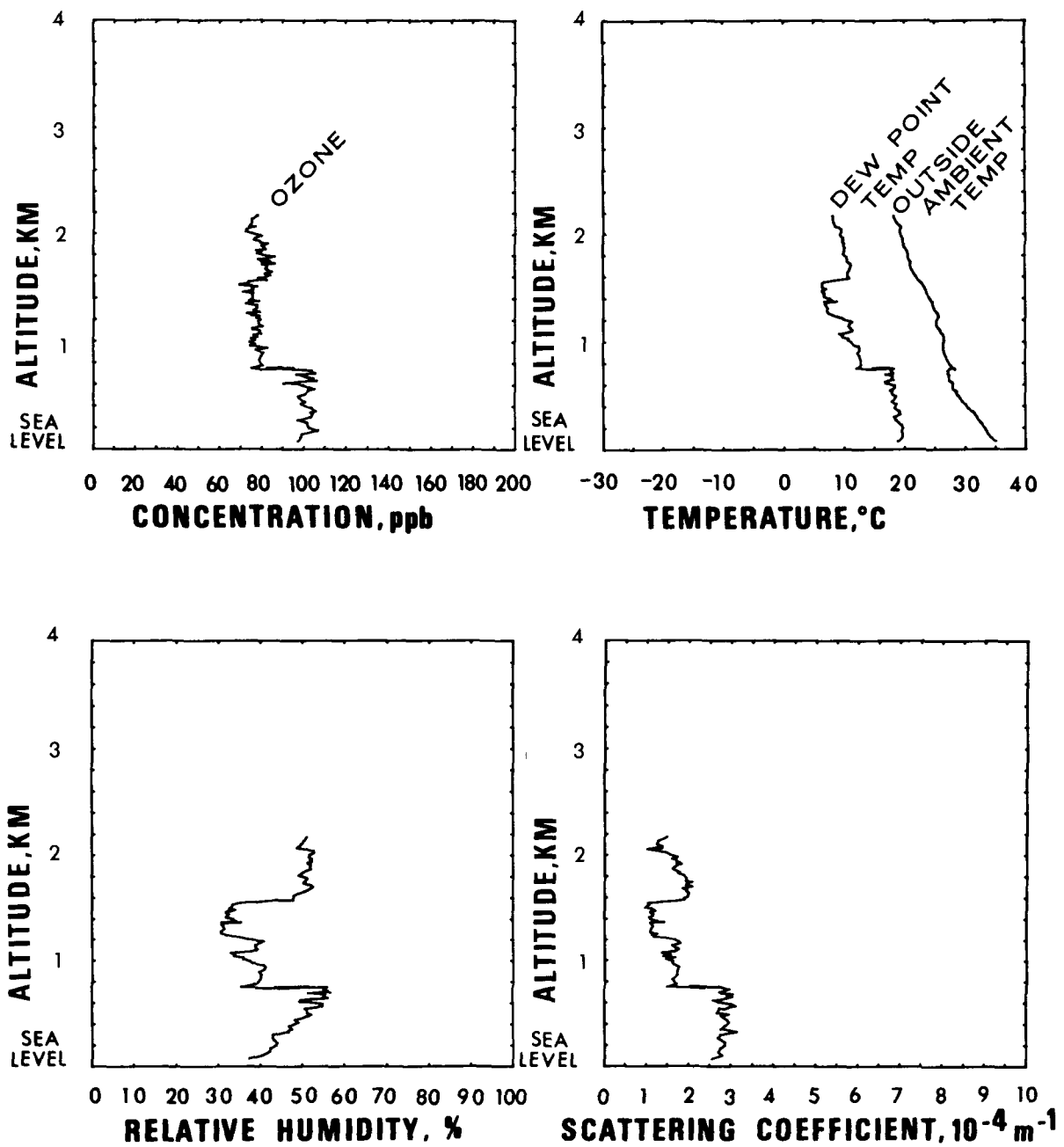


Figure 40. Flight #8: Vertical profiles of parameters for Spiral #1

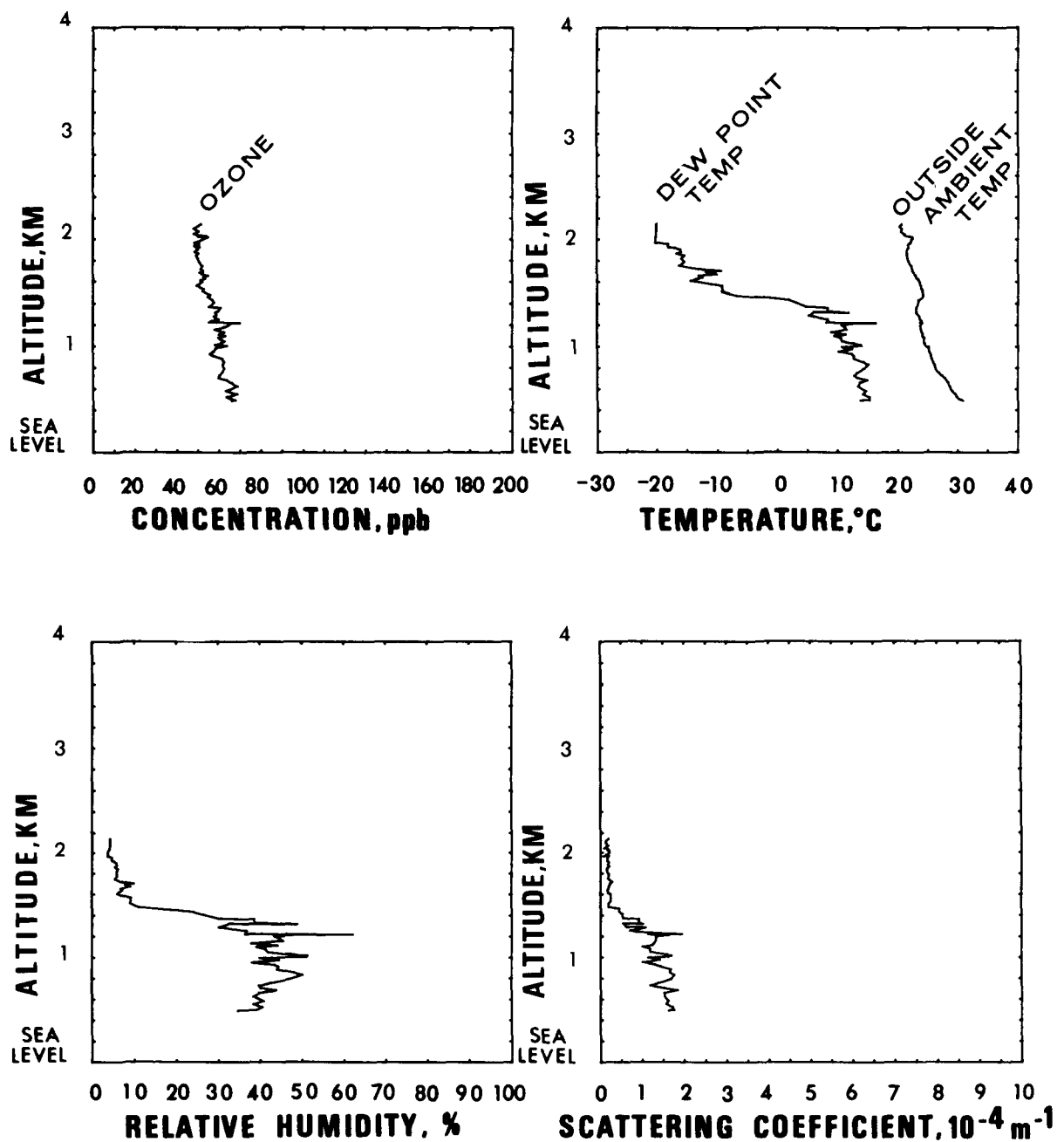


Figure 41. Flight #8: Vertical profiles of parameters for Spiral #2

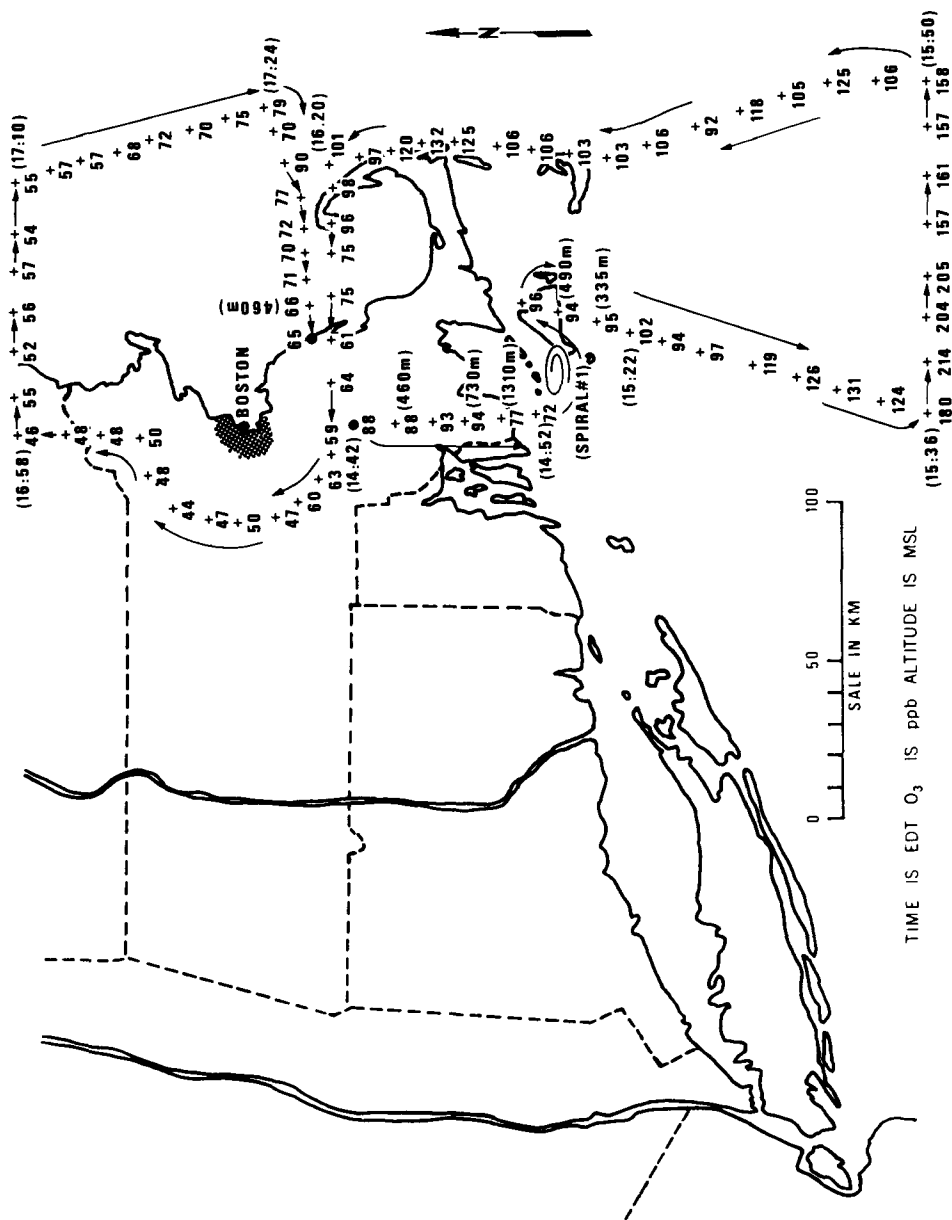


Figure 42. Flight #9 (August 14, 1975): Flight pattern and ozone distribution map

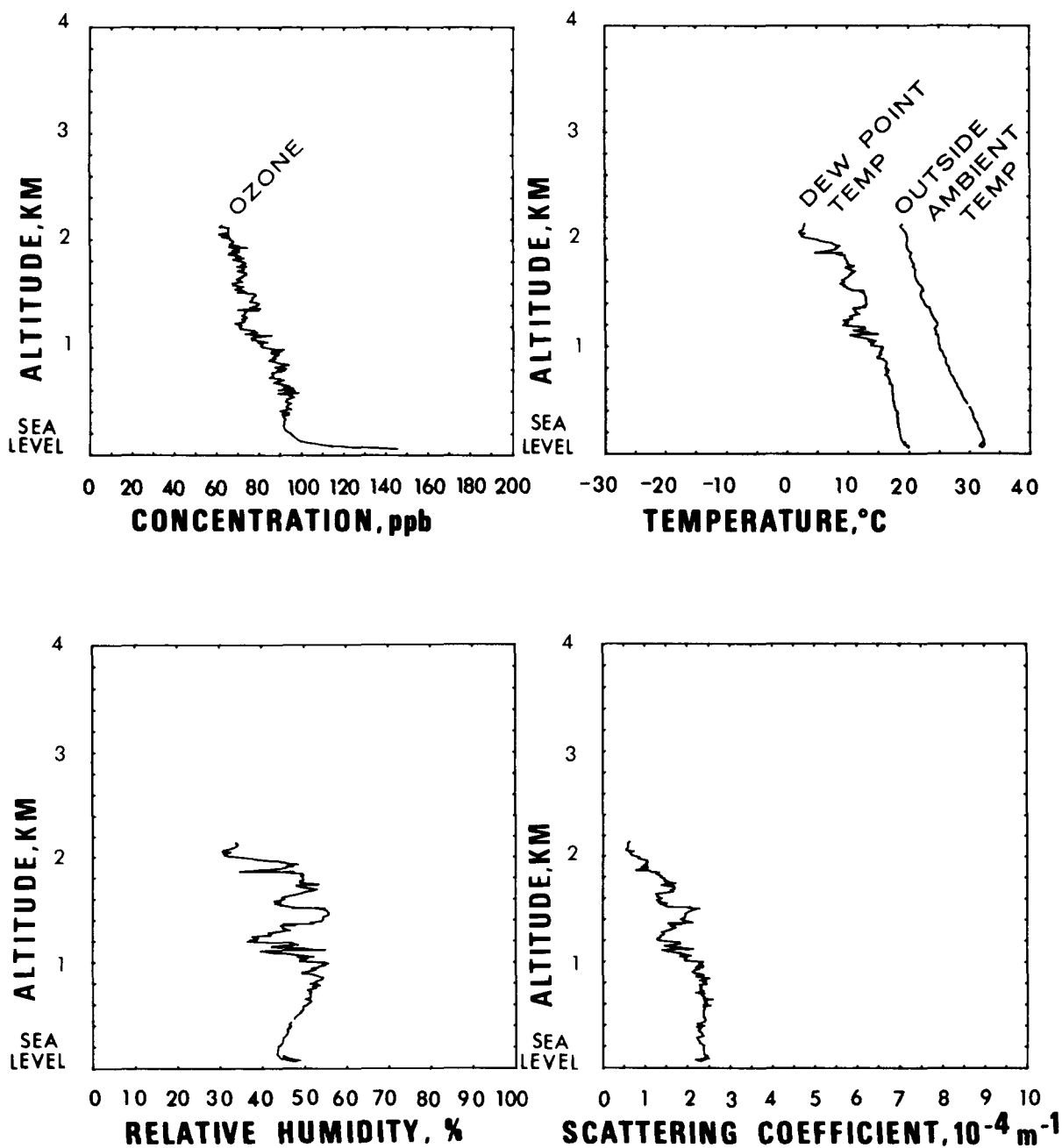


Figure 43. Flight #9: Vertical profiles of parameter for spiral #1

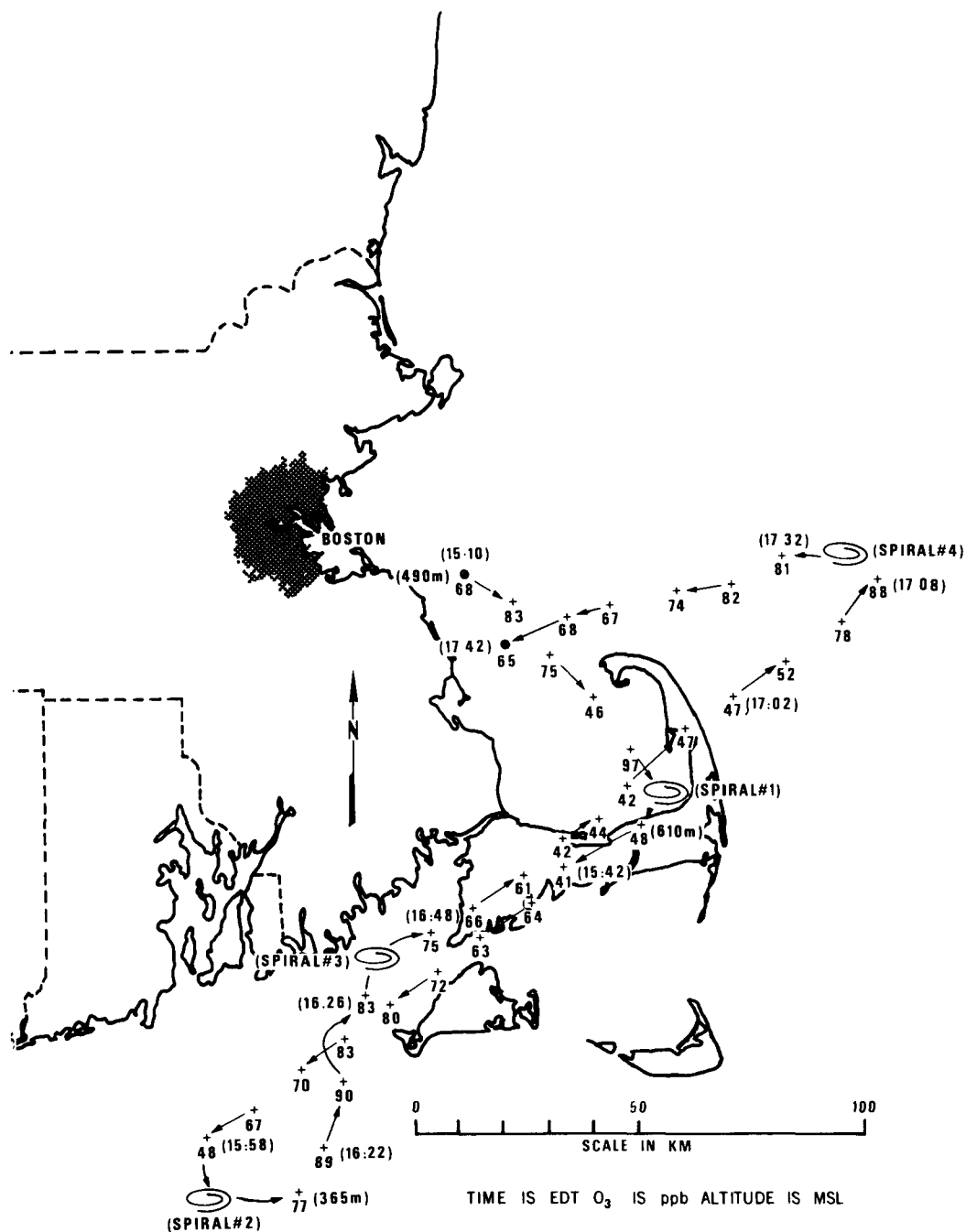


Figure 44. Flight #10 (August 15, 1975): Flight pattern and ozone distribution map

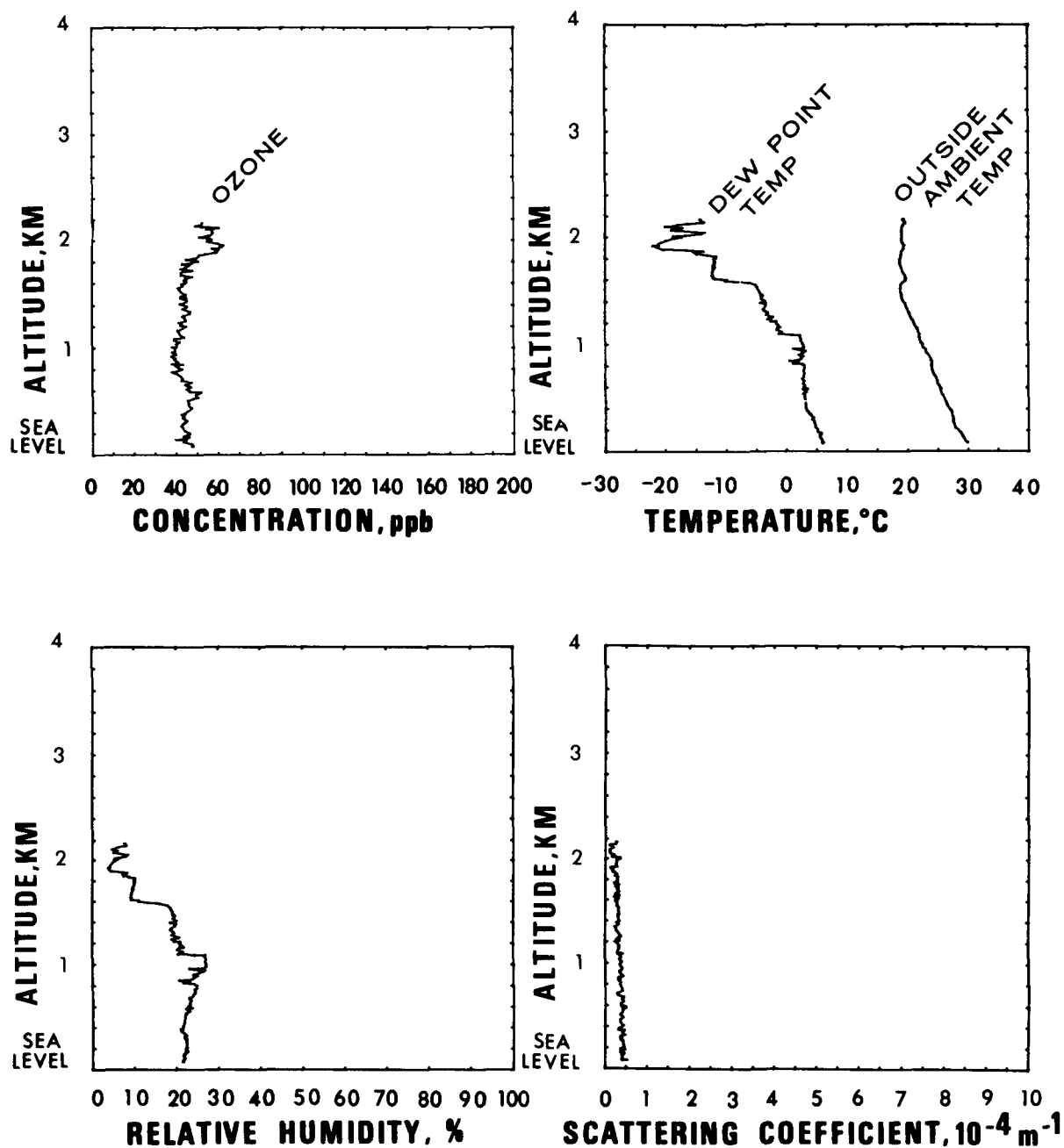


Figure 45. Flight #10: Vertical profiles of parameters for Spiral #1

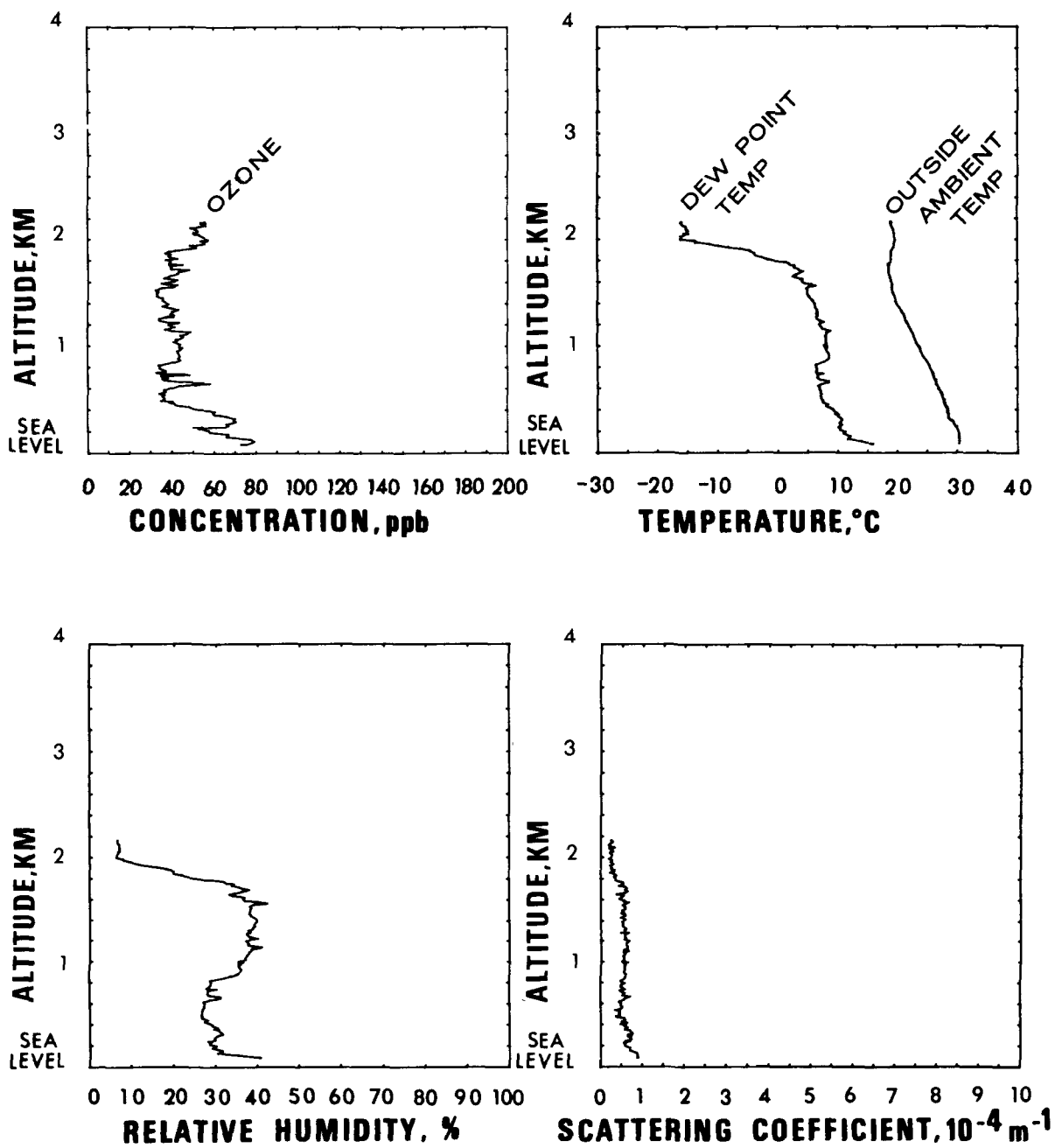


Figure 46. Flight #10: Vertical profiles of parameters for Spiral #2

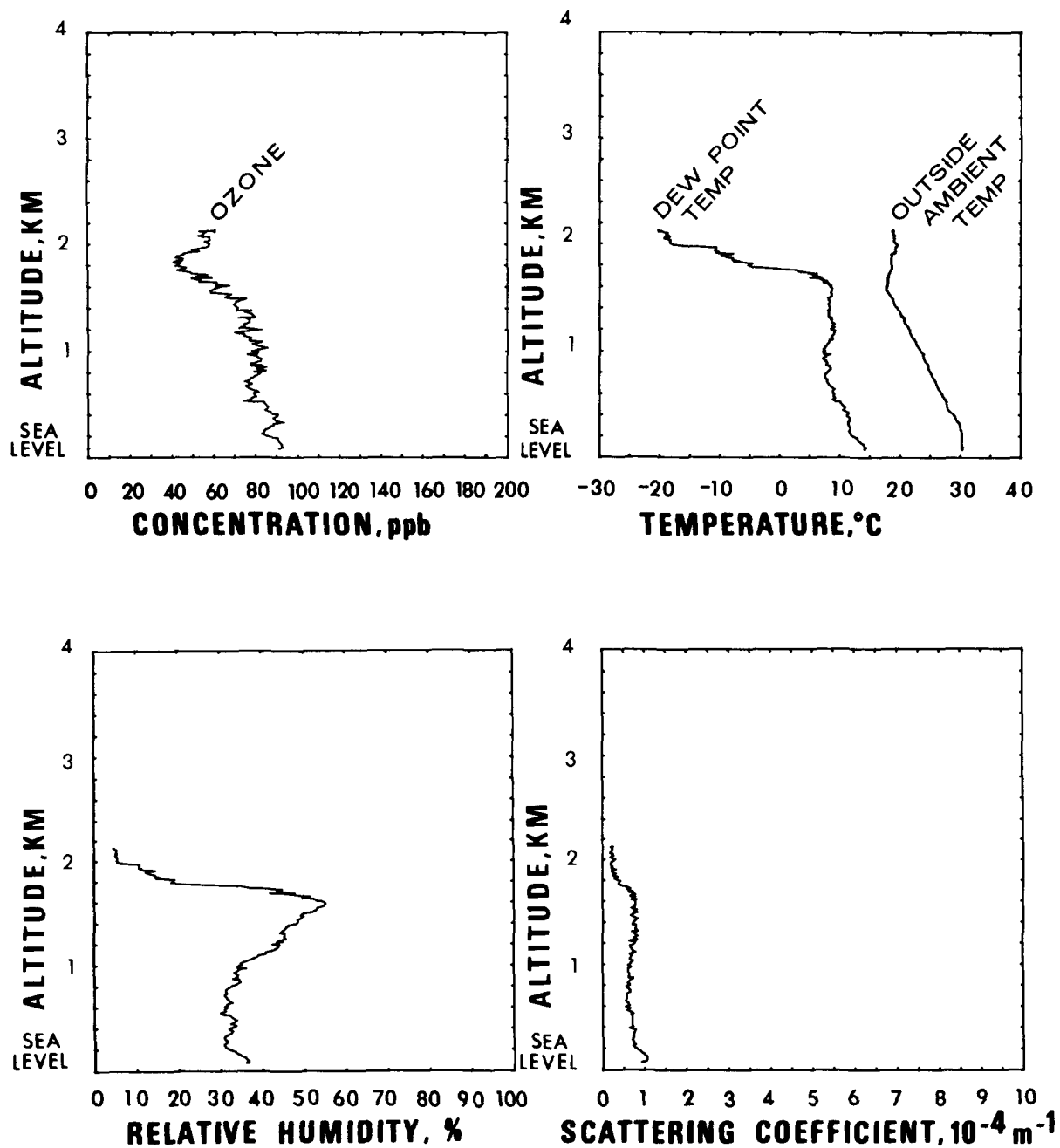


Figure 47. Flight #10: Vertical profiles of parameters for Spiral #3

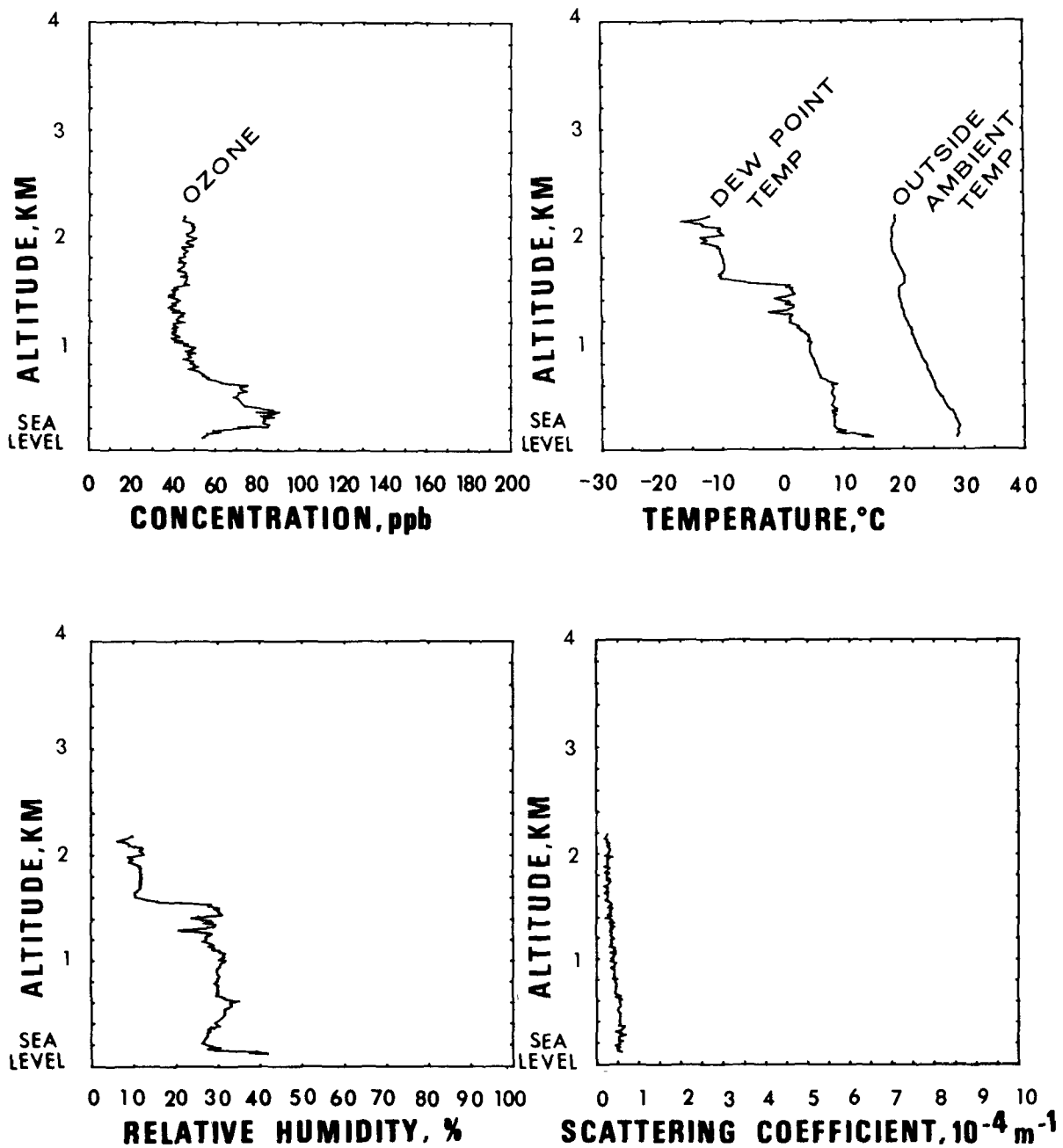


Figure 48. Flight #10: Vertical profiles of parameters for Spiral #4

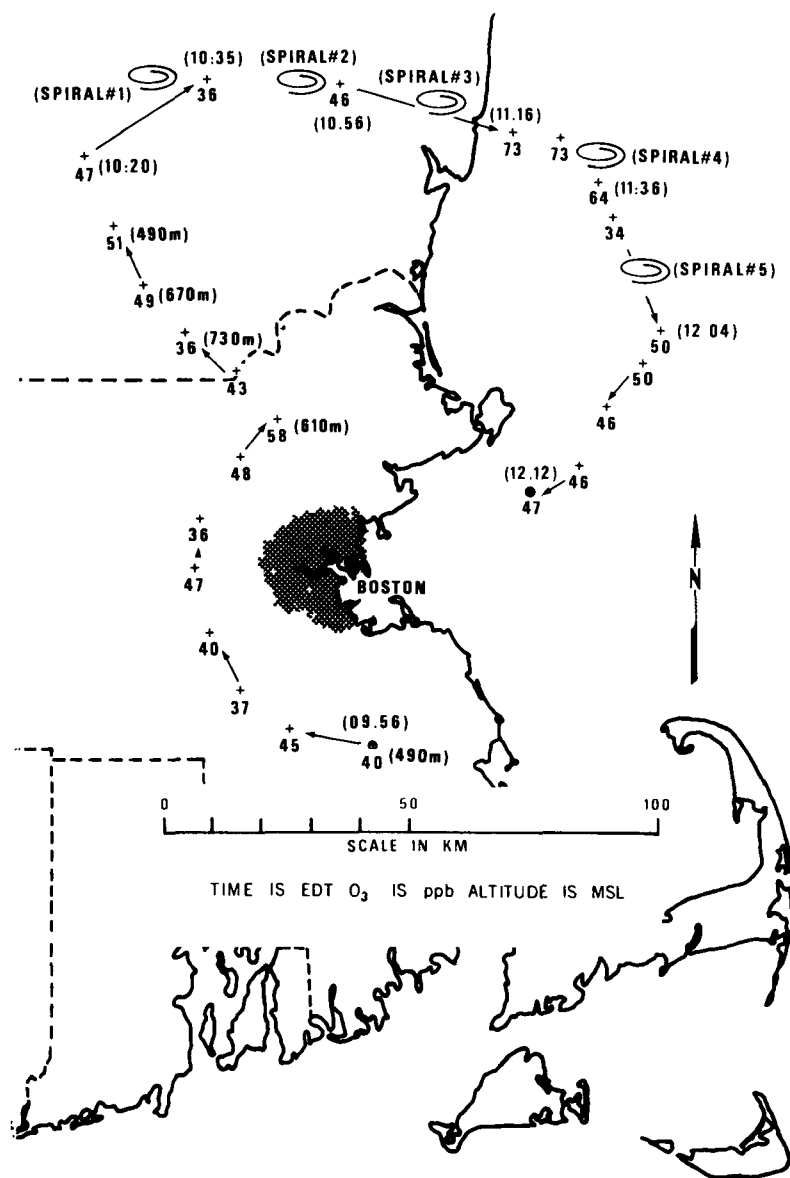


Figure 49. Flight #11 (August 17, 1975): Flight pattern and ozone distribution map

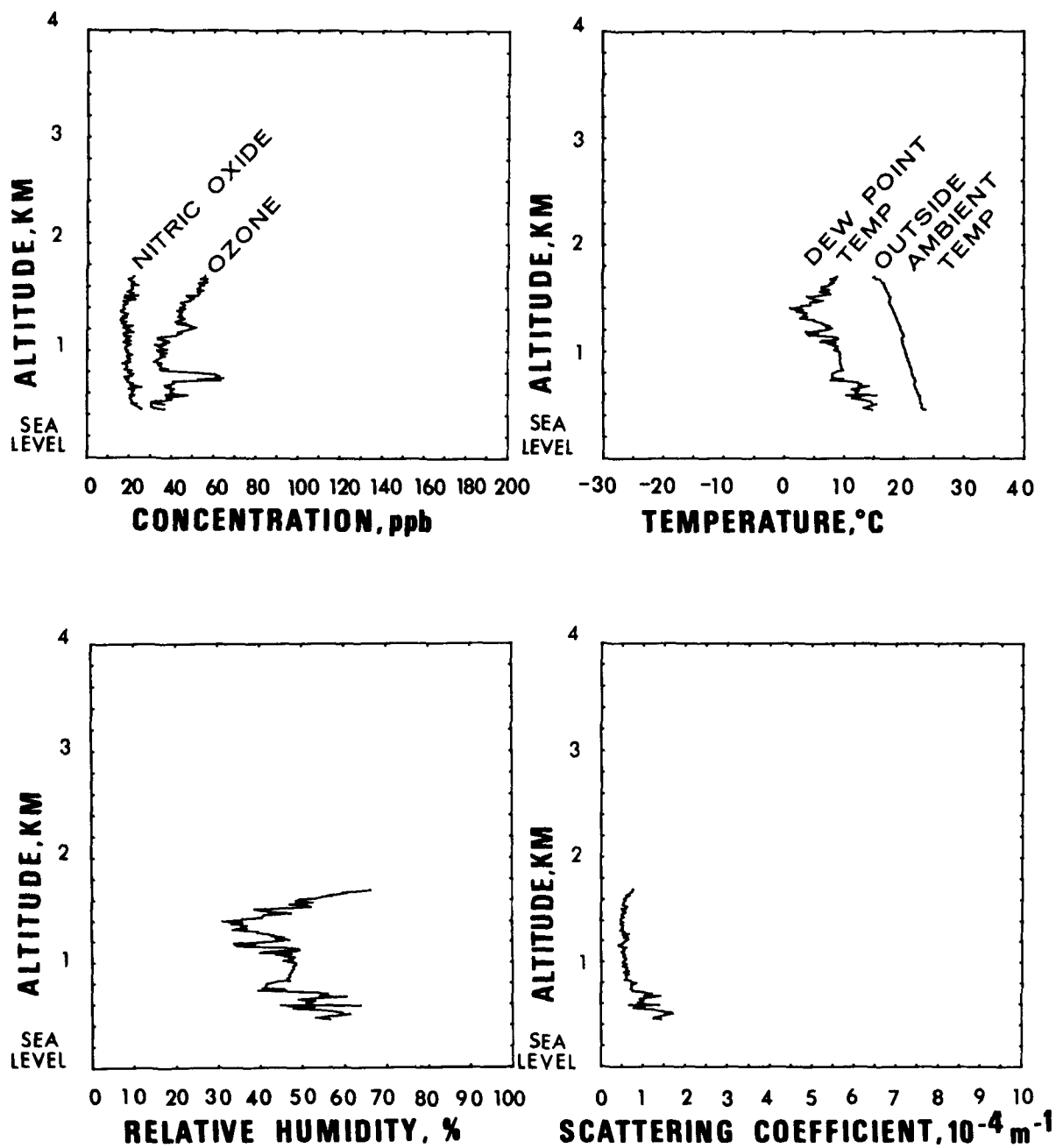


Figure 50. Flight #11: Vertical profiles of parameters for Spiral #1

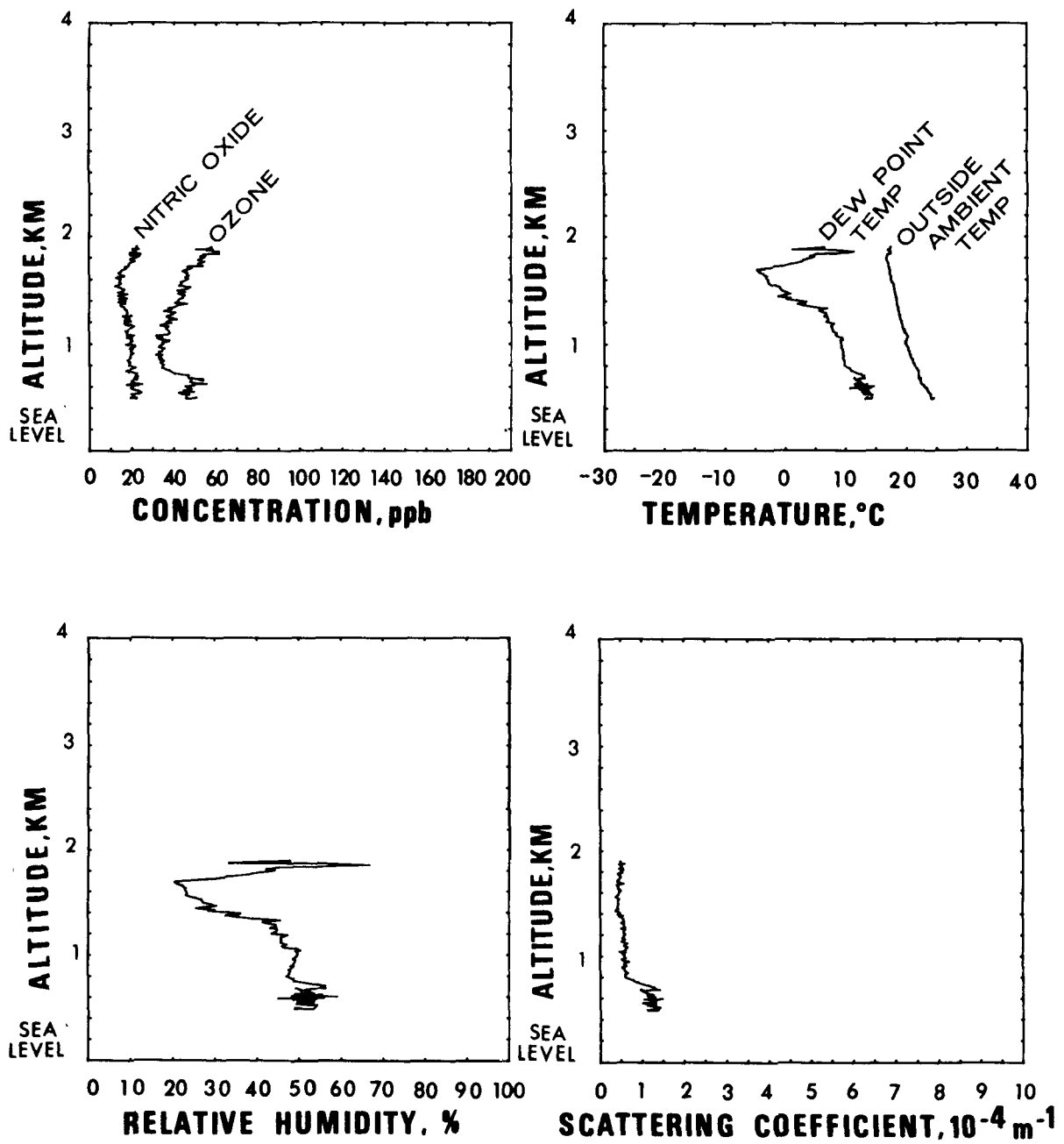


Figure 51. Flight #11: Vertical profiles of parameters for Spiral #2

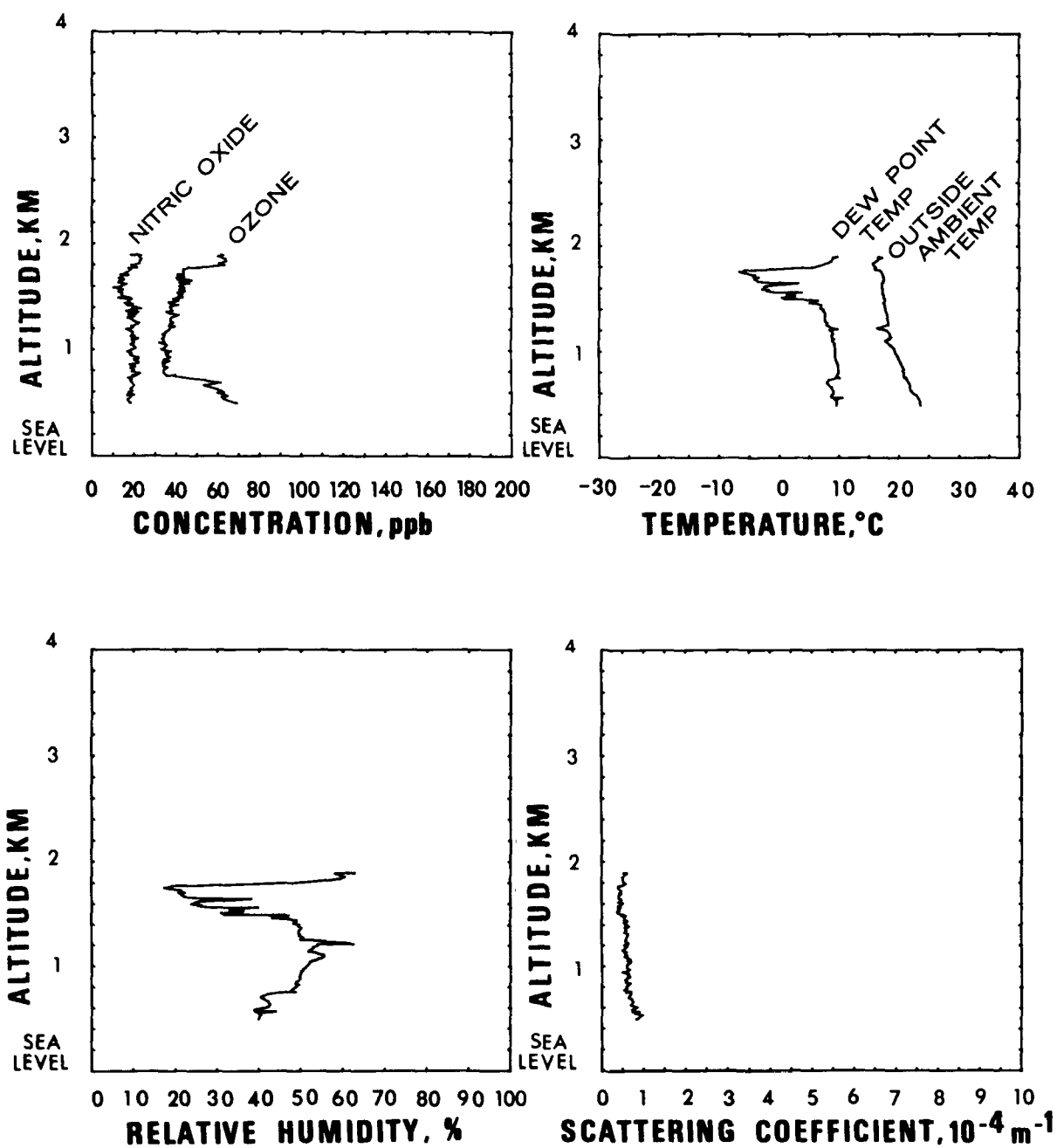


Figure 52. Flight #11: Vertical profiles of parameters for Spiral #3

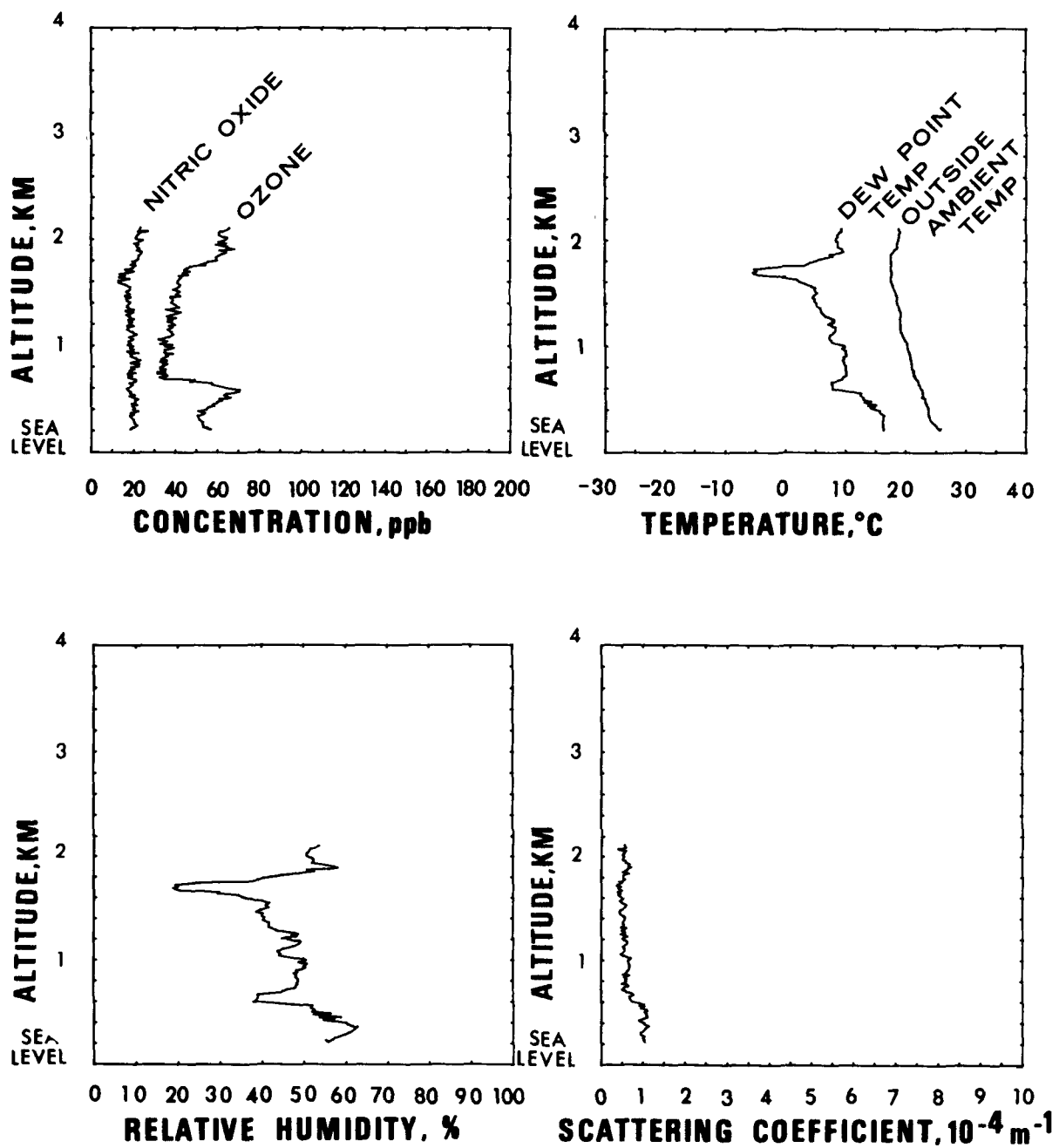


Figure 53. Flight #11: Vertical profiles of parameters for Spiral #4

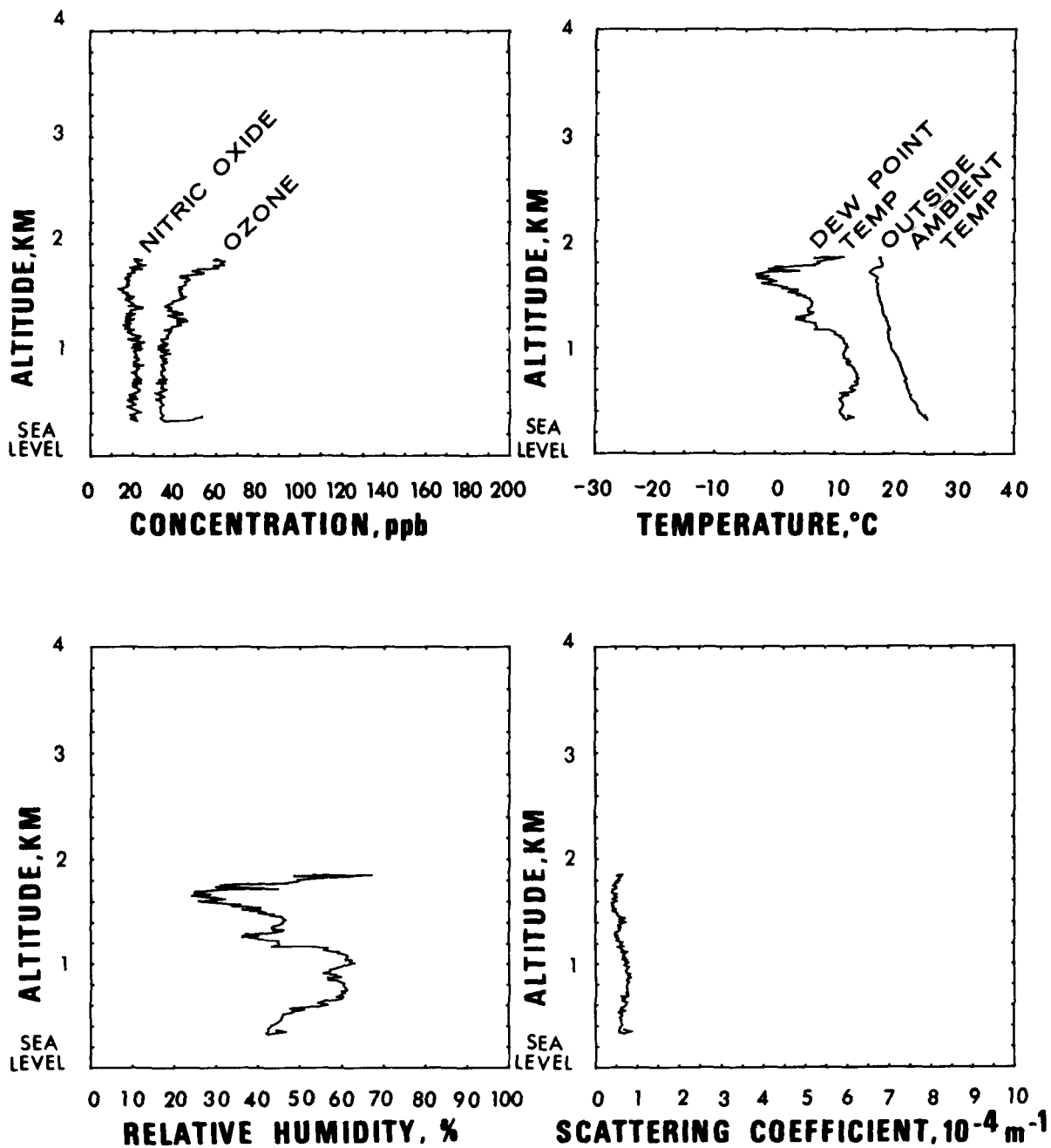


Figure 54. Flight #11: Vertical profiles of parameters for Spiral #5

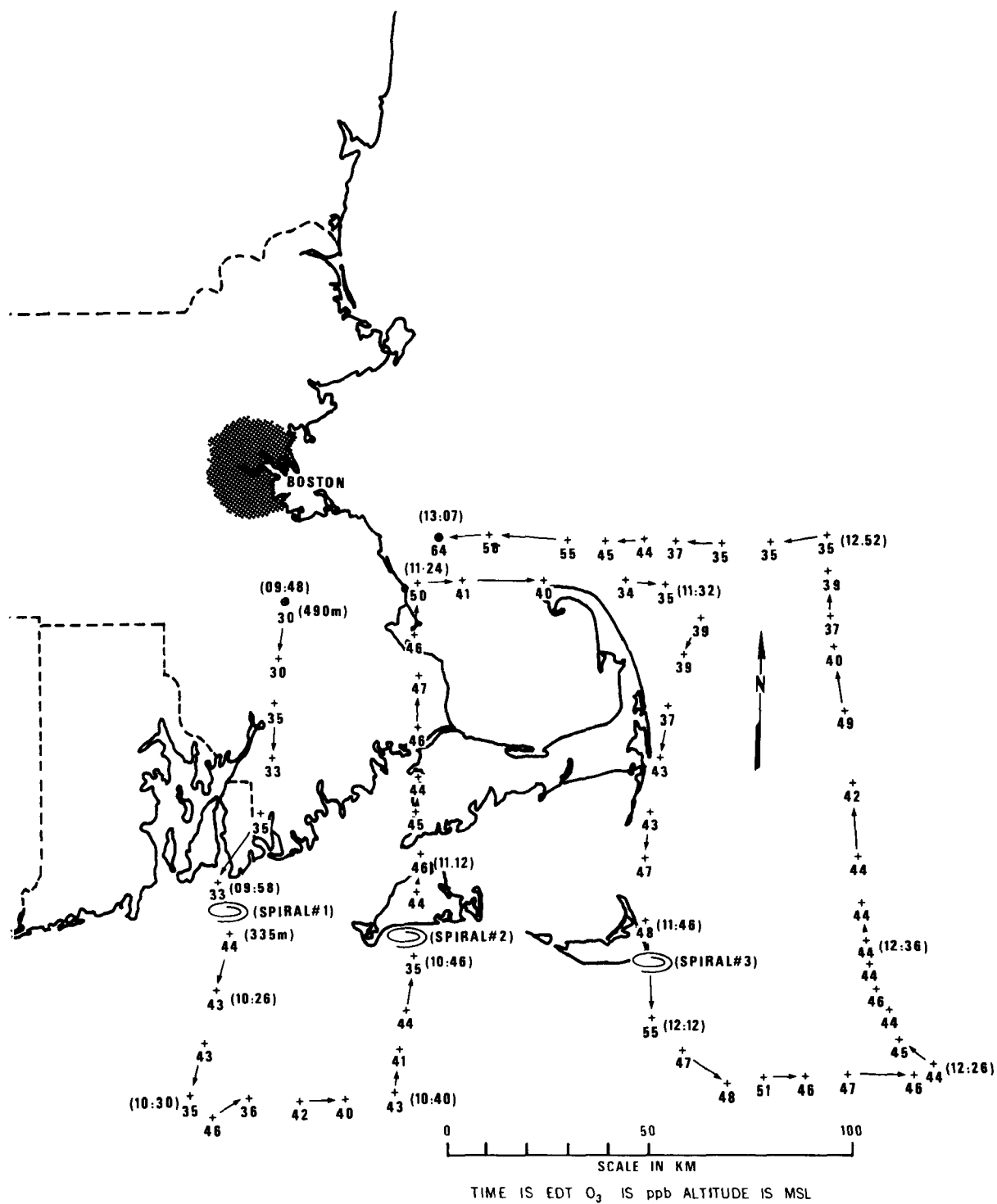


Figure 55. Flight #12 (August 19, 1975): Flight pattern and ozone distribution map

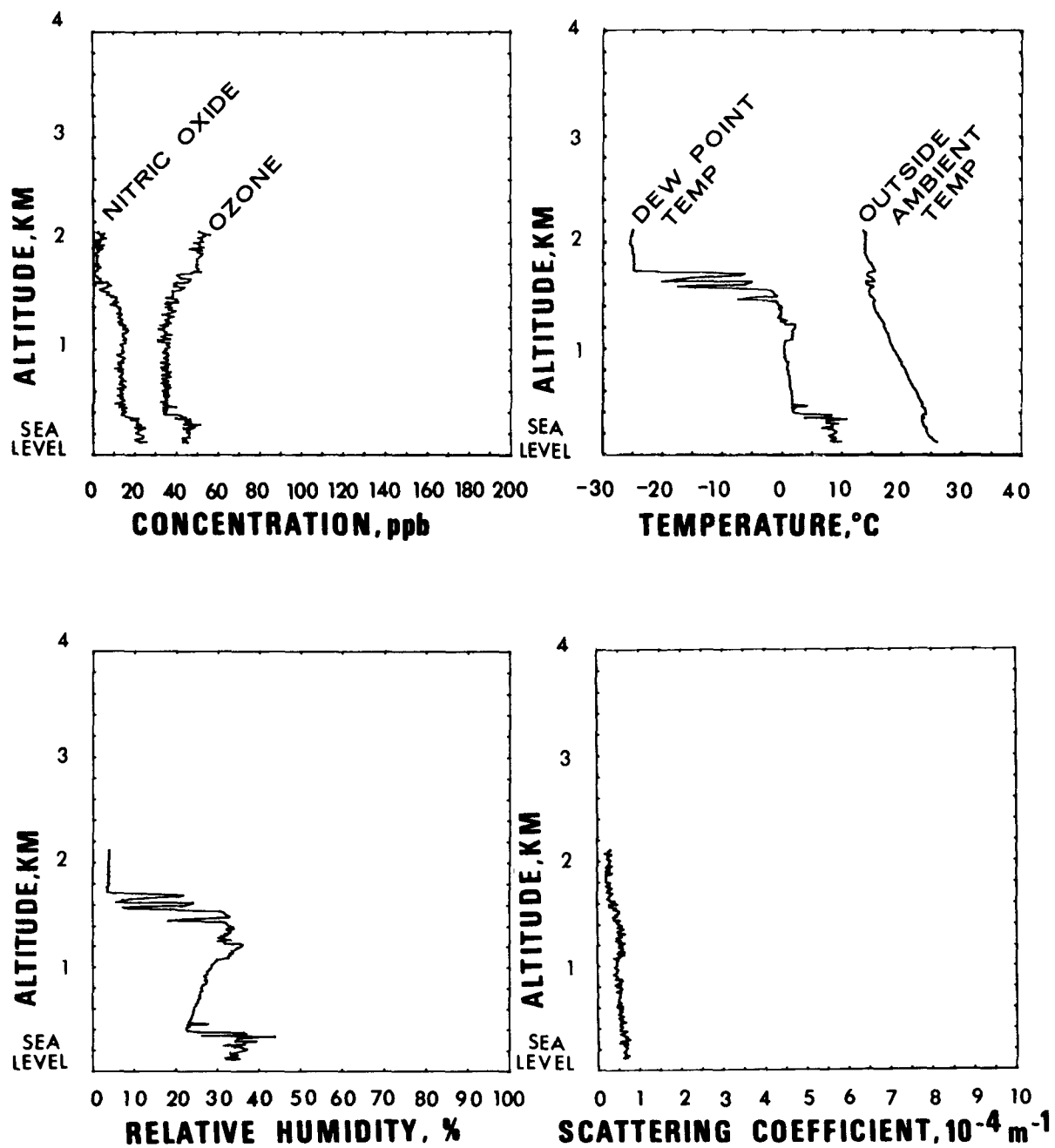


Figure 56. Flight #12: Vertical profiles of parameters for Spiral #1

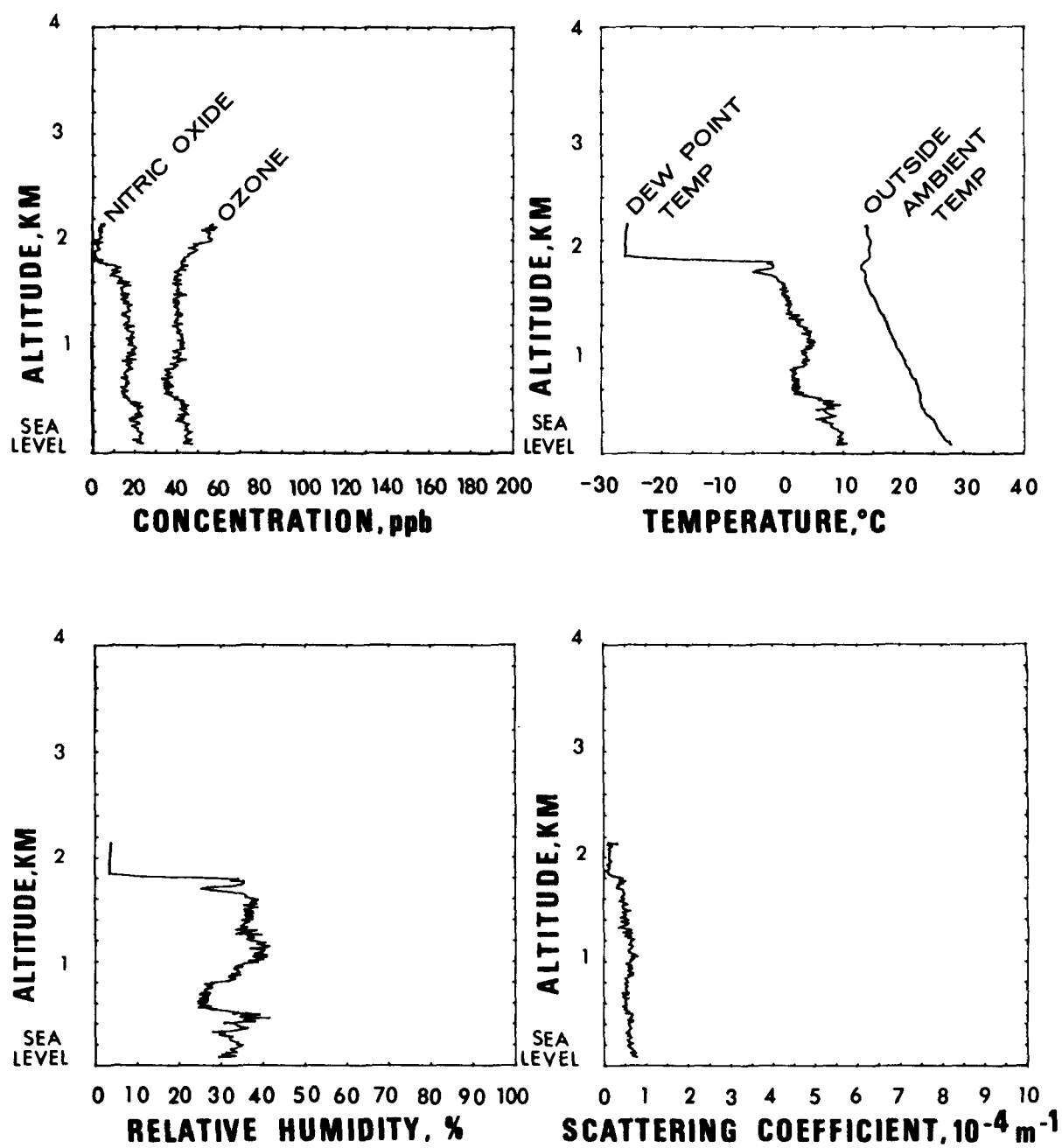


Figure 57. Flight #12: Vertical profiles of parameters for Spiral #2

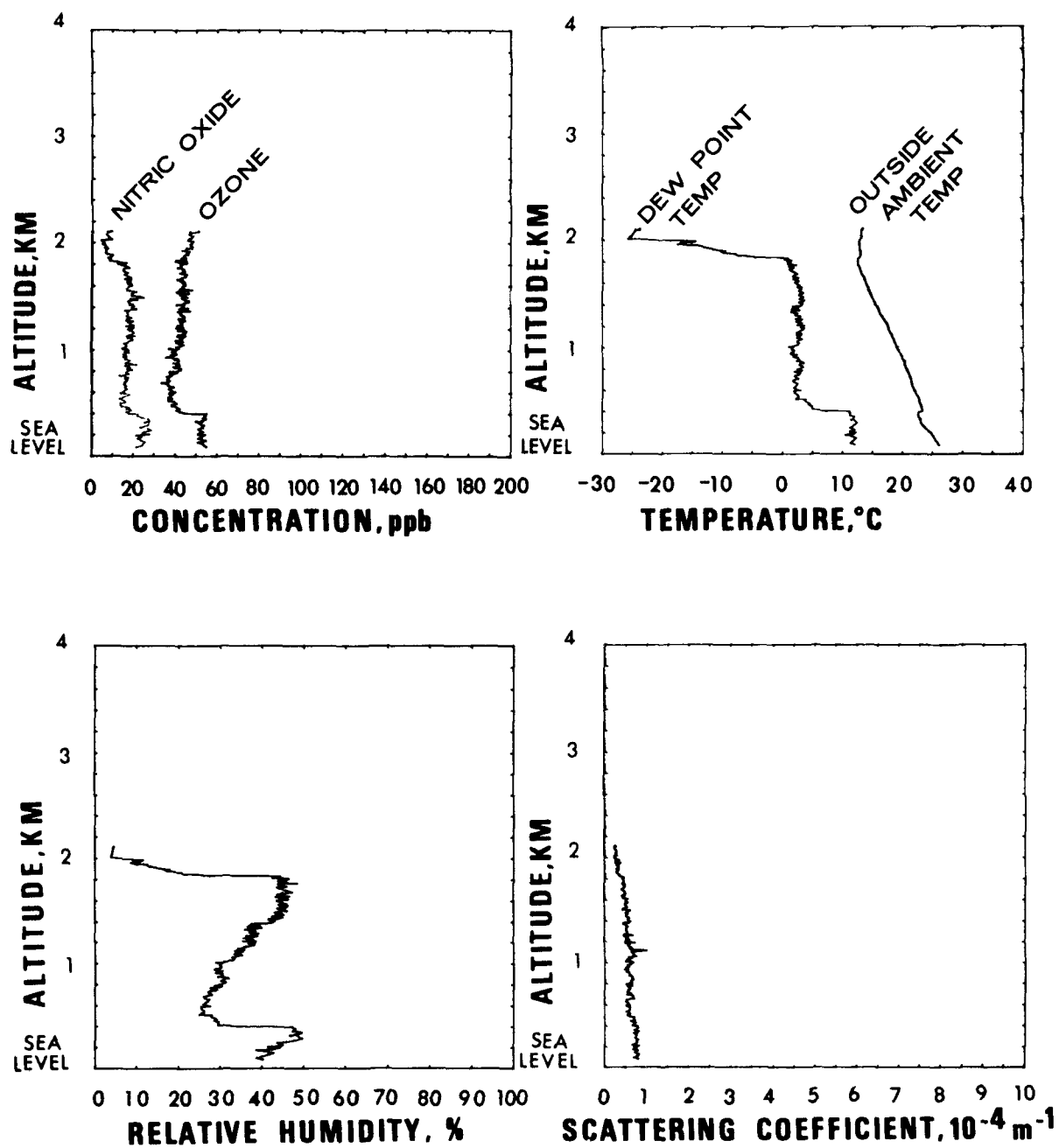


Figure 58. Flight #12: Vertical profiles of parameters for Spiral #3

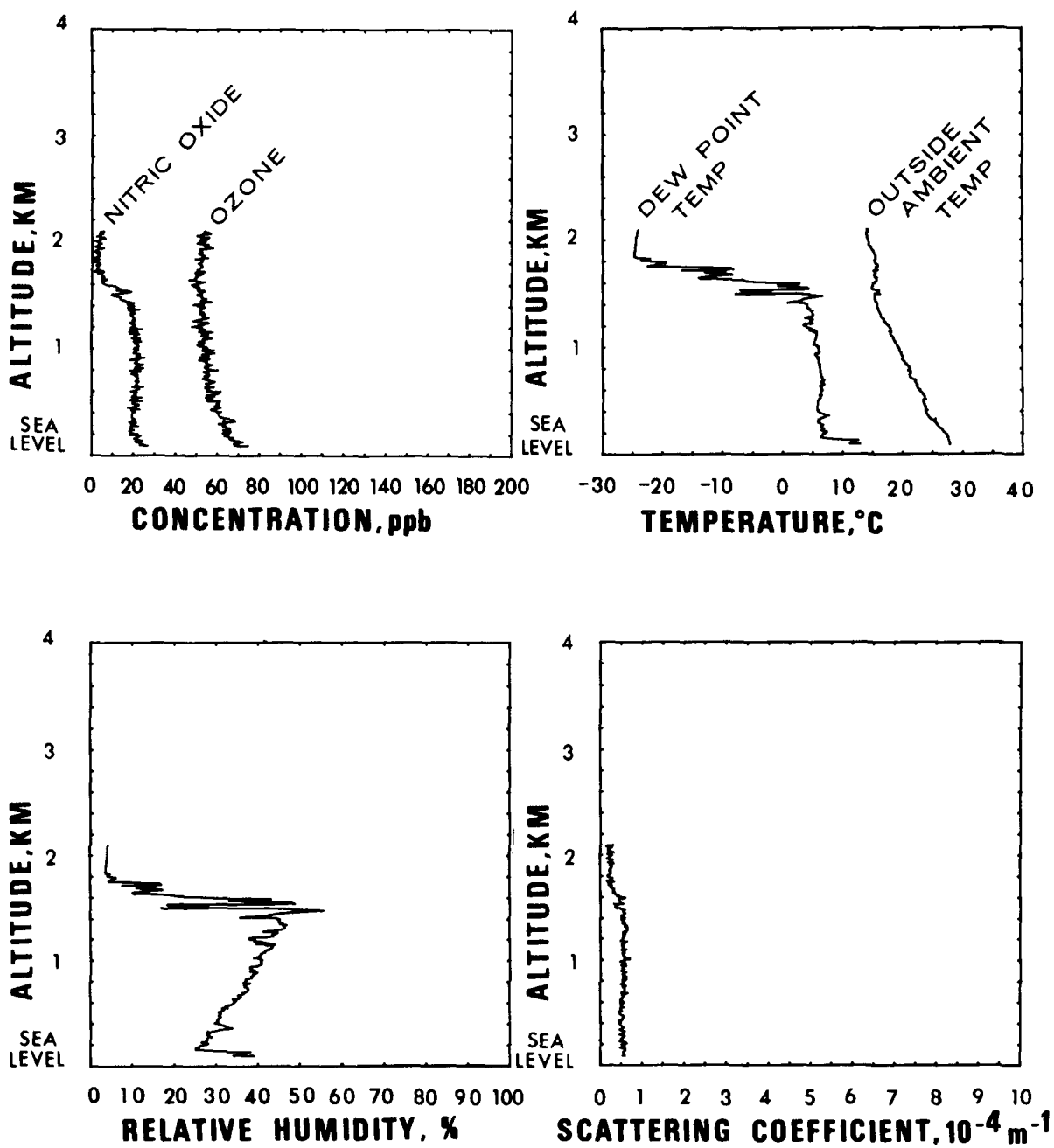


Figure 60. Flight #13: Vertical profiles of parameters for Spiral #1

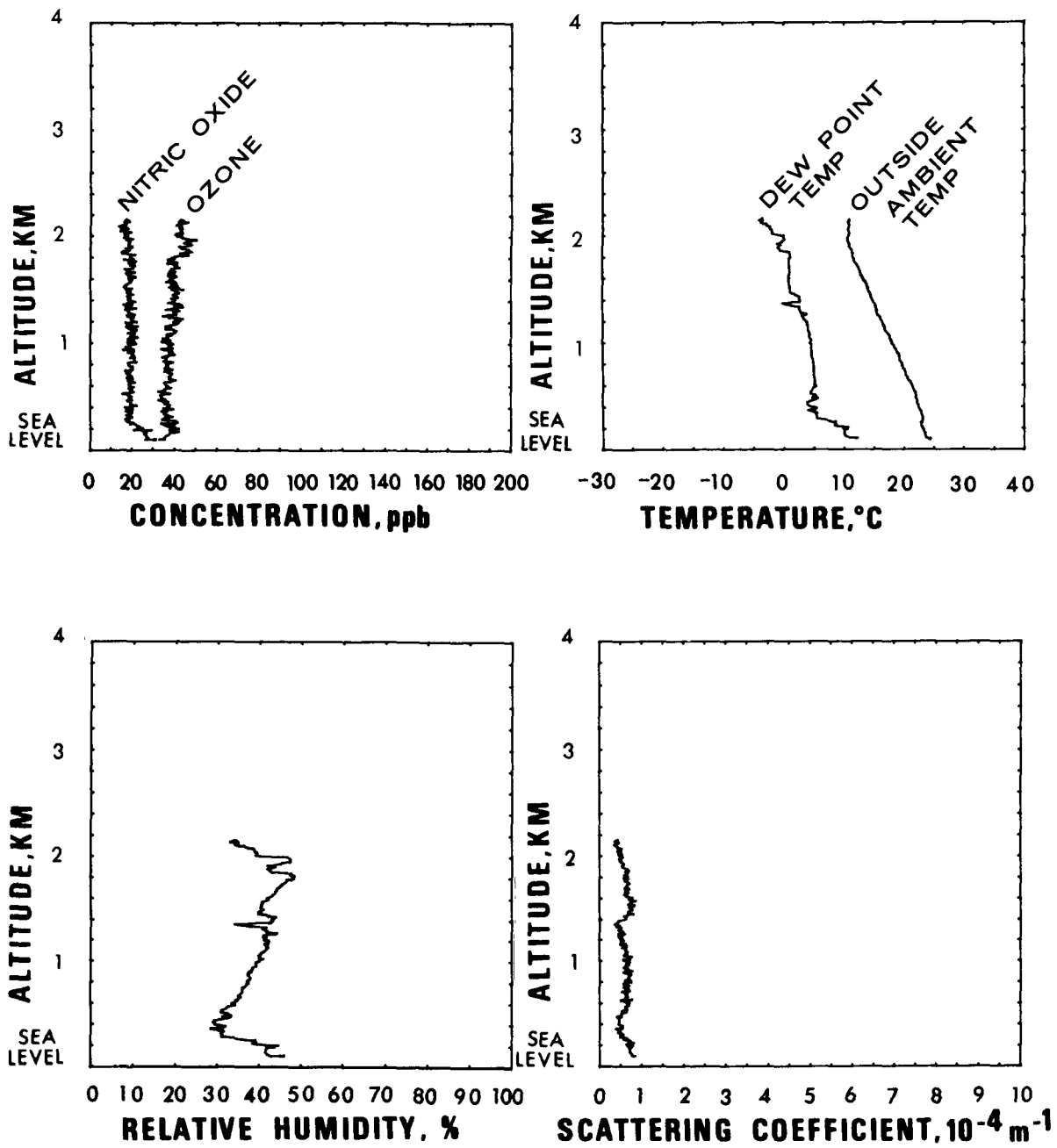


Figure 62. Flight #14: Vertical profiles of parameters for Spiral #1

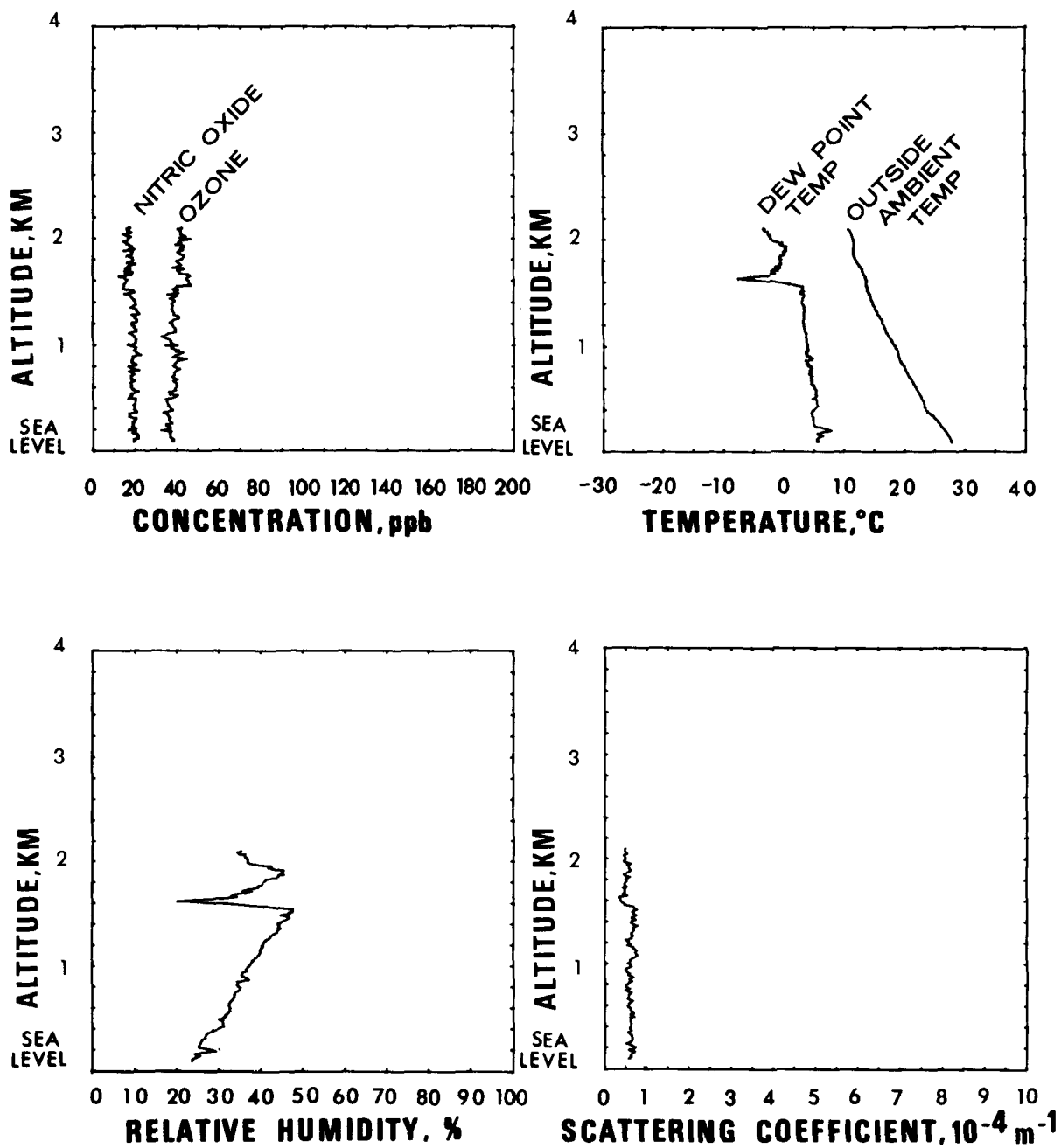


Figure 63. Flight #14: Vertical profiles of parameters for Spiral #2

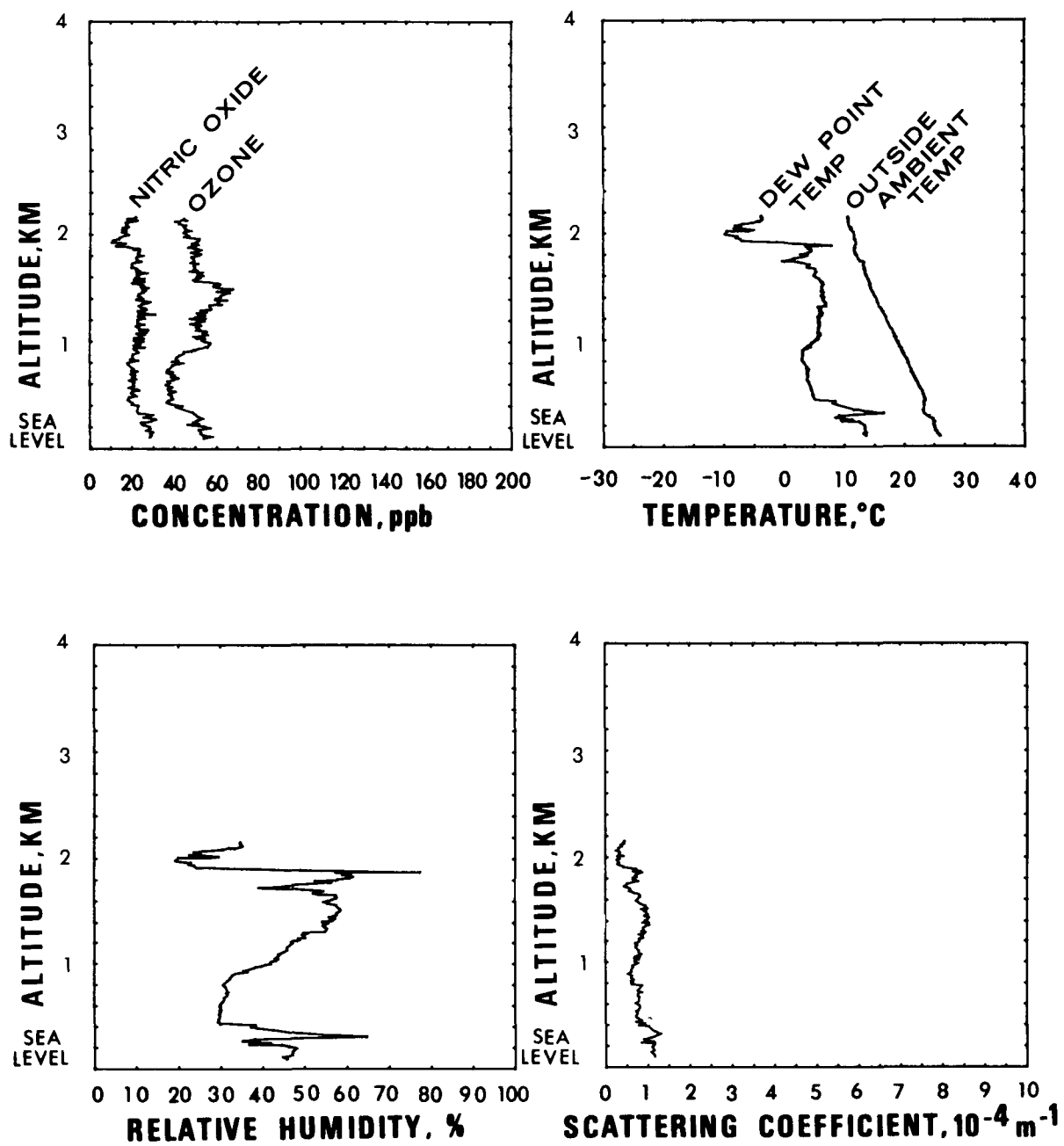


Figure 64. Flight #14: Vertical profiles of parameters for Spiral #3

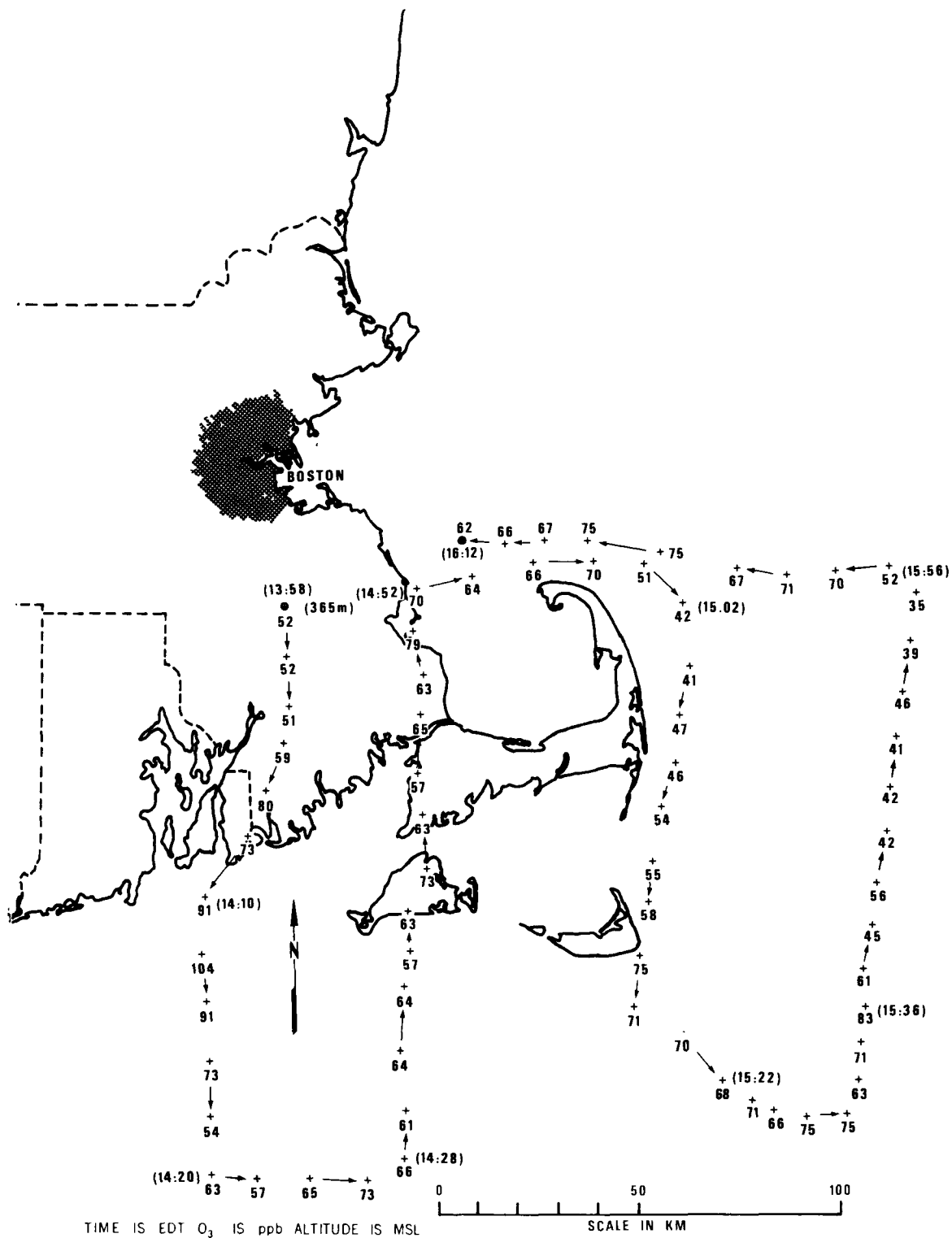


Figure 65. Flight #15 (August 20, 1975): Flight pattern and ozone distribution map

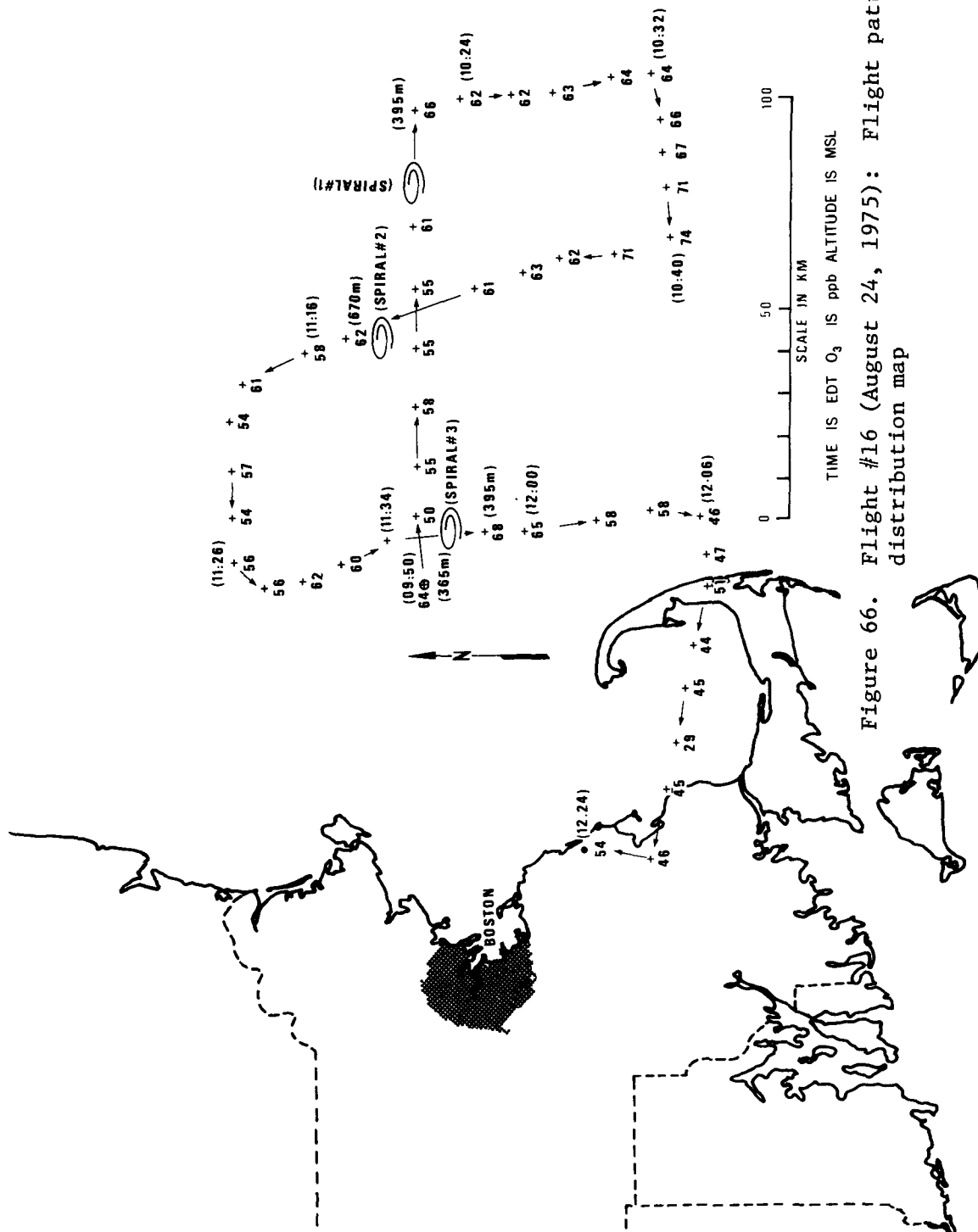


Figure 66. Flight #16 (August 24, 1975): Flight pattern and ozone distribution map

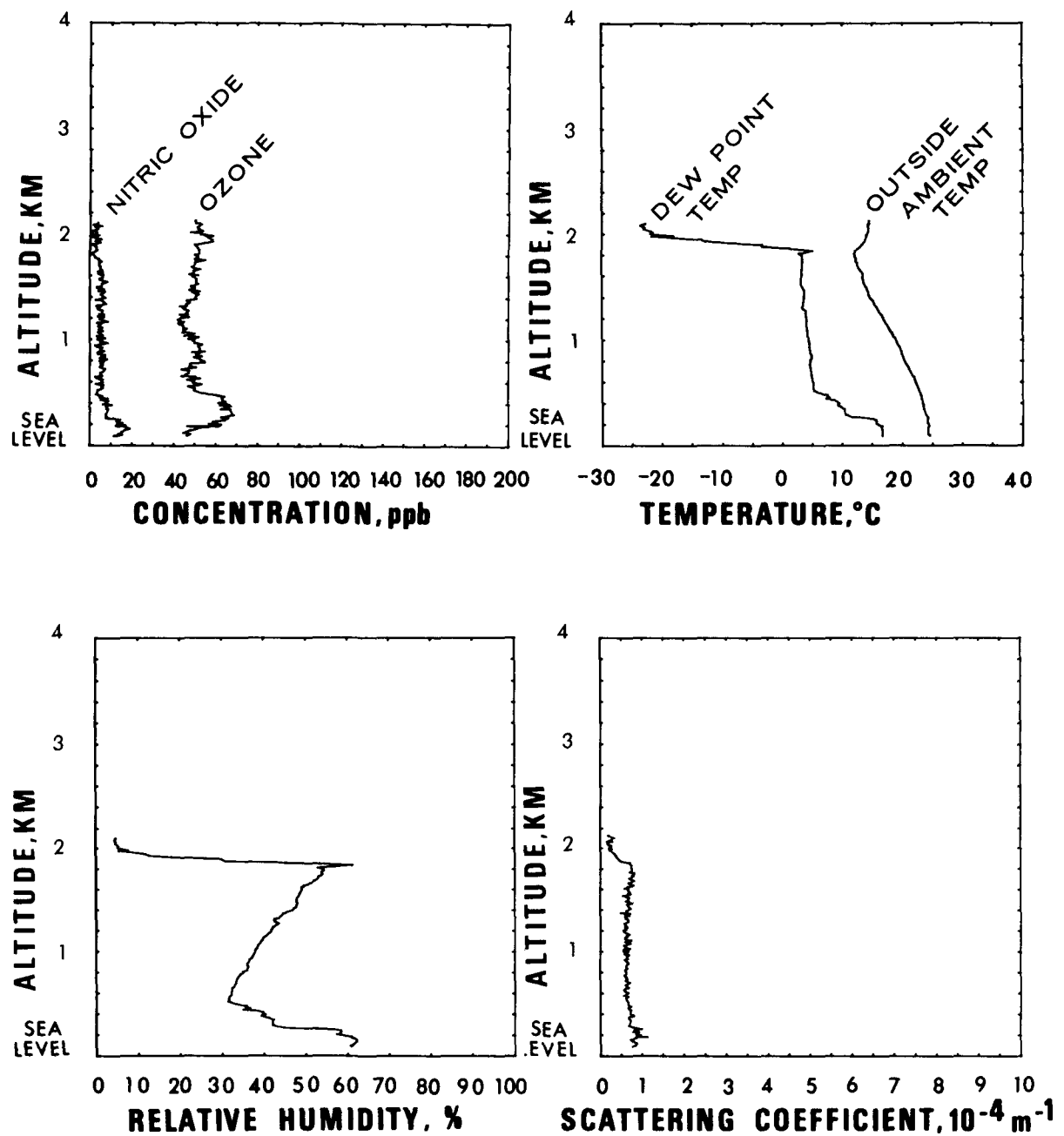


Figure 67. Flight #16: Vertical profiles of parameters for Spiral #1

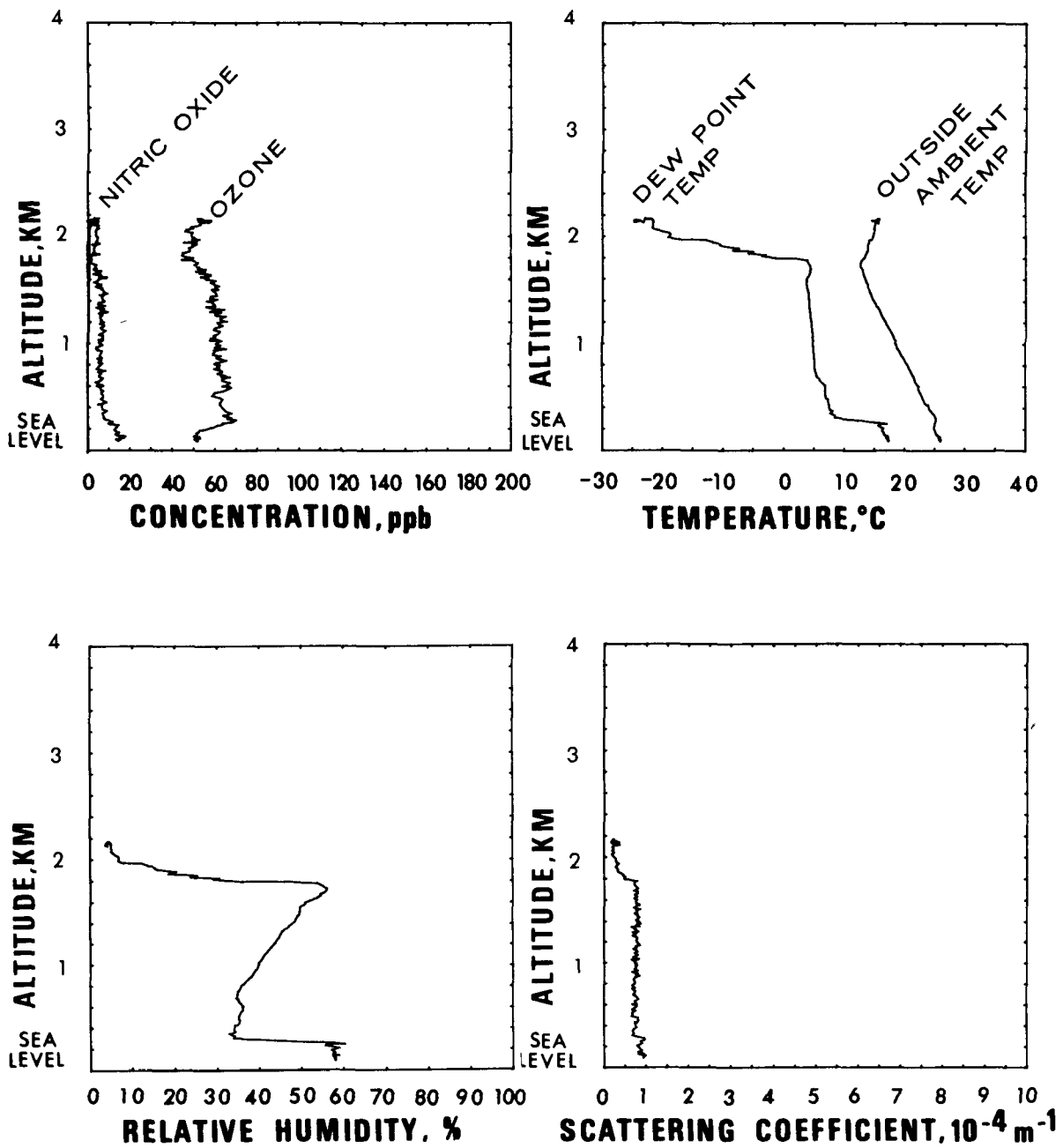


Figure 68. Flight #16: Vertical profiles of parameters for Spiral #2

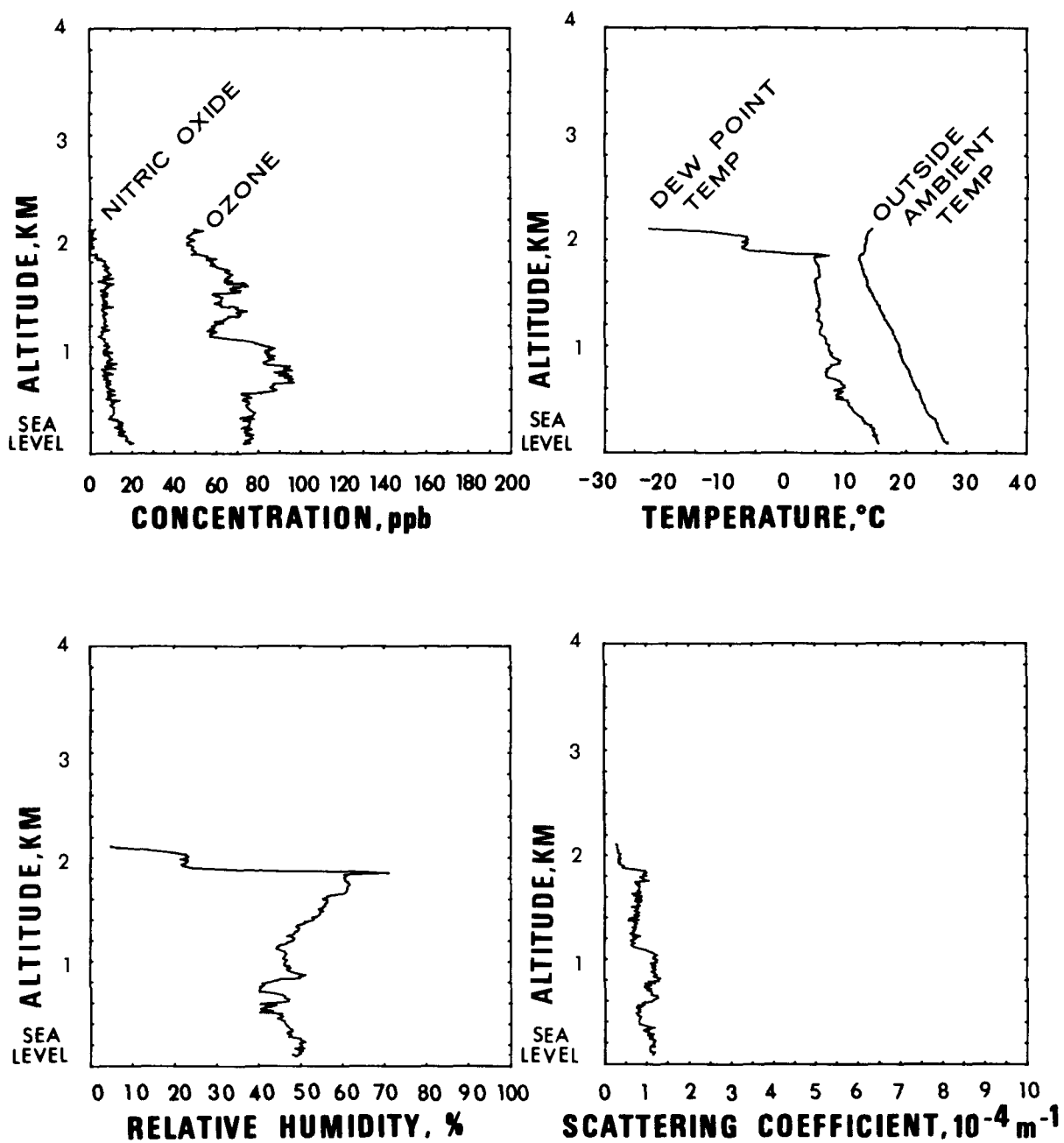


Figure 69. Flight #16: Vertical profiles of parameters for Spiral #3

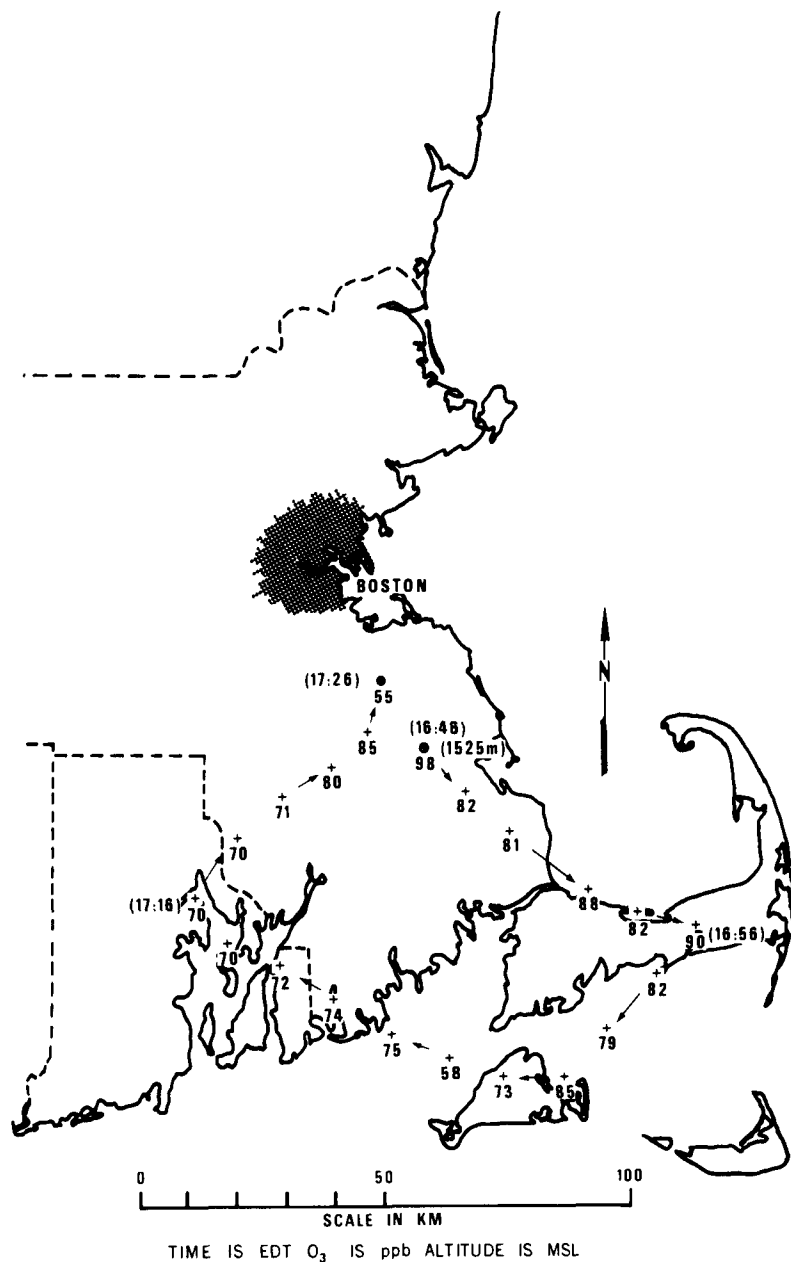


Figure 70. Flight #17 (August 26, 1975): Flight pattern and ozone distribution map

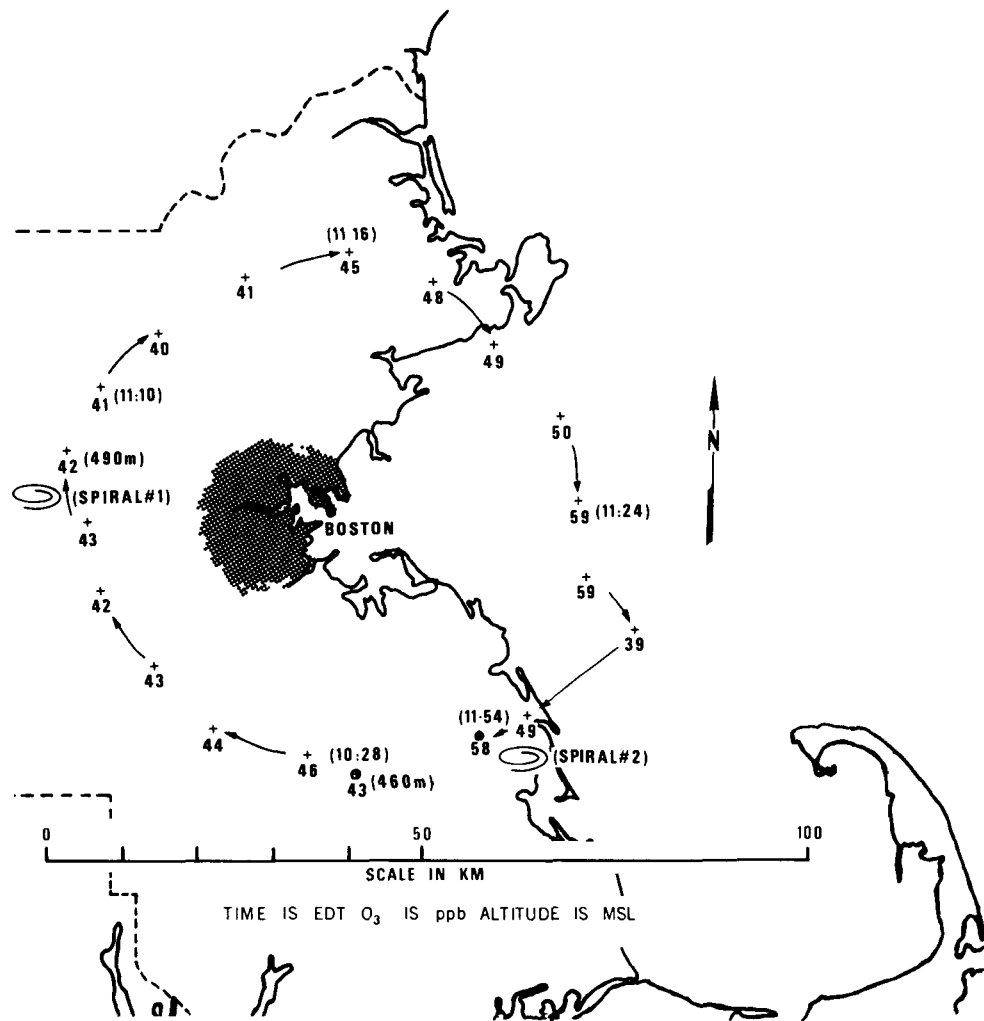


Figure 71. Flight #18 (August 27, 1975): Flight pattern and ozone distribution map

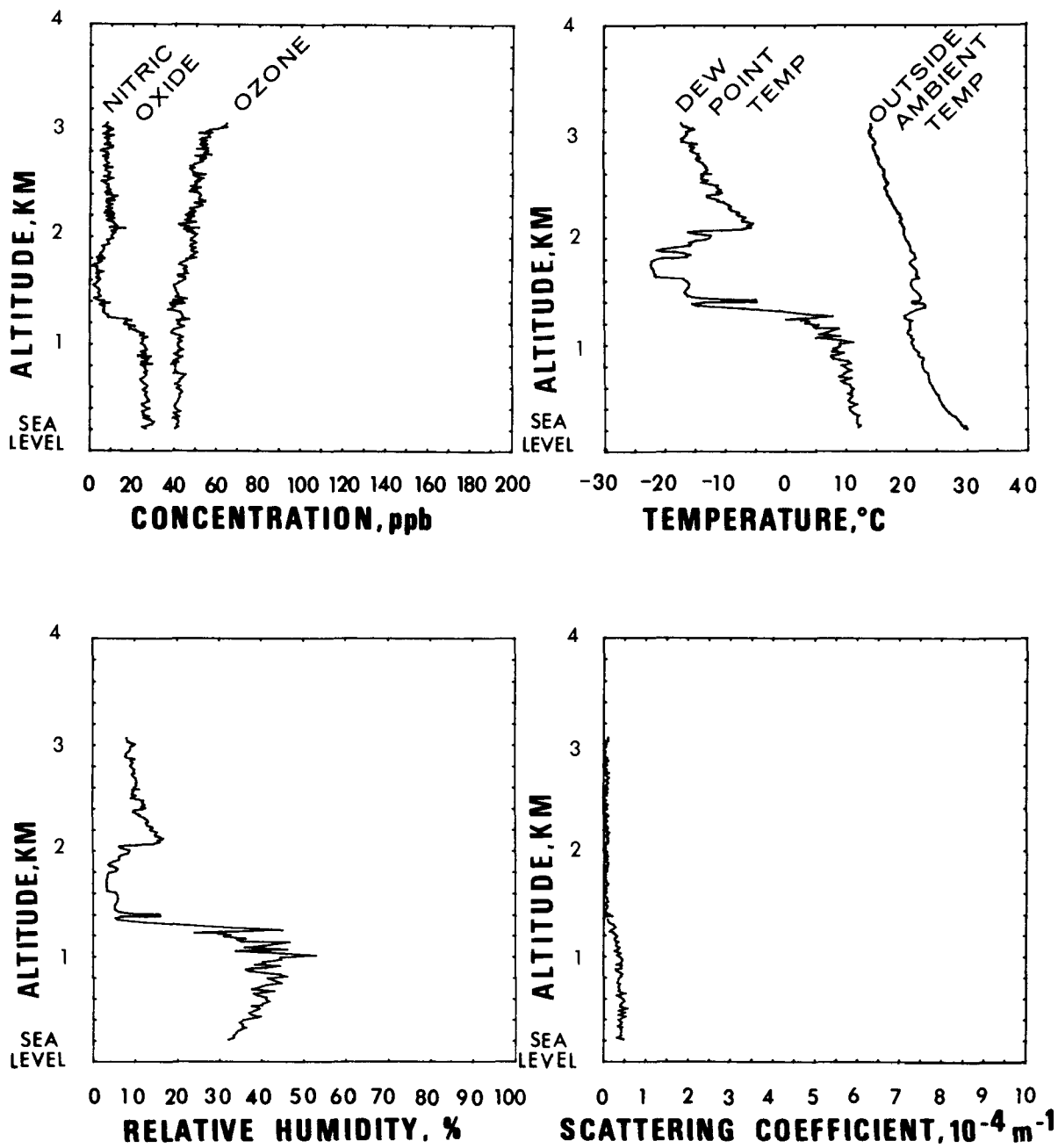


Figure 72. Flight #18: Vertical profiles of parameters for Spiral #1

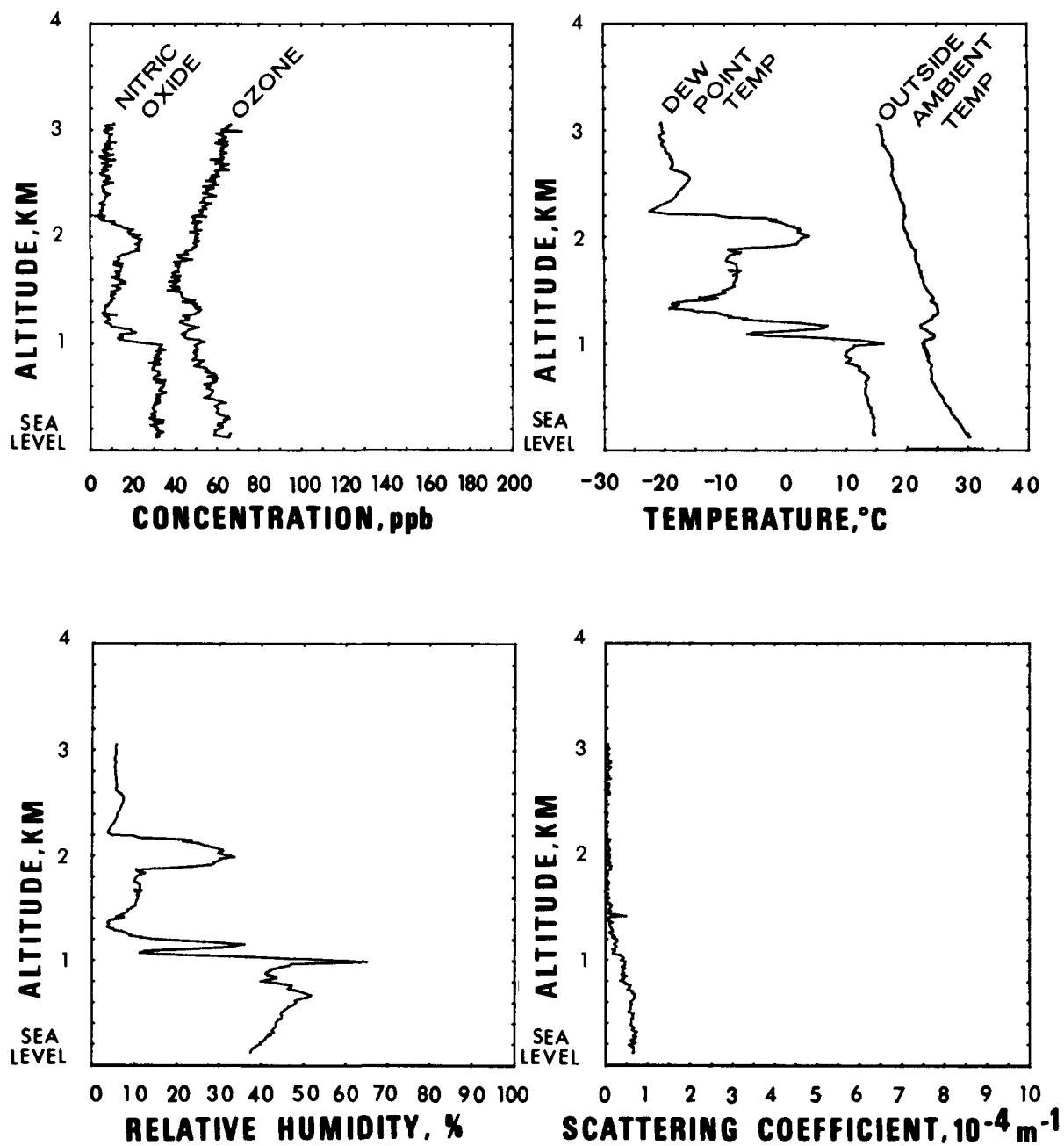


Figure 73. Flight #18: Vertical profiles of parameters for Spiral #2

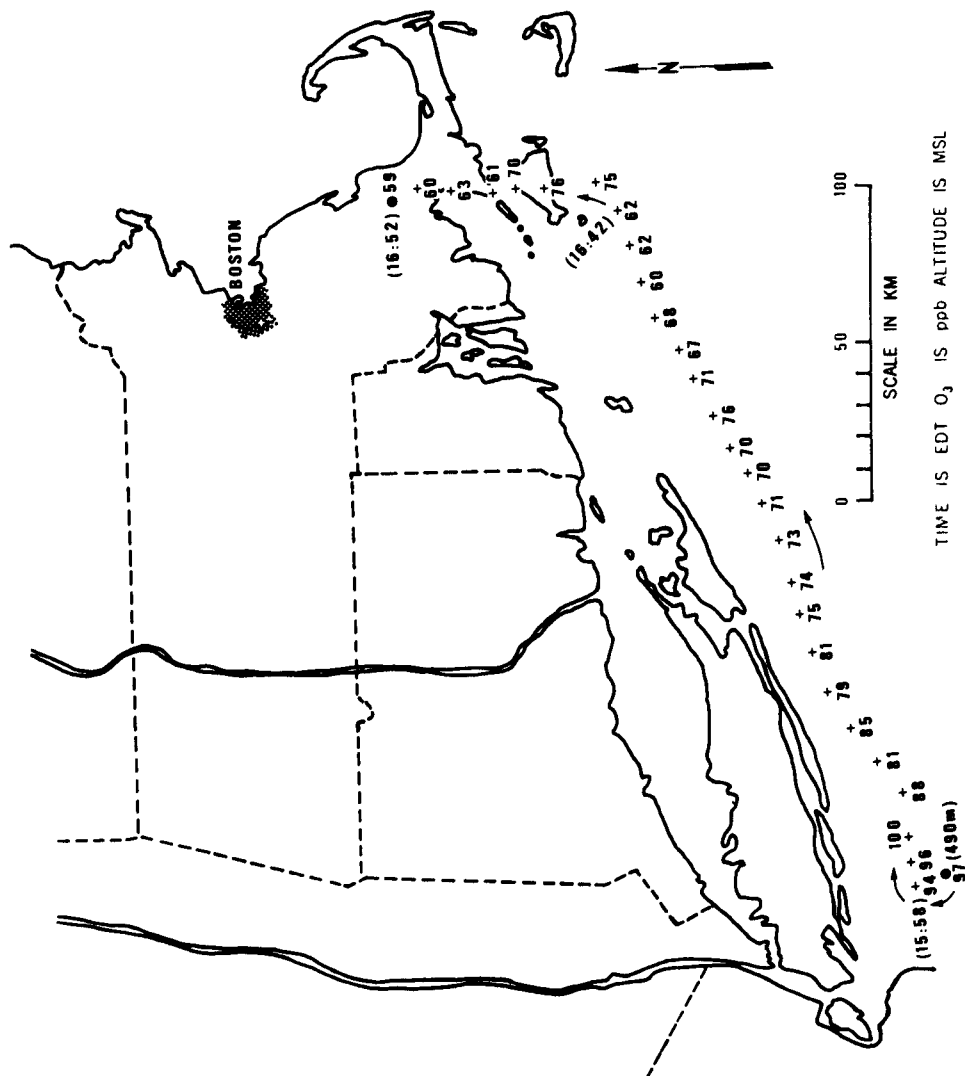


Figure 74a. Flight #19 (August 27, 1975): Flight pattern and ozone distribution map, northbound

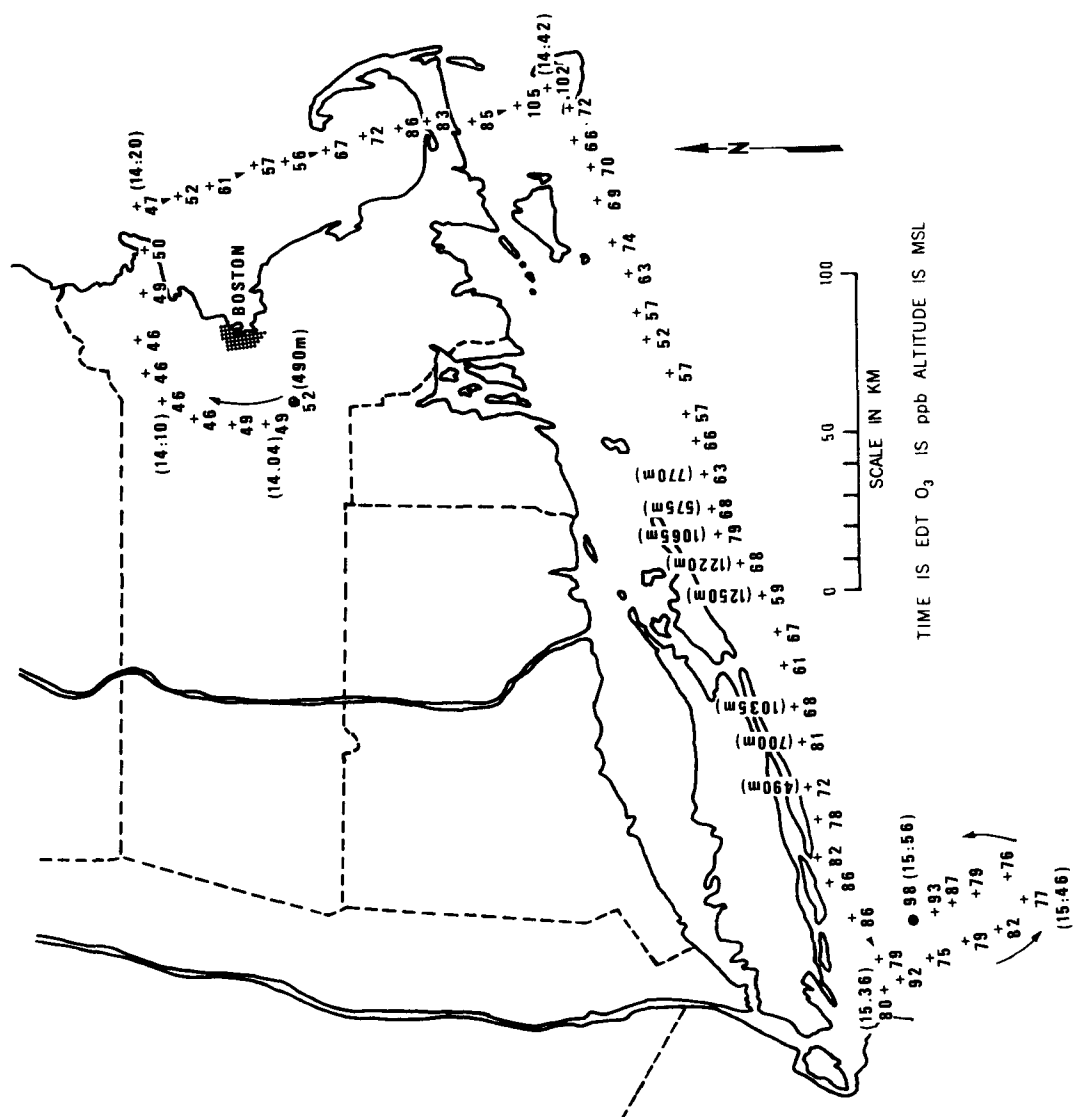


Figure 74b. Flight #19 (August 27, 1975): Flight pattern and ozone distribution map, southbound

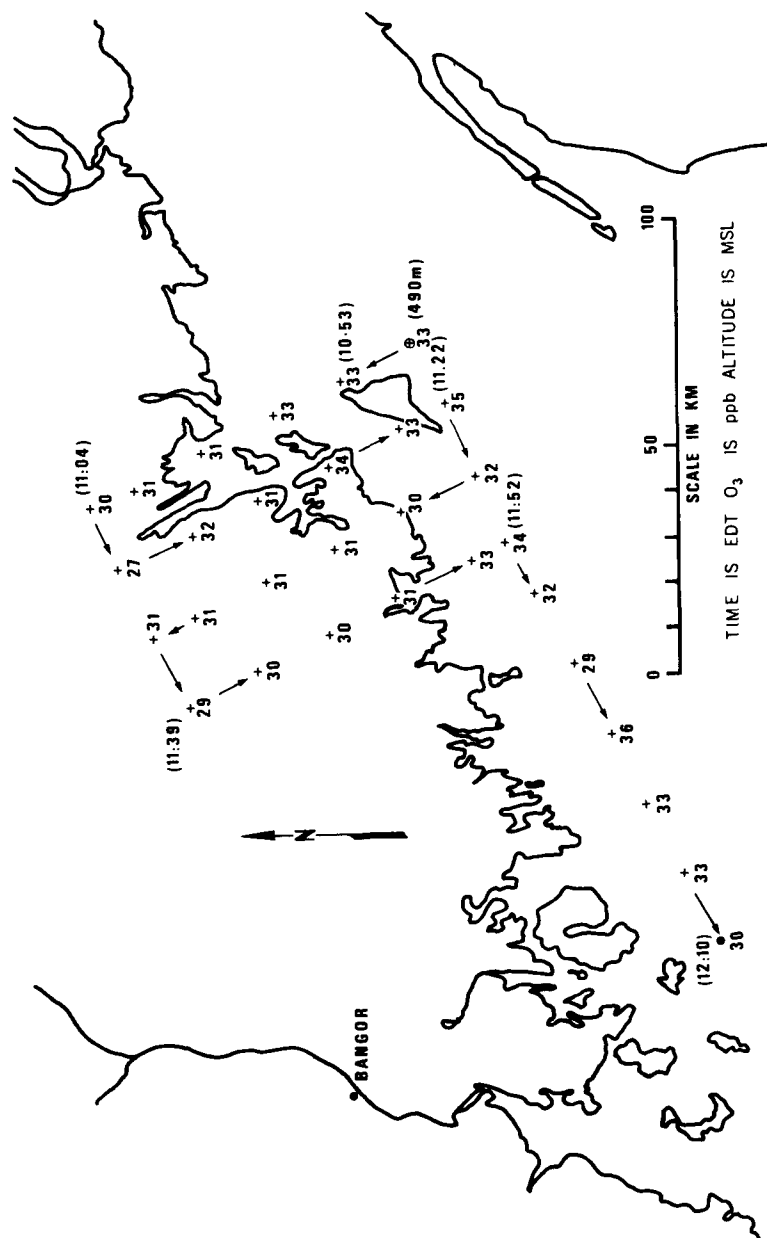


Figure 75. Flight #20 (August 28, 1975): Flight pattern and ozone distribution map

REFERENCES

- "Air Quality Criteria for Nitrogen Oxides," National Air Pollution Control Administration, Washington, D.C., Publication No. AP-84 (March 1970)
- Altshuller, A.P., and Bufalini, J.J. "Photochemical aspects of air pollution: A review." Environmental Science and Technology, Vol 5, No. 1, pp. 39-64 (1971)
- Behl, B.A. "Absolute continuous atmospheric ozone determination by differential uv absorption." Air Pollution Control Association 65th Meeting, Paper No. 72-7. Miami Beach, Florida (1972)
- Blumenthal, D.L., White, W.H., Peace, R.L., and Smith, T.B. "Determination of ozone or ozone precursors." Meteorology Research Incorporated, Prepared for U. S. Environmental Protection Agency, EPA-450/3-74-061 (November 1974)
- Boyd, A.W., Willis, C., and Cyr, R. "New determination of stoichiometry of the iodometric method for ozone analysis at pH 7.0." Analytical Chemistry, Vol. 42, No. 6, pp. 670-672 (1970)
- Breeding, R.J., Klonis, H.B., Lodge, J.P., Jr., Pate, J.B., Sheesley, D.C., Englert, T.R., and Sears, D.R. "Measurements of atmospheric pollutants in the St. Louis area," Atmospheric Environment, Vol. 10, No. 3, pp. 181-194 (1976)
- Butcher, S.S., and Ruff, R.E. "Effects of inlet residence time on analysis of atmospheric nitrogen oxides and ozone." Analytical Chemistry, Vol. 43, No. 13, pp. 1890-1892 (1971)
- Calvert, J.G. "Test of theory of ozone generation in Los Angeles Atmosphere," Environmental Science and Technology, Vol. 10, No. 3, pp. 248-256 (1976)
- Cleveland, W.S., Kleiner, B., McRae, J.G., and Warner, J.L. "Photochemical air pollution: Transport from the New York City area into Connecticut and Massachusetts." Science, Vol. 191, pp. 179-181 (1976)
- Coffey, P.E., and Stasiuk, W.N. "Evidence of atmospheric transport of ozone into urban areas." Environmental Science and Technology, Vol. 9, No. 1, pp. 59-62 (1975)

- Decker, C.D., Bach, W.D., Eaton, W.C., Hamilton, H.L., King, W.J., Ripperton, L.A., Tommerdahl, J.B., Vukovitch, F.M., White, J.H., and Worth, J.J.B. "Investigation of rural oxidant levels as related to urban hydrocarbon control strategies." Research Triangle Institute, Prepared for U. S. Environmental Protection Agency, EPA-450/3-75-036 (March 1975)
- Demerjian, K.J., Kerr, J.A., and Calvert, J.G. "The mechanism of photochemical smog formation." Advances in Environmental Sciences and Technology, Vol. 4 (J.N. Pitts, Jr., R.L. Metcalf, and A.C. Lloyd, eds.), John Wiley and Sons, New York, pp. 1-262 (1974)
- Higuchi, J.E., MacPhee, R.D., and Leh, F.K.V. "Comparison of oxidant measurement methods, ultraviolet photometry, and moisture effect." Presented at APCA Technical Specialty Conference on Ozone/Oxidants - Interaction with the Total Environment. Dallas, Texas (March 10-12, 1976)
- Hodgeson, J.A., Baumgardner, R.E., Martin, B.E., and Rechme, K.A. "Stoichiometry in the neutral iodometric procedure for ozone by gas-phase titration with nitric oxide." Analytical Chemistry, Vol. 43, No. 8, pp. 1123-1126 (1971)
- Jeffries, H.E., Fox, D.L., and Kamens, R.M. "Outdoor smog chamber studies-effect of hydrocarbon reduction on nitrogen dioxide." University of North Carolina, Prepared for U.S. Environmental Protection Agency, EPA-650/3-75-011 (June 1975)
- Johnston, D.R., Decker, C.E., Eaton, W.C., Hamilton, H.L., Jr., White, J.H., and Whitehorne, D.H. "Investigation of ozone and ozone precursor concentrations at non-urban locations in the eastern U.S." Research Triangle Institute, Prepared for U. S. Environmental Protection Agency, EPA-450/3-74-034 (May 1974)
- Kopczynski, S.L., and Bufalini, J.J. "Some observations on stoichiometry of iodometric analyses of ozone at pH 7.0." Analytical Chemistry, Vol. 43, No. 8, pp. 1126-1127 (1971)
- Mage, D.T. "Sample size requirements for statistical validity." Presented at U.S. EPA conference on Monitoring From Airborne Platforms for Air Quality Assessment, Las Vegas, Nevada (March 26-27, 1975)
- Parry, E.P., and Hern, D.H. "Stoichiometry of ozone-iodide reaction: Significance of iodate formation." Environmental Science and Technology, Vol. 7, No. 1, pp. 65-66 (1973)
- Schmitz, L.R. "Correspondence: Stoichiometry of ozone-iodide reaction: Significance of iodate formation." Environmental Science and Technology, Vol. 7, No. 7, p. 647 (1973)
- Smithsonian Meteorological Tables, Prepared by Robert J. List (sixth revised edition), Smithsonian Institute Press, City of Washington (1971)

Tebbens, B.D. "Air pollution." (A.C. Stern, ed.), Vol. I, Academic Press,
New York (1968)

TECHNICAL REPORT DATA <i>(Please read Instructions on the reverse before completing)</i>		
1. REPORT NO. EPA-600/4-77-020	2.	3. RECIPIENT'S ACCESSION NO.
4. TITLE AND SUBTITLE AIR QUALITY DATA FOR THE NORTHEAST OXIDANT TRANSPORT STUDY, 1975 Final Data Report	5. REPORT DATE March 1977	6. PERFORMING ORGANIZATION CODE
	8. PERFORMING ORGANIZATION REPORT NO.	
7. AUTHOR(S) G. W. Siple, C. K. Fitzsimmons, J. J. van Ee, and K. F. Zeller	10. PROGRAM ELEMENT NO. 1AA603	
9. PERFORMING ORGANIZATION NAME AND ADDRESS Environmental Monitoring and Support Laboratory Office of Research and Development U. S. Environmental Protection Agency Las Vegas, Nevada 89114	11. CONTRACT/GRANT NO.	
	13. TYPE OF REPORT AND PERIOD COVERED Final	
12. SPONSORING AGENCY NAME AND ADDRESS U.S. Environmental Protection Agency-Las Vegas, NV Office of Research and Development Environmental Monitoring and Support Laboratory Las Vegas, NV 89114	14. SPONSORING AGENCY CODE EPA/600/7	
	15. SUPPLEMENTARY NOTES	
16. ABSTRACT <p>During the summer of 1975, a survey was conducted in the northeastern region of the U.S. to assess the transport of oxidant and oxidant precursors through the area. This report documents the scope of participation of the Environmental Monitoring and Support Laboratory at Las Vegas Long Range Air Monitoring Aircraft in the study. The report includes a description of the monitoring system, considerations involved in the operation of the system, and a presentation of the data collected by the system.</p>		
17. KEY WORDS AND DOCUMENT ANALYSIS		
a. DESCRIPTORS	b. IDENTIFIERS/OPEN ENDED TERMS	c. COSATI Field/Group
Air masses	Oxidant Transport	01C
Air pollution	Airborne Monitoring	04A
Environmental survey		04B
Fixed wing aircraft		07B
Ozone		13B
Quality Assurance		14D
18. DISTRIBUTION STATEMENT RELEASE TO PUBLIC	19. SECURITY CLASS (This Report) UNCLASSIFIED	21. NO. OF PAGES 104
	20. SECURITY CLASS (This page) UNCLASSIFIED	22. PRICE